

Republic of Iraq  
Ministry of Higher Education  
And Scientific Research  
University of Kerbala  
College of The Engineering  
Mechanical Engineering Department



## **BUCKLING CHARACTERIZATION OF A COMPOSITE PYLON PROSTHESIS**

A Thesis Submitted to the Mechanical Engineering Department in  
College of Engineering at University of Kerbala, in Partial Fulfillment  
of The Requirements for the Degree of Master of Mechanical  
Engineering (Applied Mechanics Science)

By

**Hayder Zaher Kadhim Abdalikhwa Alkafaji**  
BSc. Mechanical Engineering / University of Babylon  
2007

Supervised By

**Prof. Dr.**  
**Mohsin A. Al-Shammari**

**Prof. Dr.**  
**Emad Qasem Hussein**

**2021 A.D**

**1442 A.H**

بِسْمِ اللَّهِ الرَّحْمَنِ الرَّحِيمِ

اقْرَأْ بِاسْمِ رَبِّكَ الَّذِي خَلَقَ ۝١ خَلَقَ الْإِنْسَانَ مِنْ عَلَقٍ ۝٢ اقْرَأْ وَرَبُّكَ

الْأَكْرَمُ ۝٣ الَّذِي عَلَّمَ بِالْقَلَمِ ۝٤ عَلَّمَ الْإِنْسَانَ مَا لَمْ يَعْلَمْ ۝٥

صدق الله العلي العظيم

من سورة العلق

# SUPERVISOR'S CERTIFICATE

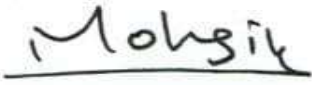
We certify that this thesis entitled

**"BUCKLING CHARACTERIZATION OF A COMPOSITE  
PYLON PROSTHESIS "**

Which is Prepared by "**Hayder Zaher Kadhim Abdalikhwa Alkafaji**"  
under our supervision at the Mechanical Engineering Department/  
College of the Engineering /University of Kerbala, as a partial  
fulfillment of the requirements for the degree of master of science in  
mechanical engineering / applied mechanics.

Supervisor

Signature:

Prof. Dr.   
Mohsin A. Al-Shammari

Date 5/9 / 2021

Supervisor

Signature:

Prof. Dr.   
Emad Qasem Hussein

Date 5/9 / 2021

# LINGUISTIC CERTIFICATE

I certify that the thesis entitled

**"Buckling Characterization of a Composite Pylon Prosthesis"**

which has been submitted by " **Hayder Zaher Kadhim Abdalikhwa Alkafaji** " has prepared under my linguistic supervision. Its language has been amended to meet the English style.

Signature:



Linguistic advisor: **Assist. Prof. Dr. Hayder Jabber Kurji**

College of Engineering

University of Kerbala

Date: 7 / 11 / 2021

## EXAMINATION COMMITTEE CERTIFICATION

We certify that we have read the thesis entitled " **Buckling characterization of a Composite Pylon Prosthesis** "and as an examining committee, we examined the student (**Hayder Zaher Kadhim Abdalikhwa Alkafaji**) in its content and that in our opinion, it meets the standard of a thesis and is adequate for the award of the Degree of Master of Science in Mechanical Engineering / Applied Mechanics.

Signature:



Name: **Prof. Dr. Mohsin A. AL-Shammari**

Date: / / 2022

(Supervisor)

Signature:

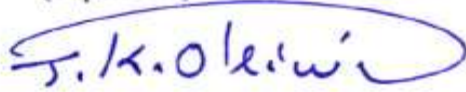


Name: **Prof. Dr. Emad Qasem Hussein**

Date: 24/ 1 / 2022

(Supervisor)

Signature:



Name: **Assist. Prof. Dr. Jawad K. Olewi**

Date: / / 2022

(Member)

Signature:

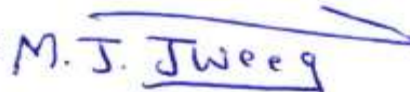


Name: **Dr. Ali I. AL- Zughaiabi**

Date: / / 2022

(Member)

Signature:



Name: **Prof. Dr. Muhsin J. Jweeg**

Date: 25/ 1 / 2022

(Chairman)

Approval of the Department of Mechanical Engineering

Approval of Deanery of the College of Engineering -University of Kerbala

Signature:



Name: **Assist. Prof. Dr. Hayder Jabber Kurji**

(Head of Mechanical Engineering Dept.)

Date: / / 2022

Signature:



Name: **Prof. Dr. Laith Shakir Rasheed**

(Dean of the College of Engineering)

Date: / / 2022

## **Acknowledgements**

I would like to express my thanks to “Allah”, the Most Gracious, and Most Merciful, his prophet “Mohammad”, and to the family of the Prophet (Muhammad), may God’s prayers and peace be upon them, for enabling me to complete this study.

I introduce my thanks to my supervisors: Prof. Dr. Mohsin A. Al Shammari, and Prof. Dr. Emad Qasem Hussain for their valuable guidance, assistance, cooperation, and motivation throughout preparing my thesis.

I would like to thank Assistant Prof. Dr. Laith Shakir Rasheed, the Dean of the College of Engineering–Karbala University.

Also, I would like to thank the Head of the Department of Mechanical Engineering Dr. Hayder Jabber Kurji, Dr. Mohammad Wahab, and the teaching staff in the Department of Mechanical Engineering for their help and support throughout my year of study.

I extend a special thanks to Eng. Mustafa Mahmood at the Babylon Center for Artificial Limbs and to all the workers there.

I extend my thanks to the staff of the laboratories in each of the Mechanical Engineering at the University of Technology, in Faculty of Physical Education at the University of Kerbala ,and the Ministry of Science and Technology, Department of Materials.

Also, I extend my heartfelt thanks to my family and all my friends, including Engs. Hussain Ibrahim, Mohammed Fahad, Muhaiman Faleh, and anyone who helped me in this work.

Hayder 2021

## الإهداء

الى من يسعد قلبي بلقياها...

الى روضة الحب التي تثبت من الازهار أزكاها ...

الى من الجنة تحت قدميها والتوفيق يأتي بدعائها ...

### أمي الحبيبة

الى رمز الرجولة والفداء ...

الى من ساندني بكل ما أوتي من قوة ...

وبه أفخر ما دمت حياً ...

أبي رحمه الله تعالى

الى من وقف بجانبني وساندني...

الى من بهم أفخر

أصدقائي وأحبي

الى من هم أقرب لي من روعي

الى من ساندني في السراء والضراء...

أخوتي أخواتي ...

الى من أنسني في دراستي ...

وشاركني أفراحي وأتراحي ...

زوجتي

الى فلذتي كبدي غلاً وفاطمة الزهراء

الى هذا الصرح العلمي الفتي الجبار...

جامعة كربلاء

أهدي هذا البحث

## ABSTRACT

The prosthetic pylon is an essential part of the artificial lower limb, and it is an exciting area of biomedical engineering today. Pylon is generally made of lightweight metal such as aluminum, titanium, and stainless steel, or an alloy of these. This research aims to develop prosthetic pylon by suggesting new composite materials to be used in its manufacture, making it lighter, less expensive, and more comfortable for the user.

Suggested samples comprise (which were with constant 2.5 mm thick) a constant number of perlon layers and different numbers (one, two, or three) layers of carbon or glass fiber layers at ( $0^{\circ}/90^{\circ}$ ) orientation relative to the applied load (as reinforcement materials) and orthocryl (617H19) (80:20) lamination as a resin. The vacuum bagging technique was used in its manufacture.

The mechanical properties test as tensile, flexural, and buckling were carried out. Besides, a physical test, as the density test, was studied.

Theoretically, these properties were calculated using appropriate equations; it was a good agreement between experimental and theoretical results as the discrepancy percentage reached (6.4 %) only.

These results showed that the modulus of elasticity, tensile strength, flexural modulus, flexural strength, and critical buckling load increase when the number of layers of reinforcement fibers increases. Also, it was found that the better composite samples contain three layers of carbon fibers oriented relative to the applied load by ( $0^{\circ}/90^{\circ}$ ). The ultimate tensile stress, critical buckling load, Young modulus, flexural strength, and flexural modulus for this sample were (204.5N, 175 MPa, 4.63GPa, 230.7 MPa, and 6.38 GPa) respectively.



Based on these results, two types of pylons were manufactured with thickness 2.5 mm), the first pylon from the sixth sample, which consists of (2 perlon, 3 carbon fibers, and 2 perlon) layers, and the other pylon from the third sample consist of (2 perlon, 3 glass fibers, and 2 perlon) layers.

The Buckling test for the two pylons made of composite materials in addition to the currently used metallic pylon made of stainless steel was performed to investigate the critical load and maximum deflection for each pylon.

Using the Finite Element Method (ANSYS WORKBENCH 17.2), maximum deformation, Von-Mises elastic strain, equivalent Von-Mises stress, critical buckling stress, and the buckling mode shape for the two composite pylons beside the metallic pylon were analyzed.

Validation of the experimental results (buckling test) was conducted by comparing with numerical results, where it was an excellent agreement between them as the discrepancy percentage did not exceed (3.01 %).

A case study was considered to verify the durability of the manufactured pylons proposed in the current study and compare it with the metallic pylons used in terms of strength, weight, flexibility, and user comfort. For this purpose, one of the patients at Babylon Center for Artificial Limbs was chosen. The patient was weighty (80 kg), height (1.7 m), and was (55) years old. The patient's left leg was amputated below the knee; the ground reaction force was tested by comparing the results of parameters for gait cycle for the patient with the new pylons (I) and pylon (II) with their counterparts of the prosthetic leg with standard pylon. Relating to the foot rotation angle, the difference was decreased between the injured leg and the regular leg, where the improvement was by (95%) and (38%). At the same time, the step length has been enhanced by (75%) and (50%). In addition, the step time improved by (88%) and (66%) in pylon (I) and pylon (II), respectively.

## List of Contents

<b>Subject</b>		<b>Page No.</b>
Abstract		<b>I</b>
List of Contents		<b>III</b>
List of Symbols		<b>VI</b>
List of Abbreviations		<b>VIII</b>
List of Tables		<b>IX</b>
List of Figures		<b>XI</b>
<b>Chapter One: Introduction</b>		
<b>1-1</b>	General Introduction	<b>1</b>
<b>1-2</b>	The Prosthesis	<b>3</b>
<b>1-3</b>	Artificial Limb Below Knee	<b>4</b>
<b>1-3-1</b>	Socket	<b>5</b>
<b>1-3-2</b>	Pylon	<b>6</b>
<b>1-3-3</b>	Ankle and Foot	<b>7</b>
<b>1-3-4</b>	The Couplings	<b>7</b>
<b>1-4</b>	Economic Pylon Fabrication	<b>8</b>
<b>1-5</b>	Aim of This Study	<b>9</b>
<b>1-6</b>	Motivation	<b>10</b>
<b>1-7</b>	Thesis Layout	<b>10</b>
<b>Chapter Two: Literature Review</b>		
<b>2-1</b>	Introduction (Historical Review for Prosthetic)	<b>12</b>
<b>2-2</b>	Prosthetic Pylon Literature Review	<b>14</b>
<b>2-3</b>	Concluding Remark	<b>18</b>
<b>Chapter Three: Theoretical Part</b>		
<b>3-1</b>	Introduction	<b>20</b>
<b>3-2</b>	Composite Materials	<b>20</b>
<b>3-3</b>	Rule of Mixtures	<b>23</b>
<b>3-4</b>	The Gait Cycle	<b>26</b>
<b>3-4-1</b>	Stance Phase	<b>27</b>
<b>3-4-2</b>	Swing Phase	<b>28</b>
<b>3-5</b>	Ground Reaction Forces	<b>29</b>
<b>3-6</b>	Mechanical Properties for Polymer Materials	<b>30</b>
<b>3-6-1</b>	Tensile Test	<b>30</b>
<b>3-6-1-1</b>	Tensile Strength	<b>30</b>

3-6-1-2	The Modulus of Elasticity	31
3-6-1-3	Elongation's Percentage at The Fracture	31
3-6-3	Bending Test	32
3-6-3	Buckling of Prosthetic Pylon	33
3-6-3-1	Introduction	33
3-6-3-2	Buckling of Column	33
3-6-3-3	The Governing Differential Equation	35
3-6-3-4	End Support Conditions and Effective Length Coefficients	37
3-7	The Design Suggested for the Pylon	38
3-8	Stress Analysis of Composite Prosthetic Pylon for a Case Study	39
3-9	Numerical Analysis	41
3-9-1	Preprocessing	41
3-9-1-1	Material Properties	41
3-9-1-2	Geometry	42
3-9-1-3	Modeling	42
3-9-1-3-1	Meshing	43
3-9-1-3-2	Convergence Test	43
3-9-1-3-3	Boundary Conditions	44
3-9-2	The Static Analysis Solution	45
3-9-3	Buckling Analysis Solution	45
<b>Chapter Four: Experimental Work</b>		
4-1	Introduction	48
4-2	Specimens Preparation	50
4-2-1	Raw Materials	50
4-2-2	The Use Equipment	55
4-2-3	Preparation of the Composite Specimens	58
4-3	Tests Conducted in This Research	63
4-3-1	Tensile Test	63
4-3-2	Flexural Test	65
4-3-3	Buckling Test	67
4-3-4	Density Test	70
4-4	Pylon Manufacturing	71
4-4-1	Equipment	71
4-4-2	Procedure of Pylon Manufacturing	72
4-5	The Pylons Buckling Test	76
4-6	The New Pylons in the Lower Limb for an Amputee (Case Study)	78
4-7	Biomechanical Test (Ground Reaction Force Test (GRF) and	81

	Measurements of Gait Cycle)	
<b>Chapter Five: Results and Discussion</b>		
<b>5-1</b>	Introduction	<b>84</b>
<b>5-2</b>	Experimental Results	<b>84</b>
<b>5-2-1</b>	Physical Properties	<b>84</b>
<b>5-2-2</b>	Mechanical Properties Results	<b>86</b>
<b>5-2-2-1</b>	Tensile Test Results	<b>86</b>
<b>5-2-2-2</b>	Flexural Test Results	<b>89</b>
<b>5-2-2-3</b>	Buckling Test Results	<b>92</b>
<b>5-2-2-3-1</b>	Critical Buckling Load and Maximum Deflection for Samples	<b>92</b>
<b>5-2-2-3-2</b>	Critical Buckling Load and Maximum Deflection for Pylons	<b>97</b>
<b>5-2-2-4</b>	Results of Gait Cycle and Ground Reaction Force (GRF) Test	<b>98</b>
<b>5-3</b>	Cost and Weight of Pylons	<b>108</b>
<b>5-4</b>	Stiffness to Weight Ratio	<b>109</b>
<b>5-5</b>	Theoretical Results	<b>110</b>
<b>5-6</b>	Results of the Numerical Analysis	<b>112</b>
<b>5-6-1</b>	Static Analysis Results	<b>112</b>
<b>5-6-2</b>	Analysis of Buckling Results	<b>118</b>
<b>Chapter six: Conclusions &amp; Recommendations for Future Work</b>		
<b>6-1</b>	Conclusions	<b>125</b>
<b>6-2</b>	Recommendations for Future Work	<b>127</b>
<b>References</b>		
<b>References</b>		<b>128</b>
<b>Appendix</b>		
<b>Appendix</b>		

## List of Symbols

Symbol	Description	Unit
<b>A</b>	Cross-Sectional Area	mm <sup>2</sup>
<b>B</b>	Width of Specimen	mm
<b>D</b>	Depth of Specimen	mm
<b>dε</b>	Change in Strain	%
<b>E</b>	Modulus of Elasticity	GPa
<b>E<sub>1</sub></b>	Modulus of Elasticity Parallel to the Fibers	GPa
<b>E<sub>2</sub></b>	Modulus of Elasticity Transverse to the Fibers	GPa
<b>E<sub>F</sub></b>	Modulus of Elasticity in Flexural Test	MPa
<b>E<sub>f</sub></b>	Young's Modulus of Fibers	GPa
<b>E<sub>m</sub></b>	Young's Modulus of The Matrix	GPa
<b>F</b>	Applied Load	N
<b>F<sub>x</sub></b>	The Axial Force	N
<b>G<sub>12</sub></b>	In – Plan Shear Modulus of Composite Materials	GPa
<b>G<sub>f</sub></b>	Shear Modulus of Fibers	GPa
<b>G<sub>m</sub></b>	Shear Modulus of Matrix	GPa
<b>k</b>	Effective Length Coefficient Factor	----
<b>K</b>	Axial Stiffness	N/m
<b>L</b>	Final Length	mm
<b>L<sub>o</sub></b>	Original Length	mm
<b>m<sub>1</sub></b>	Mass of Specimen in Air	gm
<b>m<sub>2</sub></b>	Mass of Specimen Immersed in Water	gm
<b>P</b>	Load at Fracture	N
<b>P<sub>cr</sub></b>	Critical Load	N
<b>Le</b>	Effective Length of a Column	mm
<b>V<sub>c</sub></b>	The Volume Fraction of Composite	%
<b>V<sub>f</sub></b>	The Volume Fraction of Fibers	%
<b>V<sub>m</sub></b>	The Volume Fraction of Matrix	%
<b>W</b>	Weight of Pylon	N
<b>δ</b>	Deflection of the Specimen	mm
<b>ε</b>	Engineering Strain	%
<b>v<sub>12</sub></b>	Poisson's Ratio of Composite Materials In 1 Plan	----
<b>v<sub>f</sub></b>	Poisson's Ratio of Fibers	----
<b>v<sub>m</sub></b>	Poisson's Ratio of Matrix	----
<b>ρ<sub>c</sub></b>	Density of Composite	gm/cm <sup>3</sup>
<b>ρ<sub>f</sub></b>	Density of Fibers	gm/cm <sup>3</sup>

$\rho_m$	Density of Matrix	gm/cm <sup>3</sup>
$\sigma$	Tensile Stress	MPa
$\sigma_{ult}$	Ultimate Tensile Stress	MPa
$\sigma_{cr}$	Critical Buckling Stress	MPa
$\sigma_f$	Flexural Strength	MPa

## List of Abbreviations

<b>Abbreviations</b>	<b>Description</b>
<b>AK</b>	Above Knee
<b>ASTM</b>	American Society for Testing Materials
<b>BK</b>	Below Knee
<b>CAD</b>	Computer-Aided Design
<b>CAM</b>	Computer-Aided Manufacturing
<b>CNC</b>	Computer Numerical Control
<b>COM</b>	Center of Mass
<b>COP</b>	Center of Pressure
<b>FEM</b>	Finite Element Method
<b>FF</b>	Flat Foot
<b>GRFs</b>	Ground Reaction Forces
<b>HR</b>	Heel Rise
<b>HS</b>	Heel Strike
<b>MS</b>	Mid Stance
<b>PVA</b>	Polyvinylalcohol Bag
<b>TF</b>	Trans-Femoral
<b>TK</b>	Through Knee
<b>TO</b>	Toe Off
<b>TT</b>	Trans-Tibial

## List of Tables

Sequence	Title	Page
<b>Chapter Two</b>		
<b>2.1</b>	The most important researches	<b>18</b>
<b>Chapter Four</b>		
<b>4.1</b>	Mechanical properties of perlon	<b>51</b>
<b>4.2</b>	Mechanical properties of glass fiber	<b>52</b>
<b>4.3</b>	Mechanical properties of carbon fiber	<b>53</b>
<b>4.4</b>	Mechanical properties of the orthocryl (617H19) lamination (80:20)	<b>54</b>
<b>4.5</b>	Type of the composite specimens in this study	<b>57</b>
<b>4.6</b>	Specimens specifications prepared for buckling test	<b>67</b>
<b>Chapter Five</b>		
<b>5.1</b>	Density theoretical and experimental for the samples suggested for the pylon	<b>85</b>
<b>5.2</b>	Volume fraction for the samples suggested with a thickness (2.5mm)	<b>86</b>
<b>5.3</b>	Tensile test results (Mechanical properties for all suggested samples)	<b>88</b>
<b>5.4</b>	Flexural ultimate stress and Young's modulus of all samples	<b>90</b>
<b>5.5</b>	Comparison of the results of tensile and flexural tests	<b>92</b>
<b>5.6</b>	Critical buckling load and maximum deflection for the buckling test	<b>94</b>
<b>5.7</b>	Critical buckling load theoretically and experimentally for all samples	<b>96</b>
<b>5.8</b>	Critical buckling load and maximum deflection in buckling pylons test	<b>98</b>
<b>5.9</b>	Results of step-stride and gait cycle of the amputee with standard pylon	<b>100</b>
<b>5.10</b>	Results of step-stride and gait cycle of the amputee with a pylon (I)	<b>101</b>
<b>5.11</b>	Results of step-stride and gait cycle of the amputee with a pylon (II)	<b>101</b>
<b>5.12</b>	Butterfly parameters for gait cycle of the amputee with standard pylon	<b>103</b>
<b>5.13</b>	Butterfly Parameters for gait cycle of the amputee with a pylon (I)	<b>104</b>



<b>5.14</b>	Butterfly parameters for gait cycle of the amputee with a pylon (II)	<b>105</b>
<b>5.15</b>	Percentages reduction of cost and weight for the suggested pylons relative to the standard pylon	<b>108</b>
<b>5.16</b>	Stiffness to weight ratio for all pylons when applied a unit load	<b>109</b>
<b>5.17</b>	Mechanical properties of composite samples suggested for manufacturing pylon	<b>110</b>
<b>5.18</b>	Experimental and numerical buckling results for all types of pylons	<b>123</b>

## List of Figures

No. of Figure	Title	Page
<b>Chapter One</b>		
<b>1.1</b>	The expected amputation sites in the lower leg	<b>2</b>
<b>1.2</b>	Trans-Tibial prosthetics part	<b>5</b>
<b>1.3</b>	The prosthetic pylon and adapter	<b>7</b>
<b>1.4</b>	The stainless-steel adapter	<b>8</b>
<b>Chapter Two</b>		
<b>2.1</b>	Improvement of the artificial lower limb	<b>13</b>
<b>Chapter Three</b>		
<b>3.1</b>	The levels structures analysis of the composite material	<b>22</b>
<b>3.2</b>	Location of material (Principal) coordinate system on the lamina	<b>23</b>
<b>3.3</b>	Terms used to describe foot placement on the ground	<b>27</b>
<b>3.4</b>	The normal gait stance phase	<b>28</b>
<b>3.5</b>	Ground reaction force components	<b>29</b>
<b>3.6</b>	The simple sample of three-point bending test	<b>32</b>
<b>3.7</b>	Buckling in column	<b>34</b>
<b>3.8</b>	Schematic of buckling	<b>34</b>
<b>3.9</b>	Buckling of a long straight column	<b>36</b>
<b>3.10</b>	End conditions for columns	<b>38</b>
<b>3.11</b>	Stress analysis of prosthetic pylon (case study)	<b>39</b>
<b>3.12</b>	The geometry of prosthetic pylon	<b>42</b>
<b>3.13</b>	Meshing the prosthetic pylon	<b>43</b>
<b>3.14</b>	The critical buckling stress and the number of elements	<b>44</b>
<b>3.15</b>	Boundary conditions for the prosthetic	<b>45</b>
<b>3.16</b>	Flow chart of static analysis	<b>46</b>
<b>3.17</b>	Flow chart of buckling analysis	<b>47</b>
<b>Chapter Four</b>		
<b>4.1</b>	Technical path of this study	<b>49</b>
<b>4.2</b>	Polyvinylalcohol (PVA) bag	<b>50</b>
<b>4.3</b>	Perlon fiber (polyamide 6)	<b>51</b>
<b>4.4</b>	Glass fiber	<b>52</b>

<b>4.5</b>	Carbon fiber	<b>53</b>
<b>4.6</b>	Lamination 617H19 and hardener	<b>54</b>
<b>4.7</b>	Glass mold used in this study	<b>55</b>
<b>4.8</b>	Vacuum system	<b>55</b>
<b>4.9</b>	Electronic sensitive.	<b>56</b>
<b>4.10</b>	Digital vernier	<b>56</b>
<b>4.11</b>	The stage of casting, adjusting, and smoothing the gypsum mold	<b>58</b>
<b>4.12</b>	The stage of calculating the fiber mass & its installation on the gypsum template	<b>59</b>
<b>4.13</b>	A second (external) PVA is applied to cover all fiber	<b>60</b>
<b>4.14</b>	Adding the resin to the mold & separated samples from the gypsum mold	<b>61</b>
<b>4.15</b>	Belt grinding machine	<b>62</b>
<b>4.16</b>	CNC machine	<b>62</b>
<b>4.17</b>	Tensile testing machine	<b>63</b>
<b>4.18</b>	The dimensions of the standard specimen for the tensile test	<b>64</b>
<b>4.19</b>	Stress-Strain curve for the sample (3) with three glass fiber layers	<b>64</b>
<b>4.20</b>	Specimens for tensile test	<b>65</b>
<b>4.21</b>	The dimension of the standard specimen for the flexural test	<b>66</b>
<b>4.22</b>	Three-point flexural test machine	<b>66</b>
<b>4.23</b>	Specimens of the buckling test	<b>67</b>
<b>4.24</b>	The buckling machine test	<b>69</b>
<b>4.25</b>	Specimens of the buckling test	<b>70</b>
<b>4.26</b>	Measuring of the density of samples	<b>71</b>
<b>4.27</b>	Equipment is used in pylon manufacturing	<b>72</b>
<b>4.28</b>	A sketch of the prosthetic pylon	<b>72</b>
<b>4.29</b>	Arranging(PVA),perlon, and (carbon or glass) fibers for the new pylons	<b>74</b>
<b>4.30</b>	Stages of casting pylons with vacuum technique	<b>75</b>
<b>4.31</b>	Separating the pylons produced from the metal mold and cutting it	<b>76</b>
<b>4.32</b>	Pylons during the buckling test	<b>77</b>
<b>4.33</b>	The pylons before and after the buckling test	<b>77</b>
<b>4.34</b>	Transtibial amputation (BK) for the patient had (80 kg), and fifty-five years old	<b>78</b>
<b>4.35</b>	Stages of installing the new pylon(I) in prosthesis for the	<b>79</b>

	amputated person	
<b>4.36</b>	Stages of installing the new pylon(II) in prosthesis for the amputated person	<b>80</b>
<b>4.37</b>	Ground reaction force test	<b>81</b>
<b>4.38</b>	The amputated person walks on a force plate using an available metallic pylon	<b>82</b>
<b>4.39</b>	The amputated person walks on a force plate using suggested pylon (I)	<b>83</b>
<b>4.40</b>	The amputated person walks on a force plate using suggested pylon (II)	<b>83</b>
<b>Chapter Five</b>		
<b>5.1</b>	The Stress-Strain curve for the sample (6) with three carbon fiber layers	<b>87</b>
<b>5.2</b>	Flexural Load-Extension curve for sample (6)	<b>91</b>
<b>5.3</b>	Flexural Load-Extension curve for sample (3)	<b>91</b>
<b>5.4</b>	Critical buckling load against maximum deflection for sample (6)	<b>94</b>
<b>5.5</b>	The experimental critical buckling load and aspect ratio for samples	<b>95</b>
<b>5.6</b>	The butterfly parameters of center of pressure for an amputee with metallic pylon	<b>103</b>
<b>5.7</b>	The butterfly parameters of center of pressure for an amputee with a pylon (I)	<b>104</b>
<b>5.8</b>	The butterfly parameters of center of pressure for an amputee with a pylon (I)	<b>105</b>
<b>5.9</b>	The GRF of the right (healthy) and the left (injured) legs with standard pylon	<b>106</b>
<b>5.10</b>	The GRF of the right (healthy) and the left (injured) legs with pylon (I)	<b>106</b>
<b>5.11</b>	The GRF of the right (healthy) and the left (injured) legs with pylon (II)	<b>107</b>
<b>5.12</b>	Axial stiffness for the prosthetic pylons	<b>110</b>
<b>5.13</b>	Modulus of elasticity(E1) for all samples	<b>111</b>
<b>5.14</b>	Total deformation for the standard prosthetic pylon	<b>112</b>
<b>5.15</b>	Total deformation for the prosthetic pylon (I)	<b>113</b>
<b>5.16</b>	Total deformation for the prosthetic pylon (II)	<b>114</b>

<b>5.17</b>	Comparison for total deformation of the prosthetic pylons	<b>114</b>
<b>5.18</b>	Von-Mises equivalent stress for the prosthetic standard pylon	<b>115</b>
<b>5.19</b>	Von-Mises equivalent stress for the prosthetic pylon (I)	<b>116</b>
<b>5.20</b>	Von-Mises equivalent stress for the prosthetic pylon (II)	<b>116</b>
<b>5.21</b>	Von-Mises elastic strain for prosthetic standard pylon	<b>117</b>
<b>5.22</b>	Von-Mises elastic strain for prosthetic pylon (I)	<b>117</b>
<b>5.23</b>	Von-Mises elastic strain for prosthetic pylon (II)	<b>118</b>
<b>5.24</b>	Buckling mode shape (1) for the standard prosthetic pylon	<b>119</b>
<b>5.25</b>	Buckling mode shape (1) for prosthetic pylon(I) with three carbon	<b>119</b>
<b>5.26</b>	Buckling mode shape (1) for prosthetic pylon (II) with three glass layers	<b>120</b>
<b>5.27</b>	Comparison of the total buckling deformation numerically for pylons	<b>120</b>
<b>5.28</b>	Max. buckling stress for prosthetic standard pylon	<b>121</b>
<b>5.29</b>	Max. buckling stress for prosthetic pylon (I)	<b>121</b>
<b>5.30</b>	Max. buckling stress for prosthetic pylon (II)	<b>122</b>
<b>5.31</b>	Comparison of the critical buckling stress for pylons	<b>123</b>
<b>5.32</b>	The experimental and numerical buckling stresses of all pylons	<b>124</b>

---

# CHAPTER ONE

## INTRODUCTION

### 1.1 General

From the blessings of ALLAH almighty upon us which are countless, that we were created in this integrated form. Also, he provided us with these senses and abilities such as hearing, sight, and the ability to move like walking jogging. We may encounter natural or unnatural misfortune, accidents, sicknesses, or any other reason we lose this ability or cause loss of body limbs like legs, arms, teeth, etc. So, the prosthesis is designed to compensate for the missing limb, helping amputees return to normal life and do their activities.

Continuously, and in all places, efforts have always been made to make up for the amputee and help him regain mobility and walk with a prosthesis, which is a significant challenge for a person who undergoes an amputation. For this, the engineer who designs the prosthesis and his clinical team must be well versed in the mechanics of rehabilitating an amputee for human walking.

There are no accurate statistics for the number of amputees worldwide, but which is estimated in millions. This is because of the difficulty in collecting and analyzing data from various countries worldwide; this lack of data is an area of concernment that requires future study [1].

**Amputation** is a surgical procedure that involves the removal of organs, limbs, or a portion of a limb to save the patient's life by removing dead or damaged tissue. The leading cause of amputation are wars and what is left of them from mines (they have produced 300,000 amputees worldwide per year). In addition to terrorist

.....

attacks, emergency accidents in transportation, industrial facilities, etc. Also, diseases such as diabetes, which has recently spread, cancer, or people were born incomplete part (The deformity congenital), and other causes. All these led to increasing the number of amputations at an alarming rate [2].

To help make the prosthesis in the correct size, the design and manufacturing process begins with a precise and detailed measurement process. Before surgery, a prosthetist maybe needs to start taking measurements, if at all possible, where the prosthetist and doctor meet to go over the specifics of the procedure. The size of the portion to be removed, the incision's ability to heal, and the capability to make an effective residual limb all influence the level of amputation; there are several levels for amputation in the lower limp of the human body, as shown in figure (1.1). Still, there are three main levels, which are [3]:

1. Hip disarticulation: it is an amputation at or near the hip joint.
2. Knee disarticulation: it is an amputation throughout the knee.
3. Symes: it is an ankle disarticulation while preserving the heel pad.

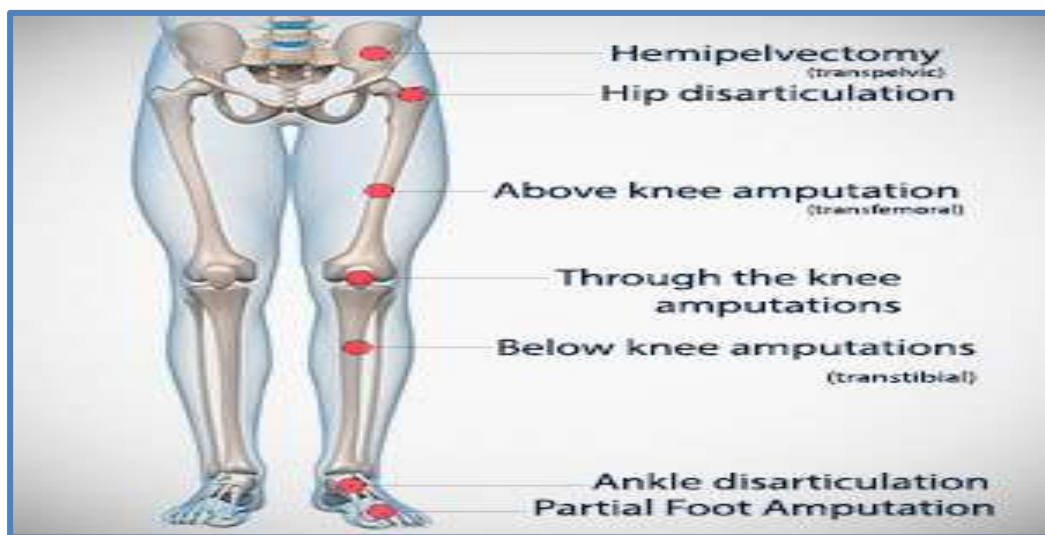


**Figure (1.1)** The Expected amputation sites in the lower leg [3].

Psychologists, physiatrists, and prosthetists physiotherapists may be involved in the amputee's rehabilitation to address the loss of function and pain. It is worth mentioning, the prosthesis is selected according to the type of amputation.

## 1.2 The Prosthesis

Prosthetics is defined as internal or external devices that replace lost organs or functions of the neuroskeletonotor system and can control it either orthopedic or externally [4]. Prosthetics is one of the most important applications of biomedical engineering, which has witnessed significant progress. The advancement in surgical practice, medication, engineering materials, and instrumentation has been successfully helped in this field. Biomedical engineers have an essential role in prosthetics where they are shared in the design of some of the commercial components for prostheses such as foot, knee joint, and development CAD-CAM [Computer-Aided Design (CAD) and Computer-Aided Manufacturing (CAM)] system. They have solved significant problems facing amputees and have directed attention to satisfying their human function, performance, comfort, and cosmesis [5].

Prosthetic components must meet the general design aims of user acceptance, comfort, ease of use, durability, efficient locomotion, and reliability during gait. Several complex interactions affect comfort and locomotion, but these are influenced by one of three factors: the prosthetic components, the prosthetist, and the patient [6].

The main objective of a prosthetic below the knee (which will be the focus of the current research) is to supply means of replacing the lost structure and function of the skeleton and muscles of the shank, ankle, and foot. The plaster mold is then used as a residual limb's duplicate to test the prosthetic limb's suitability as it is



.....

being built. The patient's residual limb will usually shrink over a few months as the tumefaction goes down, and the muscles initiate atrophy because of lacking use. To accommodate the size reduction, layers of sock-like dressings can be adjusted to accommodate the residual limb's changing dimension. Sometimes a new socket may be required for this. Also, new technologies enable computerized digital measurements to be taken. It can predict these changes.

The structure of the residual limb is also essential, involving the location of bones, tendons, or muscles. Other considerations in the prosthesis's design include the patient's health and skin condition. Physical therapy and prosthetic device fitting are critical after an amputation. Walking with a prosthesis can be difficult, needing several months of training and rehabilitation. In particular, a prosthetist must try carefully with children to ensure that the prosthetic limb is suitable for their growth because residual limb forms change permanently, leading to prosthetic collapse. The amputee will need a visitation to the prosthetist in all for his life.

The numbers of below-knee amputees in Iraq have increased for the reasons mentioned previously. Still, unfortunately, little researches have dealt with manufacturing pylon from composite material just as socket and foot are manufactured from it.

This study deals with the artificial limb below the knee, which generally consists of the following interchangeable parts that are usually custom-built to the individual's anthropometric specifications:

### **1.3 Artificial Limb Below Knee**

The artificial limb below the knee consists of the parts as shown in figure (1.2):

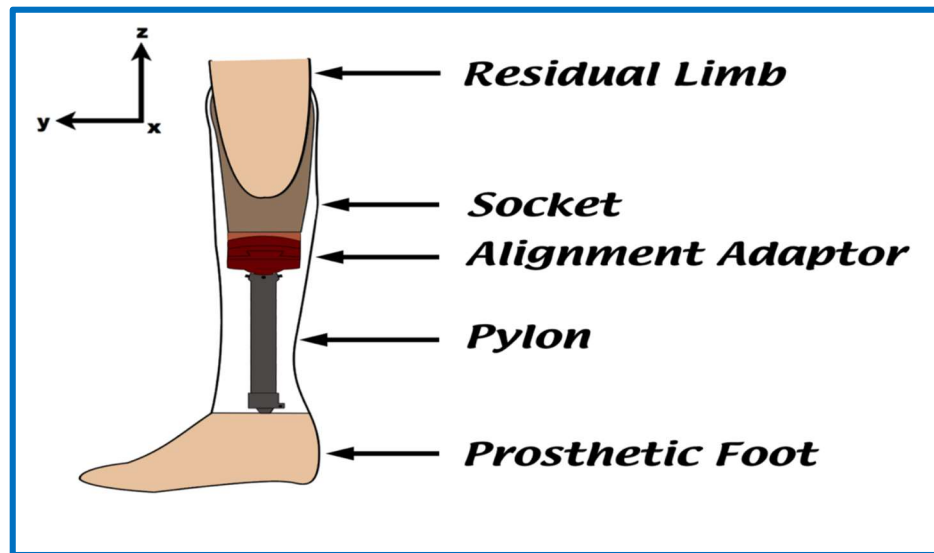


**Figure (1.2)** Trans-Tibial (TT) prosthetics part.

### 1.3.1. Socket

It is the essential part of the prosthesis because it connects the amputated person to the prosthesis. It must contact the residual limb part of the amputated limb comfortably and firmly. So, it must be comfortable, stationary, and strong enough to bear the weight of the amputated person; if not, the amputee will not wish to wear the prosthesis constantly or will not be glad about it [7, 8].

The socket manufacturing process went through many stages. Where it was earlier carved out of wood. After that, it formed from aluminum. It was performing the purpose. However, the manufacturing process was not easy and needed a long time. With the development of modern technology. It has become a manufacturing socket process possible from polymers, glass fibers, and other fibers, which are strong, lightweight, easy to form, and cheap, leading to increasing amputees' acceptance of the limb [9]. The perfect socket of prosthetic must be characterized by:

1. Efficient gait function.
2. Safe structural.

### **1.3.2 Pylon**

It is a rod commonly made of lightweight metals such as aluminum, titanium, stainless steel, or an alloy of these, to produce more strength and safety; as shown in figure (1.3), pylon will link the socket to the foot joint through the prostheses if the amputation is Below the Knee (BK), while it will connect the knee joint to the socket if amputated Above the Knee (AK). Sometimes pylons are made from two rods to offer additional impact absorption, especially with high-level activity [10], but this metallic pylon is characterized by its heavyweight that consumes more energy, imbalance during walking or running, and is very expensive.

On the design side, the prosthetic's pylon radius and length about (15mm) and (400mm), respectively; these dimensions depend on the amputee's weight and length.

The pylon is subjected to the compression load of the amputee's weight, which may be led to the buckling phenomenon. When connected to the prosthetic socket, the pylon takes place the tibia and fibula bones as the support structure for the amputee. Sometimes, the pylons are enclosed by a covering to add the prosthetic limb's most vibrant manifestation; the cover can be formed and varicolored to match the amputee's skin tone. Lately, pylons have evolved from simple static shells to dynamic devices capable of axial rotation and energy absorption, storage, and release [11]. In the current research, this part that provides structural support in BK prosthetics will be studied.



**Figure (1.3)** The prosthetic pylon and adapter [Ottobock Company].

### 1.3.3. Ankle and Foot

The prosthetic foot is the lowest part of the prosthetic lower limb. It works as a regular foot; in a perfect world, it should emulate all the activities of a regular foot. This foot must have to ability to stable base of support, muscle activity simulation, trauma absorbing. There are several designs for the prosthetic foot used to suit the various requirements of amputees. It can be classified the prosthetic feet into two types, the foot with movable joints, and the foot without movable joints [10, 12].

### 1.3.4 The Couplings

The almost universal standardization of coupling components of BK prosthetics allows for the easy interchanging of components by this part [13]. Figure (1.4) illustrates the stainless-steel adapter.



**Figure (1.4)** The Stainless-steel adapter [Ottobock Company].

In the current research, the composite technology will be selected to manufacture prosthetic pylon to try making the pylon have characterized as good strength, cheap, lighter weight, lower deformation, and longer life, which are very important factors. Composite lamination polymers include binding the reinforcement fiber layers with each other to produce a lamination. This lamination process occurs under the vacuum bagging technique; it was used to create the pylon with high properties compared to the pylon made of metal [14].

## 1. 4 Economic Pylon Fabrication

Given the difficult economic conditions experienced by countries at war or subject to terrorist attacks, which usually leads to an increase in amputations, it was necessary for engineers working in the biomedical field were required to have lower-cost and more comfortable prosthetics to serve this segment of society. So, attention turned to the selection of composite materials. Besides their low cost and ease of fabrication, the composite materials have high mechanical properties. Also,

.....

it is an environmentally friendly material; therefore, its uses are widely spread in biomedical applications such as socket, foot, and others [15].

### **1.5 Aim of This Study**

The main objective of this work is to design and manufacture a pylon in BK prosthetic limb by choosing a composite material. This selection was according to the better results of samples which made of constant perlon layers and a different number of (carbon or glass) fibers layers as reinforcement materials at (0°/90°) orientation relative to the applied load and the orthocryl (617H19) (80:20) lamination as a resin. To make the prosthetic pylon more economical, lighter weight, more balanced, and more comfortable to help the user return to normal life and do their activities.

This work contains the following points:

1-Study the effect of reinforcing fiber types, a number of these fiber layers, aspect ratio, and volume fraction on the mechanical properties of composite specimens suggested for the prosthetic pylon.

2-Study the static and buckling analysis of the composite prosthetic pylon; this work included two significant parts; experimental and numerical using (ANSYS-17.2) techniques (to determine the best materials that can be used to manufacture pylon with long life according to the required specifications.

3-Design and produce a pylon that is resistant to buckling failure from a composite material. After that, manufacture a prosthetic lower limb for a case study (a person amputee below the knee weighting (80 kg), and aged (55 years). This prosthetic can withstand the weight of the patient and the loading encountered in the different stages of the gait cycle, mainly at the heel strike position.

.....

## 1.6 Motivation

The cases of amputation in Iraq wars-torn country through the last thirty years increased at an alarming rate. Also, the significant terrorist attacks, car crashes, industrial accidents, and diseases like gangrene, diabetes, and other reasons besides the low level of medical capabilities, all these causes together faced our people and led to large numbers of people have lost limbs.

Therefore, there is an actual need for economical prosthetics as an alternative to the currently used prosthetic pylon that is usually made of light metals like titanium, aluminum, and stainless steel or an alloy of these but, in addition to their high cost, these materials characterize heavyweight, and rigidity, which caused failed prosthetic limp.

## 1.7 Thesis Layout

This thesis consists of six detailed chapters that cover the general theme of it, as follows:

- The current chapter one gives a general introduction to amputation, levels, its causes, and components of prosthetics below-knee and introduces the main aim to be achieved.

In chapter two, the historical aspects of the prosthetic by the historical review are summarized, giving a general idea about the materials used, manufacturing methods of the prosthetic pylon, and presenting the literature review.

- Chapter three consists of a theoretical study that includes an introduction, gait cycle, composite material, mixtures rules characteristics required for the prosthetic pylon proposed. Also, it consists of the steps of numerical analysis using the finite element method (ANSYS - 17.2) for the product prosthetic pylon.

- .....
- The experimental part is presented in chapter four, which gives properties of the materials suggested for prosthetic pylon manufacturing. Also, it explains the method of manufacturing composite specimens and measuring the mechanical characteristic, a requirement by tensile, flexural, and buckling tests. This chapter includes the manufacturing process of the proposed pylon, using it in the prosthetic lower limb for an amputee person, and conducting some of the required tests.
  - Chapter five presents the results reached and discussion it, which included the mechanical properties of composite materials and the experimental and numerical results and compares them.
  - The last chapter (six) presents the conclusions drawn from the current study and the suggestions for future research.



## **CHAPTER TWO**

### **LITERATURE REVIEW**

#### **2.1 Introduction (Historical Review for Prosthesis)**

Prosthesis term originates from the Greek verb (*Bprostithenai*), whose meaning is (to add to), ancient literature includes references to prosthetic limbs in stories and poems. The earliest prostheses that have registration had their origin in ancient Egypt. Where in the year (2000) scientists have reported finding in Cairo, a prosthetic toe made of wood and leather was found attached to the nearly (3,000) year-old mummified remains of an Egyptian noblewoman. This prosthesis was used to complement the body form rather than being functional [16, 17].

The prostheses design has improved over time in their functional aspect. In (1858), in Italy, an artificial leg manufactured from iron and bronze beside a wooden nucleus dating from (300 BC) had functional use for the lower limb amputees.

In (1560), a shank was designed as a functional prosthetic leg made of metal, leather, paper, and glue by the French surgeon Ambroise Paré and the French artisan Le Petit Lorrain to ensure certain moves the amputee makes use of a mechanism of activation by the cord [18].

The prostheses developed in the nineteenth century until (1912), aviator Marcel Desoutter, who lost his leg in World War I, designed and manufactured the first aluminum prosthesis in history [19].

After the end of the Second World War and increasing amputees' numbers suddenly, this led to new prosthetic feet and related components [20].

.....

In (1960), Ambroise Paré and Le Petit Lorrain began using new low- resistance composite materials for manufacturing prostheses. After that, with the development of new composite materials, fundamentally using carbon fiber and thermosetting resins, significant growth occurs in designing prostheses and orthopedic appliances [21].

So, it can be said from the twentieth century, and prostheses were significantly developed clearly in terms of design and materials.

Nowadays, most prosthetic limb parts are made of composite materials like plastic and carbon fiber. Which is lighter, stronger, and its shape is like the form of the natural human limb such as socket and foot. Figure (2.1) shows the development of artificial lower limbs.



**Figure (2.1)** Improvement of the artificial lower limb [22].

## 2.2. Prosthetic Pylon Literature Review

**Wevers H. and Durance J.P. (1987)** [23] investigated dynamic tests experimentally for components of prosthetic lower limb (socket, pylon, and foot). This is to find out how many cycles each compound will fail. These tests showed the pylon made of aluminum (6061-T6) with applied load (1350N) failed in (897,600) cycles in a fatigue test.

**Thurston A.J. et al. (1989)** [24] were concerned with manufacturing a semi-rigid pylon for below-knee prosthetic employing (carbon, glass, and Kevlar) fibers were laminated by mold without the tensile elements being pre-stressed, in methyl methacrylate matrix (30% of flexible orthocryl, and 70% of rigid orthocryl). The pylon was flexible to certain limits, allowing the use of energy storage properties while walking; these compound materials can be changed according to the needs of each amputee. Fatigue testing results showed that the material lasted a long time before it failed, equivalent to thirty months of vigorous use.

**Bern N., P. Lawes, and Solomonidis S. (1994)** [25] focused on measured prosthetic forces and moments during amputee gait using a shorter pylon transducer. The strain gauged tubular structure and flanges were machined as one component from aluminum bar adapters fitted to flanges to fix the prostheses. The shortened pylon transducer is supplied to be a very effective tool in the biomechanical analysis of the gait for an amputee.

**Coleman et al. (2001) K. L.** [26] presented a study that compared two types of pylons, one made of aluminum (solid) and the other of nylon (flexible). In terms of the effect of flexibility on the ground reaction force (GRFs) and the extent to which this affects the user's comfort. The results revealed that the nylon pylon is more flexible and comfortable, allowing the amputee to walk faster.

.....

**Ross Stewart and Ian Brown (2001)** [27] studied the crack growth problem using FEM by building a model to know the expected life for the pylon of the prosthetic, and they investigated fatigue failure and the stress distribution for the pylon adapter. The model was compared to manufactures testing and the cyclic test. They focused on finding the stress distribution for two types (titanium and aluminum) of pylon; the results were reached ( $1.74 \times 10^6$ ) cycles without breakage, and the crack length stretched (51mm) for the aluminum pylon.

**Winson C. C. Lee et al. (2004)** [28] studied using FEM the stiffness effect for three different forms of the monolimb pylon on the stress distribution at the socket interface through the walk. These forms were elliptical, circular, and the cross-section for the third type was elliptical at one end and circular at the other. The term "monolimb" indicates a single piece molded made of thermoplastic materials containing pylon and socket. The results displayed that when the pylon stiffness decreased, Von-mises stresses applied to the limb dropped. Maximum Von-mises stresses were found in the first type of pylons.

**Prasanna Lenka K. et al. (2008)** [29] focused on designing a new prosthetic limb with an adjustable shank made of polypropylene and nylon using FEM. The new pediatric prosthetic is a scientific mechanical device; with three principal components: a socket, adaptable pylon (comprising two portions, upper and lower), and foot. It was lightweight, cheap, and easy to manufacture, for this can be used with patients in developing countries, particularly for growing children, where the prosthetic has to be replaced repeatedly.

.....

**Shasmin H.N. et al. (2008)** [30] presented a study about low-cost pylon made from bamboo. Bamboo natural fiber-reinforced composite material- with superior mechanical characteristics to ensure using it as a structural material rather than metallic materials like aluminum and titanium. It is designed and manufactured for amputees who have lost their lower limbs and cannot afford the high cost. The results found through (compression, flexural, and tensile) tests that bamboo pylons have suitable mechanical properties, such as strength and modulus of elasticity. Also, the bamboo pylon is more robust than pylon made of aluminum.

**Shasmin H.N. et al. (2008)** [31] performed studying the effect of the mass of two types of pylons on amputees while walking, the first pylon made of bamboo, and the other from stainless steel. Through the comparison between these two pylons generally, the results showed no discernible impact on gait characteristics, stride velocity, and cadence for the two types. But, the use of bamboo pylon provided advantages in terms of cost and mass. To reduce the mechanical power required during walking, the older persons used the bamboo pylon in prosthetics.

**Muhsin J. Jweeg et al. (2010)** [32] studied pylon made of composite materials experimentally and analytically. These pylons are made of a different number (6, 9, 12) layers of perlon as reinforcement materials and acrylic as a matrix. The (tensile, impact, and fatigue) tests have been done. The results show that with an increase in perlon layers, the mechanical properties increase. Also, all pylons were inexpensive and lightweight.

**Muslim M. Ali et al. (2012)** [33] studied the effect of angle dorsiflexion on the prosthetic pylon's flexural stress. The study involved two parts: numerical and

theoretical. In the numerical part, the authors used FEM (ANSYS) to determine bending stress in the gait cycle with ankle dorsiflexion and Von- Mises stresses. The theoretical part included an analytic solution. The results showed that the bending stress would increase with the increase in dorsiflexion angle and the increase in the length of the pylon. It will also increase with the decrease in the diameter of the pylon.

**Albert E. Yousif, and Ahmed Ali Sadiq (2012)** [34] focused on designing TK (through the knee) prosthetic lower limb; it contains of (knee joint, adjustable pylon, ankle joint, and foot). Also investigated total deformation, shear stresses, and maximum Von-Mises stress using FEM. They developed this lower limb where the adjustable shank consists of two parts. The lower part was made of beach wood, and the upper part was made of aluminum. The results indicated that total deformation occurs at the end of the lower part of the adjustable pylon. In contrast, the Von-Mises stress and shear stress are happening at the upper part's contact point with the support.

**Pitkin M., J. Pilling, and G. Raykhtsaum (2012)** [35] studied the bending strength for two types of shanks; the first shank was composed of porous titanium only, while the other shank was composite materials (solid core titanium with drilled holes surrounded by and a porous sintered titanium shell). The results showed the shanks composed of only porous titanium have bending strength and stiffness less than the composite pylons

**Jawad K. Oleiwi and Shaymaa J. Ahmed (2015)** [36] presented a study on designing a new prosthetic pylon made of composite materials to make prosthetics more comfortable and economical for the amputee. Two types of fibers were used as reinforcing layers: artificial and natural. The artificial layers were perlon, and

hybrid (carbon + glass) fibers. Whilst the natural layers were the jute fibers. Also, polymethyl methacrylate (PMMA) was used as a matrix. Tensile, impact, bending, hardness, and creep tests were performed on the suggested samples. They used FEM to analyze; critical buckling stress and total deformation for all types of a composite prosthetic pylon. The results showed that the best laminated composite specimens have three hybrids (carbon + glass) layers that have mechanical properties higher than specimens that have three jute layers. Still, specimens of jute fibers were lighter weight.

This study has been developed (in current research), using new materials (carbon or glass) fibers as reinforcing layers and orthocryl lamination (617H19) as (matrix) due to its availability in the market and its relatively low cost. Two types of pylons were manufactured, with a difference in pylon's length from the research 36. Also, in current research, a buckling test was conducted for practically manufactured pylons, and then they were used in a prosthetic limb for an amputee, and a GRF test was performed.

### 2.3 Concluding Remarks

The most important studies are outlined in Table (2.1).

**Table (2.1)** The most important researches

No.	Material used	Parameters studied
[31]	Bamboo and stainless steel	Compression, flexural, and tensile tests
[32]	Acrylic reinforced by different layers (12, 9, 6) perlon	Tensile, impact, and fatigue tests
[36]	Artificial layers (perlon layers, hybrid (carbon + glass) fibers) and	Tensile, impact, bending, hardness, and creep tests

---

	natural layers (jute fibers), and polymethyl methacrylate (PMMA) matrix	
--	---	--

Most research into the lower prosthesis has focused on designing and manufacturing the socket and the foot without exposure to the pylon. Even in the research that dealt with the prosthetic pylon, it has been noticed that a few of them the prosthetic pylons were made of composite materials or have been actually tried it in a prosthetic limb for the amputated person as a substitute for the pylon currently used made of metals, which are usually very expensive and heavy.

In this research, the design and manufacturing of two types of pylons of the proposed composite materials; the first pylon was made of three layers of carbon fibers and four layers of perlon. Whilst, the other pylon was made of three layers of glass fibers in addition to four perlon layers as reinforcement fibers in orthocryl (617H19) (80:20) lamination as a resin. Then the manufactured pylons were used in the prosthetic limb of an amputee below the knee to substitute for the metallic pylon.



## **CHAPTER THREE**

### **THEORETICAL ANALYSIS**

#### **3.1 Introduction**

Lower limb amputees below the knee usually show deformities such as step length, slow walking, and unbalancing. The main reason for this is that the natural limb contains muscles and enough flexibility, which the prosthesis lacks. That is beside the difference in weight between the unaffected limb and the prosthesis and other reasons. The functions of the prosthetic pylon can be summarized as follows [37]:

- 1- Transfer the load from the socket connected with the amputee's body to the foot.
- 2- Set the socket and the foot in the correct position in the prosthetic limb.
- 3- Provide cosmeses (when using a cover over a prosthetic pylon).

High-performance composites and thermoplastics have increasingly replaced conventional prosthetic and orthotic materials like lacing, wood, titanium, and stainless steel. Fiber-reinforced plastics are very appealing in this field due to their low weight, longevity, size reduction, stability, and energy conservation requirements.

The socket frame component, which connects by the residual limb and carries a load, and transmits this load for the pylon component, which backs the load over the ground, was made of composite in Trans-Tibial (TT) and Trans-Femoral (TF) prostheses [38].

#### **3.2 Composite Materials**

The most straightforward states of composite materials generally are composed of the two phases: a continuous, less stiff, and weakly, called the

“matrix”. At the same time, the other is an intermittent one, powerful and stiffer, which is knowing “strengthening”, but in several cases, maybe accrue the chemical interaction or other effects led to an additional phase is called “interphase,” occurring between the matrix and the strengthening [39].

Reinforcement fibers make up the most significant part of the volume fraction of composite materials and account for a significant portion of the acting force on the construction of the composite according to fibers length, fiber type, and fiber orientation with a load applied [40].

The fibers' tasks are to supply stiffness, strength, decrease cost with some fillers, and prevent the crack spread. While the matrix functions were summarized in providing a good finishing for the product, arranging the fibers together at a particular shape, keeping the fiber surface from the damage. Also transmitting applied stress to the fibers (distributes the loads equally between fibers so that subjected to the selfsame amount of stress) [41].

In the current research, polymer composites were used, which divided into [42]:

1-Thermoplastics composites reinforced with (natural fibers or carbon, kevlar, glass fibers). They are characterized by their powerful intermolecular bonds that cause significant kindly biocompatibility and resistance to moisture damage.

2-Thermosetting composites, these materials are brittle and have a high interlocking density that leads to breakage and cannot be reshaped, such as epoxy and polyurethane.

The arrangement of the fibers into a composite material is related to composite requirements. Composite materials contain plies or lamina, which are thin layers; the fibers of each lamina can be aligned in the same direction (unidirectional) or different directions as weaving. Lamina contains short fibers oriented and distributed in the same direction or at random. A laminate is consisted of stacking

the lamina to the required shape of the laminate. The structure is made of these laminates shown in figure (3.1) [43].

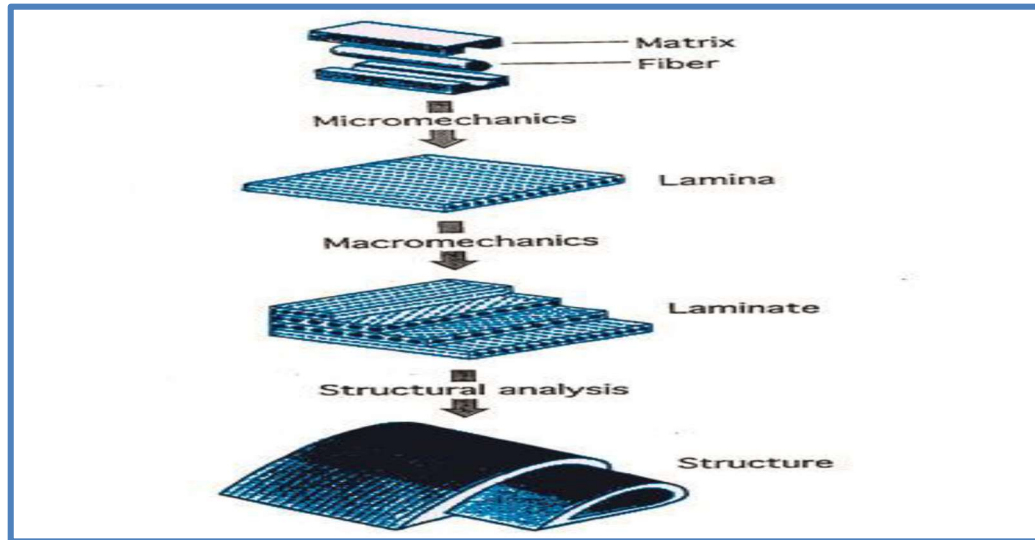


**Figure (3.1)** The levels structures analysis of the composite [43].

The mechanical properties of composite material have different in three reciprocally perpendicular directions. Therefore, it is necessary to specify a system of three orthogonal coordinates directed along the planes of material symmetry.

This coordinate is directed along the planes of the material (principal) coordinates system. The first axis of the material is directed toward the direction of the fibers; it is called the fiber axis (axis-1). While the second axis (axis-2) is placed on the lamina plane, its direction is perpendicular to that of the fiber is called the matrix axis.

The third one is called the normal axis (axis-3); this axis is perpendicular to the lamina plane. Figure (3.2) shows the position of the material coordinates system on the lamina [44].

In case the mechanical properties of the composite material were equal in three reciprocally perpendicular directions, this composite material is called isotropic. In

comparison, it is called orthotropic when the mechanical properties of the composite material are equal in only two reciprocally perpendicular directions.

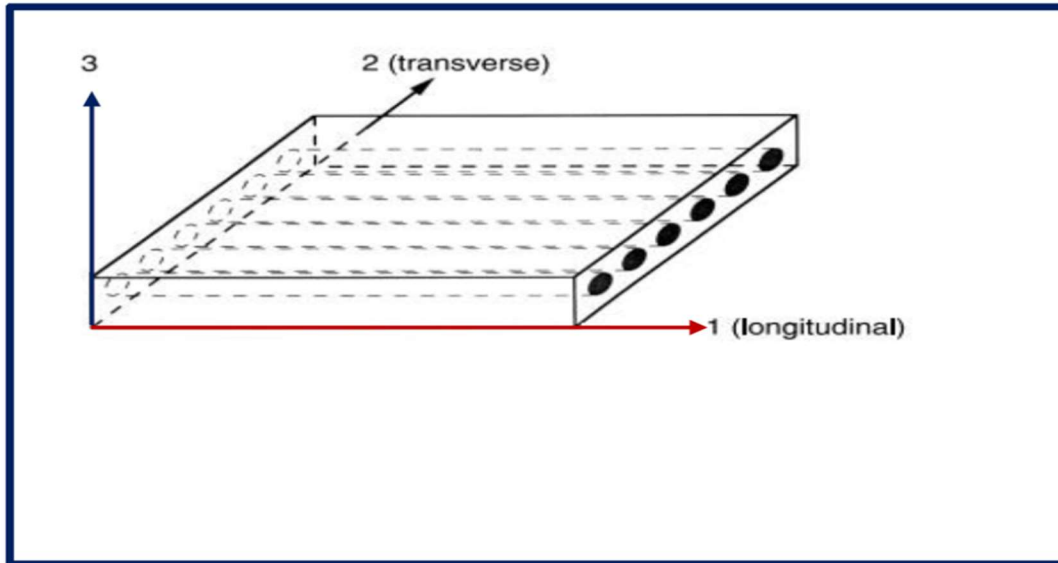


**Figure (3.2)** Location of material (principal) coordinate system on the lamina [44].

### 3.3 Rule of Mixtures

The ply (lamina) is a single layer of a composite of resin reinforced by proper fibers as illustrated in Figure (3.2). Using the rule of mixtures, the mixtures' properties for the unidirectional lamina can be predicted from the properties of the reinforcement fibers and the matrix [45].

The materials model mechanics utilizes simple analytical equations to reach the efficient composite characteristics, depending on simplified hypotheses concerning the distribution of strain and stress in a representative volume element. The typical (mixtures rule) equations for composites are the result of this process. These properties are proportionate to the matrix and fiber volume fraction.

The volume fraction for fibers can be calculated from [46]:

$$V_f = \frac{V_f}{V_c} * 100\% \quad \dots (3.1)$$

And the volume fraction of the matrix can be calculated from:

$$V_m = \frac{V_m}{V_c} * 100\% \quad \dots\dots (3.2)$$

Where:

$V_f$  and  $V_m$ : volume fractions of the fibers and matrix, respectively.

$V_f$ ,  $V_m$ , and  $V_c$  : volumes of the fibers, matrix, and composite, respectively.

$$V_f + V_m = 1 \quad \dots\dots (3.3)$$

The volume of the fibers can be expressed as:

$$V_f = \frac{M_f}{\rho_f} \quad \dots\dots (3.4)$$

where  $M_f$ : Mass of fiber,  $\rho_f$  : Density of fiber

While the volume of matrix material can be expressed as:

$$V_m = \frac{M_m}{\rho_m} \quad \dots\dots (3.5)$$

where  $M_m$ : Mass of a matrix,  $\rho_m$ : Density of matrix

The total mass of the composite material can be calculated as [47]:

$$M_c = M_f + M_m \quad \dots\dots (3.6)$$

The volume of composite constituents can be evaluated as:

$$V_c = V_f + V_m \quad \dots\dots (3.7)$$

And can be calculated the density for composite (fiber reinforced polymer) from:

$$\rho_c = \rho_f V_f + \rho_m V_m \quad \text{or} \quad \dots\dots (3.8)$$

$$\rho_c = \rho_f V_f + \rho_m (1 - V_f)$$

$\rho_c$ : the density of the composite.

To describe the mechanical characteristics of the composite material (resin reinforced by fiber) through assumed as an orthotropic material in its plane (plane 1-2) in Figure (3.2), four elastic stiffness characteristics are required. These were ( $G_{12}$ ,  $\nu_{12}$ ,  $E_1$ , and  $E_2$ ) [47].

In the fiber reinforcement direction, Young's modulus for lamina composite materials, here axial strain (isostrain) in both the reinforcement fiber and the resin.  $E_1$  is determined by the following [47]:

$$E_1 = E_f V_f + E_m V_m \quad \dots (3.9)$$

While the transverse modulus of elasticity (Isostress) is assumed to apply to both the reinforcement fiber and the resin,  $E_2$  is calculated as follows [47]:

$$\frac{1}{E_2} = \frac{V_f}{E_f} + \frac{V_m}{E_m} \quad \text{or} \quad E_2 = \frac{E_f \cdot E_m}{E_m V_m + E_f V_f} \quad \dots (3.10)$$

Where:

$E_m, E_f$  : Modulus of elasticity for matrix and reinforcement fibers, respectively.

$\nu$ : Poisson's, which define as [ $\nu = (\text{transverse strain}) / (\text{axial strain})$ ].

Poisson's ratio calculated using the mixture rule as follows:

$$\nu_{12} = \nu_f V_f + \nu_m V_m \quad \dots (3.11)$$

$$\nu_{21} = \nu_{12} \frac{E_2}{E_1} \quad \text{or} \quad \frac{\nu_{21}}{E_2} = \frac{\nu_{12}}{E_1} \quad \dots (3.12)$$

$$\frac{\nu_{13}}{E_1} = \frac{\nu_{31}}{E_3} \quad \dots (3.13)$$

$$\frac{\nu_{23}}{E_2} = \frac{\nu_{32}}{E_3} \quad \dots (3.14)$$

Where:

$\nu_m$ : Poisson's ratio of the matrix.

$\nu_f$  : Poisson's ratio of reinforcement fibers.

The rigidity modulus for the fiber and the matrix of the composite material can be calculated as [47]:

$$G_{12} = \frac{G_m \cdot G_f}{V_m G_f + V_f G_m} \quad \text{or} \quad \frac{1}{G_{12}} = \frac{V_m}{G_m} + \frac{V_f1}{G_f1} + \frac{V_f2}{G_f2} \quad \dots (3.15)$$

$$G_{13} = G_{23} = G_m = \frac{E_m}{2(1+V_m)}, \quad \text{where:} \quad \dots (3.16)$$

$G_m$ : Shear modulus of the matrix

$G_f$ : Shear modulus of fibers.

### 3.4 The Gait Cycle

Walking is a repetitive sequence of limb motions that move the body forward while with each other maintaining stance stability. Also, walking is defined as a type of movement that involves using both legs alternately to provide the two push and support. [48].

To complete a gait cycle, a stride is two equal steps; the length of the step can be known as the distance amongst the right foot heel contact and the left foot heel contact. The length of the step is proportional to the walking speed, where if the walking speed increased, the length of step will improve [49]. The number of steps taken per minute is called the cadence, or walking speed, which can change significantly as the cadence is up to (130) steps per minute in fast walking, while in slow walking, the cadence is up to (70) steps per minute [50]. One gait cycle generally happens through the time it takes for two sequential events to occur involving the same limb, when the foot first impacts the supporting surface or ground. This process includes two phases: the “stance phase”, during which the foot contacts the ground. It may be defined as the time between the heel striking the ground and the toe of the same foot leaving the ground. This time involves (60- 62) % of the overall gait cycle time and the “swing phase”, through which the foot does not touch the ground. This phase can be defined as the time the toe leaves the ground to the time the heel of the same foot strikes the ground, which takes nearly (38-40) % overall the time of the gait cycle as shown in figure (3.3) [51, and 52].

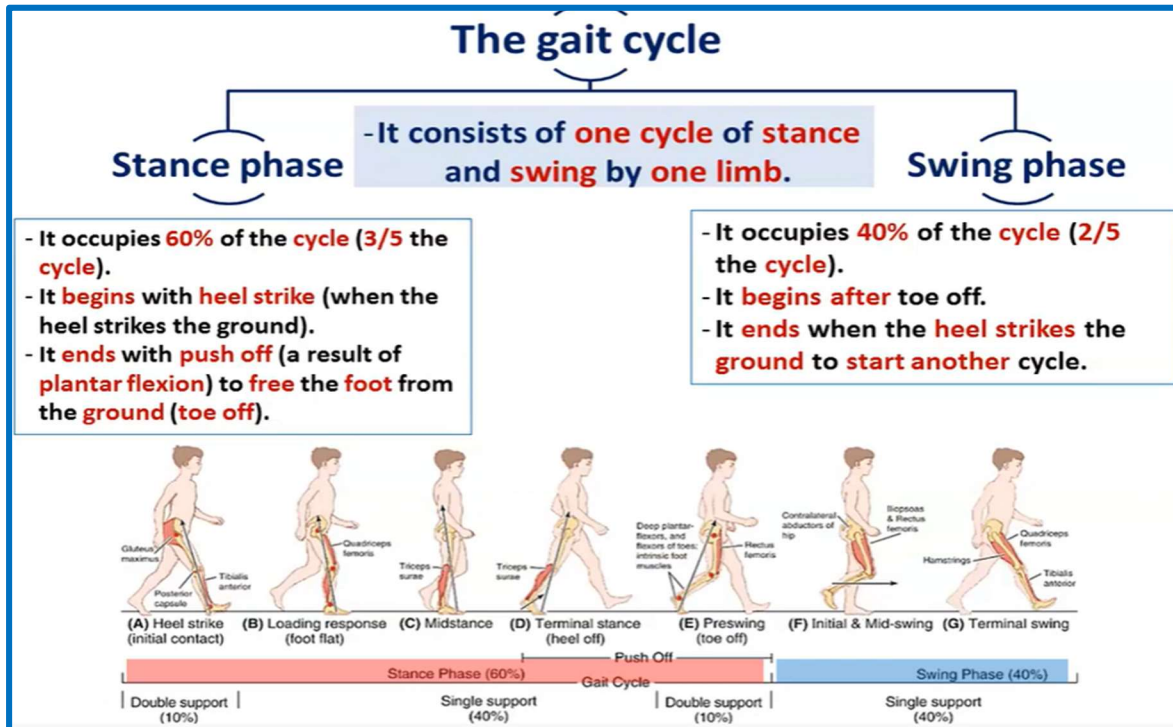


**Figure (3.3)** Terms used to describe foot placement on the ground [49].

A person's gait cycle usually consists of the two major components listed below [52].

### 3.4.1 Stance Phase

The stance phase consists of the following points and, as shown in figure (3.4):

- 1- Heel Strike (HS) or Initial contact: The stance phase starts with it, at which point the contact with the ground is made.
- 2- Flat Foot (FF) or Loading response: The foot is closely controlled to go down towards the floor after the heel contacts the ground, at FF, to supply a steady backing basis for the rest body.
- 3- Mid Stance (MS): The ankle joint is exactly located under a hip joint, and the ankle serves as a pivot point as the entire body rolls over the foot.
- 4- Heel Rise (HR) or terminal stance (heel off): At it, the heel loses contact with the ground, it occurs in a critical time instant, where the objective of the lower limb



from that MS point onwards was to propel the mass body center ahead through the phase of (push-off).

5- Toe-Off (TO): It is the ending of the stance phase, usually when the foot leaves the floor, the toe is the last point of touch with it, for this, called the toe-off phase.

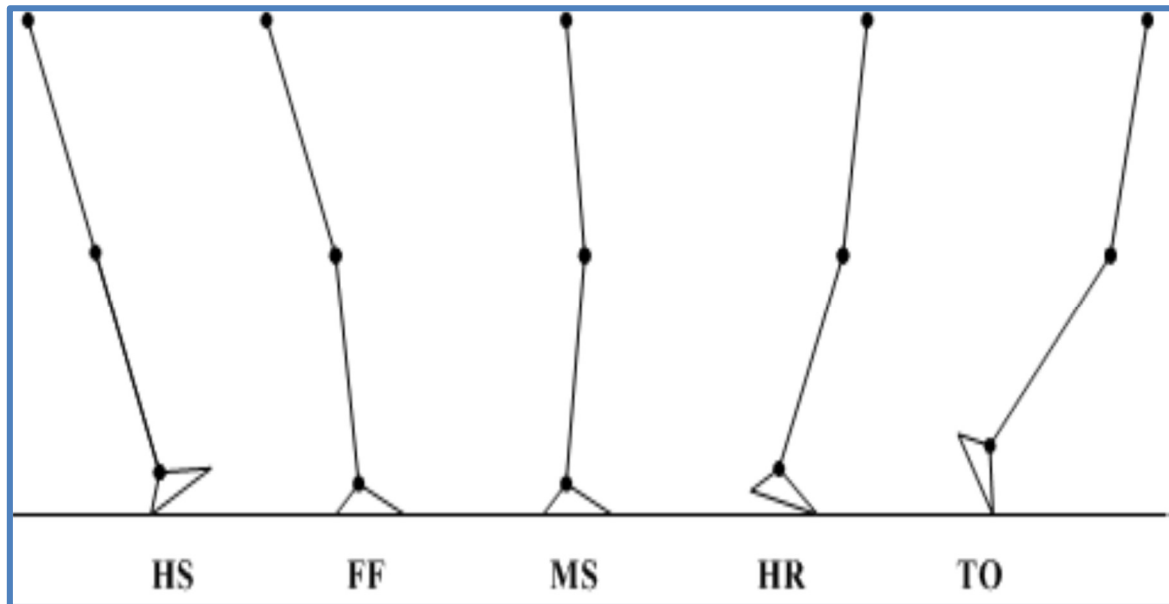


**Figure (3.4)** The normal gait stance phase [52].

### 3.4.2 Swing Phase

The swing phase begins when the end of the stance phase, which can be defined as the period between the toe-off is leaving the floor and the heel touches it, for the same leg, the swing phase consists of:

- 1- Initial swing: At the moment the foot loses touch with the ground, acceleration begins, and the subject speeds up the leg forward by activating the hip flexor muscles
- 2- Mid swing occurs when the foot passes right down the body, coinciding with the other foot's mid-stance.
- 3- Terminal swing: The muscles stabilize the foot and slow the leg, preparing for the suffix heel strike.

### 3.5 Ground Reaction Forces (GRFs)

The Ground Reaction Force (GRF), is precisely defined as “the force exerted by the ground on a body in contact with it,” there is no ground reaction force if the leg is not in touch with the ground

As shown in figure (3.5), GRF is a three-component vector that represents forces in the vertical, anterior-posterior, and medial-lateral planes. Each part assesses a distinct aspect of the movement. The vertical aspect is the most significant and is primarily caused by the body's vertical acceleration. GRF data is easily available, and it is commonly expressed as a percentage of body weight versus gait stages. The lateral aspect has been ignored since it is negligible compared to the vertical force [53,54].

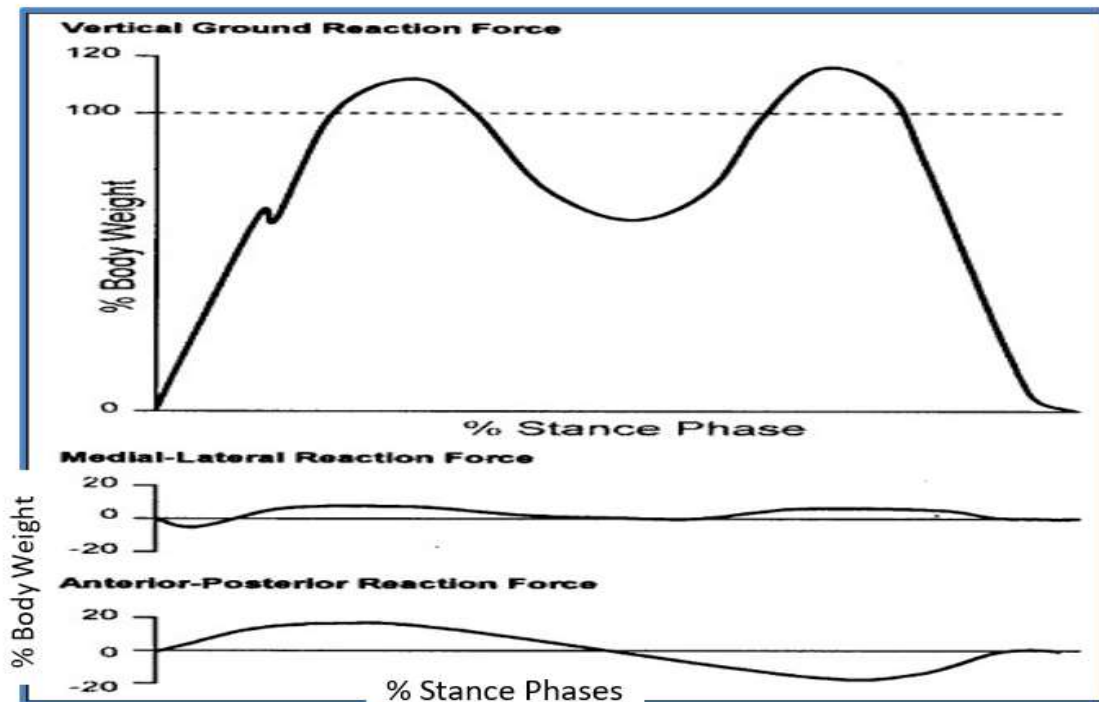


Figure (3.5) Ground reaction force components [52].

HS and TO will show the usual force, denoted by the percentage of body weight applied to the pylon and is approximately equal to (120 %). The horizontal force is about (18 %). At full heel strike, the limb's angle was (30°) [55].

## 3.6 Mechanical Properties for Polymer Materials

### 3.6.1 Tensile Test

The tensile test is one of the basic tests used to know the properties of the materials. This led to knowing their optimal uses to develop necessary designs for the parts in proportion to the forces imposed on them. It also provides the primary checks for control quality of materials. From the tensile test, can be obtained:

- 1 -Tensile stress
- 2- Modulus of elasticity.
- 3- Elongation percentage at break [56].

**3.6.1.1 Tensile Strength** is calculated by dividing the load at the break by the original minimum cross-sectional area as shown in the following:

$$\text{Tensile strength at break} = \frac{\text{Load at break}}{\text{Cross sectional area}}$$

$$\sigma = \frac{F}{A} \quad \dots\dots (3.17)$$

Where:

$\sigma$ : Longitudinal stress for specimens (*MPa*).

F: The applied load (*N*).

A: Area of the cross-section before the test (*m<sup>2</sup>*).

### 3.6.1.2 The Modulus of Elasticity (Young's Modulus)

A material constant is obtained from the slope of the linear portion of the stress-strain curve. It can be expressed mathematically with:

$$E = \frac{\Delta \sigma}{\Delta \epsilon} \quad \dots (3.18)$$

Where:

$E$ : Young's Modulus (GPa)

$\sigma$  : Longitudinal stress for specimens (MPa).

$\epsilon$  : Engineering strain (%).

### 3.6.1.3 Elongation's Percentage at the Fracture

Calculation of the elongation's percentage at fracture point is done by dividing the changing in the length of gage (extension) at the point of sample laceration over the original length of the gage and multiplying by (100), as will be showed in the equation (3. 21).

$$\text{Elongation's percentage } (\epsilon) = \frac{L - L_0}{L_0} * 100\% \quad \dots (3.19)$$

Where:

$\epsilon$  : Engineering strain (%).

$L$ : Specimen's length after the test (mm).

$L_0$ : Original length of specimen (mm).

### 3.6.2 Bending Test

The flexural modulus is the criterion of the material's stiffness during bending; it can be obtained from the bending (flexural) test. Also, this test is provided with the strength at which the beam was bend with three-point load conditions. The bending test data helps select the materials used to manufacture parts that support loads without bending [57]. Figure (3.6) illustrates the simple sample of the three-point bending test.

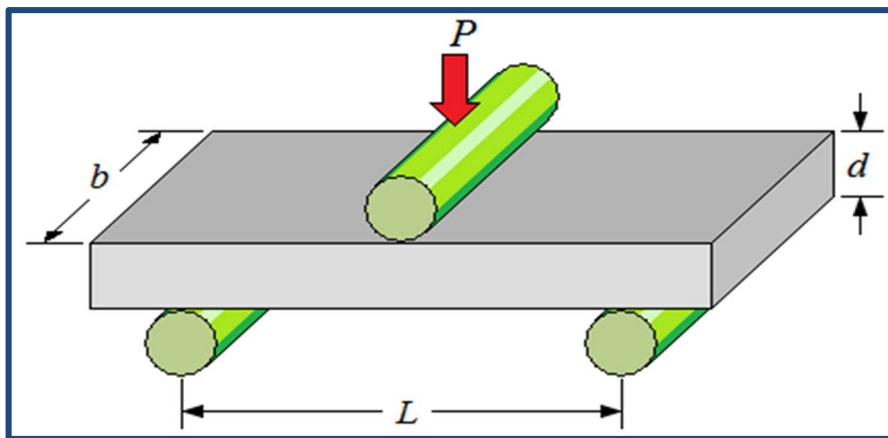


**Figure (3.6)** The simple sample of three-point bending test [57].

The flexural strength ( $\sigma_f$ ) can be defined as the maximum stress at failure on the specimens being tested, and it is computed for any point on the load-deflection curve by the following [58].

$$\sigma_f = \frac{3PL}{2bd^2} \quad \dots\dots (3.20)$$

$\sigma_f$ : Bending (flexural) strength (MPa).

P: The fracture load (N)

L: The sample length(mm).

d: The sample thickness(mm).

b: The sample width (mm).

For this, the maximum bending stress happens in the midpoint of the test specimen. The flexural modulus ( $E_F$ ) can be determined by [58]:

$$E_F = \frac{L^3 P}{4bd^3 \delta} \quad \dots\dots (3. 21)$$

Where:

$E_F$ : Flexural Modulus ( $MPa$ ).

L: The sample length (the span of the support) (mm).

P: The fracture load ( $N$ )

d: The sample depth ( $mm$ ).

$\delta$ : The deflection of a sample ( $mm$ ).

### 3.6.3 Buckling of Prosthetic Pylon

#### 3.6.3.1 Introduction

Buckling is a treacherous phenomenon that occurs in engineering structures; any slight increase in the applied load may lead to sudden catastrophic failure. It occurs when the body is subjected to an axially compressive force that exceeds the critical bending load of the body.

#### 3.6.3.2 Buckling of Column

For example, when an ideal column, as in figure (3.7-a), is subjected to a specific axial compressive force  $F$  with a low value, only a shortening of the column length and deflection will occur. If the values of  $F$  are low, the column will return to its straight position, even with force  $F$  remaining in place. This means the column is in a steady state. If the axial force  $F$  is increased, and there is a new value for it; until the lateral deflection (deformation) reaches a specific limit (exceeding the critical point). The column will remain deformed, even with the

force  $F$  removed; by then, the column will have failed structurally. That is called buckling, and this force is called critical buckling load, as shown in figure (3.7-b).

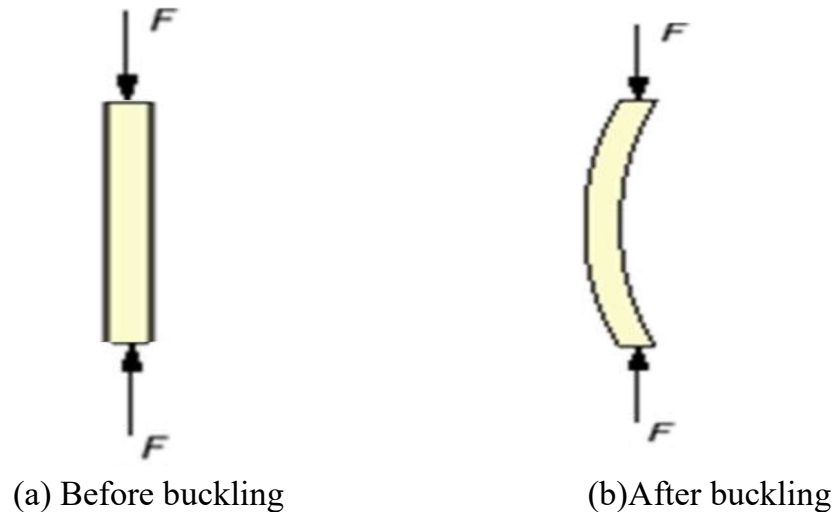


**Figure (3.7)** Buckling in column [32].

The critical load is reached during the bending of the column (when the column begins to bend). Sometimes, the load can be removed without causing permanent damage since yielding deformation does not occur. The curve in the right part of figure (3.8) shows how to get the critical buckling load for the column.

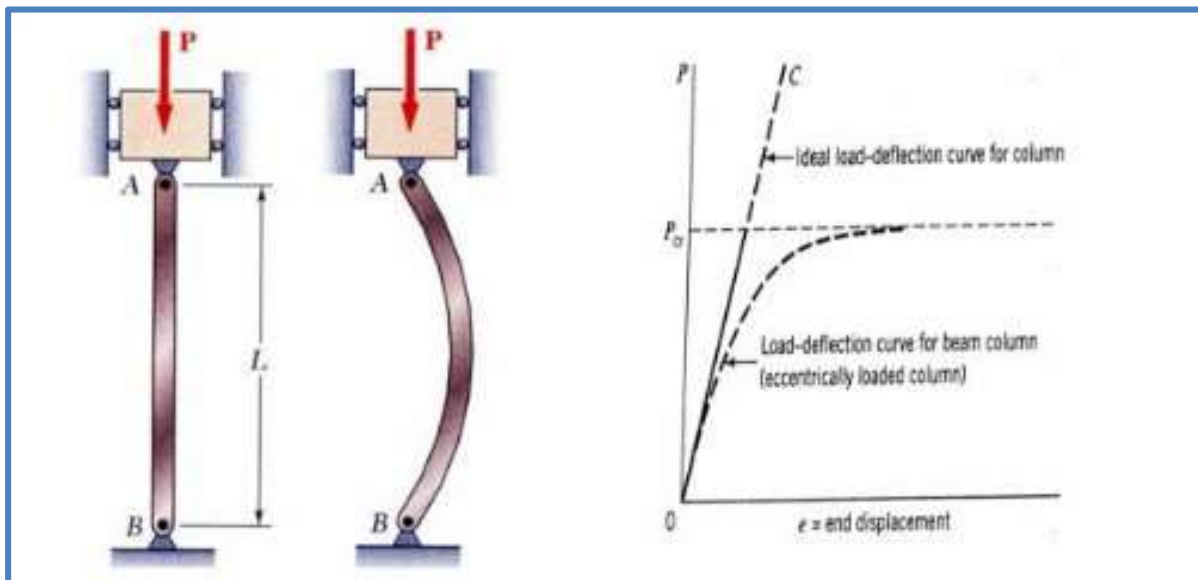


**Figure (3.8)** Schematic of buckling [59].

---

Therefore, buckling can be depicted in easy words as curvature or bending of a column by a compressive load, according to their prorated lengths and cross-sectional dimensions. The structural members that are capable of carrying compression loads can be split into two broad groups.

1- In compression of the slender, long columns or members, before arriving at the yield stress, the buckling occurs.

2- Columns are short, thick members that typically fail by crushing when the material's yield stress in compression is exceeded.

The main reasons that cause buckling failure:

(a) It is not possible to apply the load entirely along the member's axis.

(b) The member might not be completely straight at first.

A medium or long column will buckle and fail when the applied axial load exceeds a critical value [60]. At the time of buckling, the compressive stress can be well below the materials' yield strength.

### 3.6.3.3 The Governing Differential Equation

An external axial compression force  $P$  is applied to a buckled fixed-pin supported column of length  $L$ ; the left part of Figure (3.8) shows that. The buckled column's transverse displacement is performed by  $(\delta)$ . The moments and forces that act on the cross-section of the buckled column are depicted in the right schematic of figure (3.9).



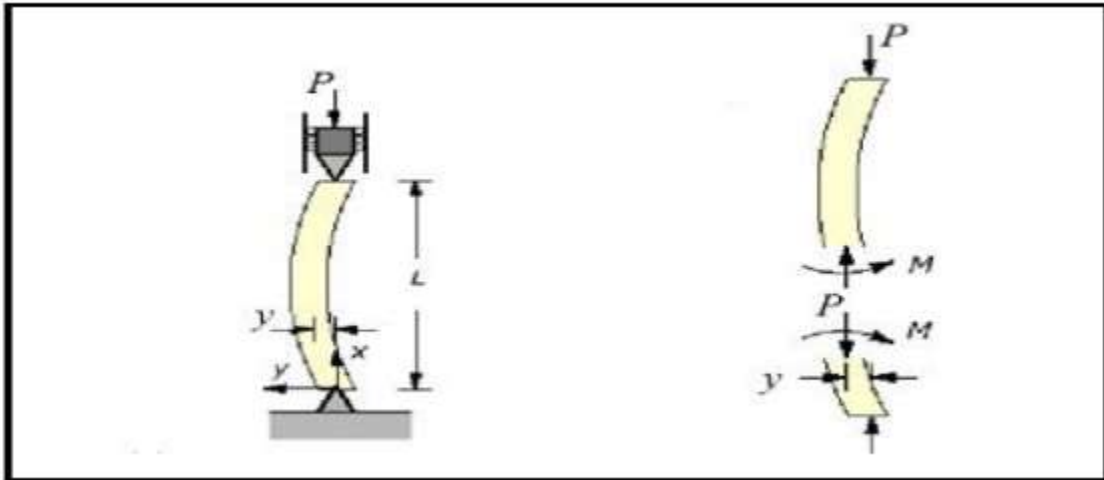


**Figure (3.9)** Buckling of a long straight column [61].

The internal bending moment  $M$  is solved by moment equilibrium on the lower free body,

$$PY + M = 0 \quad \text{..... (3.22)}$$

Recall in the elastic curve the connection between transverse displacement ( $y$ ) and moment  $M$ ,

$$EI \frac{d^2y}{dx^2} = M \quad \text{..... (3.23)}$$

$$\frac{d^2y}{dx^2} + \frac{PY}{EI} = 0 \quad \text{..... (3.24)}$$

Eliminating  $M$  from Eqs. (3.23) and (3.24) the buckled slender column has a governing equation, a second-order homogeneous ordinary differential equation with constant coefficients, solved using a characteristic equations method. The solution has been discovered as follows:

$$y(x) = A \sin(Px) + B \cos(Px) \quad \text{..... (3.25)}$$

$$\text{Where } p^2 = \frac{P}{EI}$$

The two boundary conditions,  $y(0) = 0$  and  $y(L) = 0$ , can determine the coefficients  $A$  and  $B$ , yielding  $B=0$

$$A \sin (P L) = 0 \quad \dots (3.26)$$

The coefficient (A) must be equal to zero for the majority of values of (M x L), but the particular cases of (M x L, A) cannot be equal to zero, causing the column to buckle. The limitation on (M x L) also applies to the loading values (F); these particular values are known as Eigen values in mathematics. Any other values of F produce solutions that are fiddling (viz, the deformation is zero).

$$\sin (P L) = 0$$

$$P = 0, \frac{\pi}{L}, \frac{2\pi}{L}, \frac{3\pi}{L}, \frac{4\pi}{L}, \dots, \frac{n\pi}{L} \quad \dots (3.27)$$

Since  $p^2 = \frac{P}{EI}$  therefore

$$P = 0, \frac{\pi^2 EI}{L^2}, \frac{(2)^2 \pi^2 EI}{L^2}, \frac{(3)^2 \pi^2 EI}{L^2}, \frac{(4)^2 \pi^2 EI}{L^2}, \dots, \frac{(n)^2 \pi^2 EI}{L^2} \quad \dots (3.28)$$

or

$$P = EI \left( \frac{n\pi}{L} \right)^2 \quad \text{For } n = 0, 1, 2, 3, \dots \quad \dots (3.29)$$

The critical load when (n = 1) is the lowest load that causes buckling [61].

$$P_{cr} = \frac{\pi^2 EI}{L^2} \quad \dots (3.30)$$

Where:

E: Young's Modulus.

I: Moment of Inertia.

Le: Column effective length

### 3.6.3.4 End Support Conditions and Effective Length Coefficients

In theory, end supports are either pinned or fixed, but they are designed to be rigid or pinned in reality and may fall somewhere in between pinned or fixed.

The effective length of the column will be affected by the support conditions which can be different in each plane.

The distance between points on a column where the moment is zero (inflection points) is known as the effective length of a column ( $L_e$ ).

$$L_e = k L \quad \dots\dots (3.31)$$

Where:

$L$ : The actual length of the column in the buckling plane.

$k$ : The coefficient factor of the effective length. It depends on the column's ending condition support, as shown in figure (3.10) [62].

$$\text{Then, } P_{cr} = \frac{\pi^2 E I}{L_e^2} \quad \dots\dots (3.32)$$

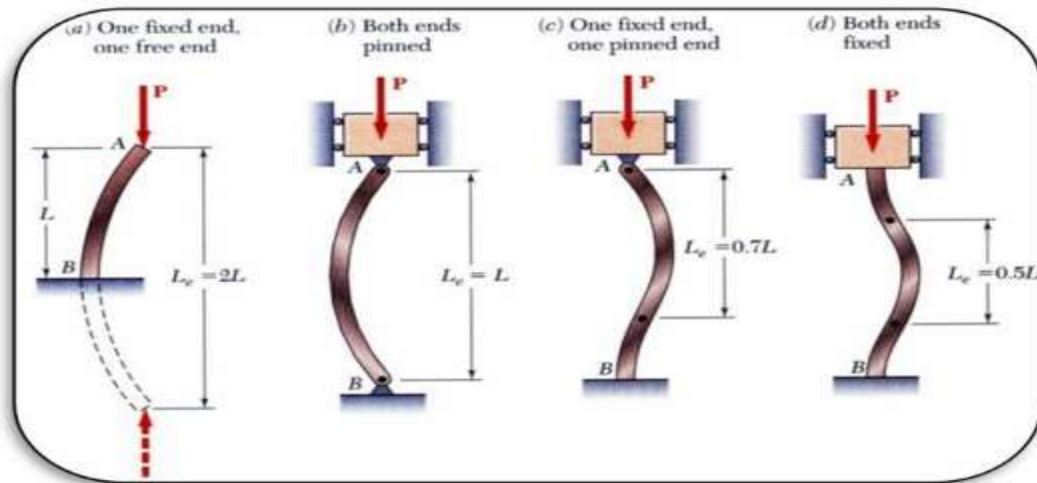


**Figure (3.10)** End conditions for columns [63].

### 3.7 The Design Suggested for the Pylon

Sometimes, complex and expensive designs may not be needed, even if they contain new ideas and shapes. But if it was rather a lighter, stronger, sleeker design, or one of higher quality and value than the standard parts that have been used in the market for long periods, that is what is required. The pylon used nowadays has made from metals such as steel or aluminum, which does not possess good impact absorption compared with composite materials. For this, it is possible to manufacture a practical, simple pylon to get specific performance criteria.

The new pylon must be rendering the essential assignments, which contain:

1-Backup the body against gravity through walking and standing.

2-Flexibility to absorb impact through heel touch.

3-The principle of storing energy as the prosthetic lower limb with the new pylon accepts-body weight and returns this energy to other limb functions.

Emphasis has been placed during the manufacturing of the new pylon to be lightweight and economical so that amputees of the elderly and children with limited income can use it. Therefore, the composite materials were chosen in its manufacture, making the pylon more durable, strong, and flexible.

These proposed composite materials are powerful enough to protect the pylon from breaking while altering the vertical and horizontal impulses during weight-bearing [64].

### 3.8 Stress Analysis of Composite Prosthetic Pylon for a Case Study

The vertical and horizontal load were based upon an (80 kg) subject, assuming that the length of the pylon (210 mm), the inner and outer diameter (25 mm), (30 mm) respectively, as shown in figure (3.11) as follows:

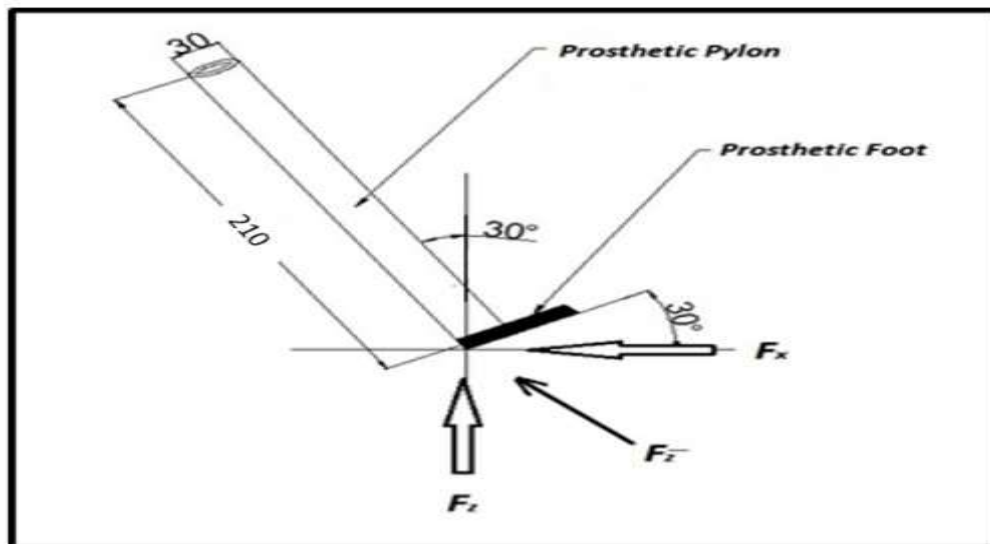


**Figure (3.11)** Stress analysis of prosthetic pylon (case study).

$$\mathbf{F}_x = (-0.18) (80 \text{ kg}) (9.81 \frac{\text{m}}{\text{s}^2}) = -141.264 \text{ N}$$

$$\mathbf{F}_z = (1.2) (80 \text{ kg}) (9.81 \frac{\text{m}}{\text{s}^2}) = 941.76 \text{ N}$$

$$\begin{aligned}\mathbf{F}_z^- &= \mathbf{F}_x \sin 30^\circ + \mathbf{F}_z \cos 30^\circ \\ &= (-141.264 \text{ N}) (\sin 30^\circ) + (941.76 \text{ N}) (\cos 30^\circ) \\ &= 744.956 \text{ N (The load that applied in static analysis).}\end{aligned}$$

$$\begin{aligned}\sigma_{Fz}^- &= (\mathbf{F}_z^-) / ((\pi / 4) * (D_o^2 - D_i^2)) \\ &= (744.956 \text{ N}) / ((\pi / 4) * (30^2 - 25^2)) \\ &= 3.446 \text{ N/mm}^2\end{aligned}$$

### **3.9 Numerical Analysis**

The numerical model was attained using finite element analysis for standardized tests, experimentally verified, so being able to be used for the manufacture of big structures. Essentially, the Finite Element Analysis requires dividing the area of geometry into tiny sub-elements in a process called meshing [65].

#### **Finite Element Analysis**

The finite element method (ANSYS WORKBENCH) software, version 17.2, was used to analyze the model adopted in the current research. This method provides all of the functions for layers construction, composite material analysis, and ply layup. Also, it defines the element, demonstrates the design of complex composites made up of various materials, thicknesses of layers, and texture orientations [66].

ANSYS software is one of the systems that has been developed and updated since (1992); it has been beneficial because it has been improved and extended to apply to electrical, mechanical, environmental, chemical, and biomedical engineering disciplines, among others.

#### **3.9.1 Preprocessing**

It is essentially defining the problem and the main parts of it; the preprocessing is divided into:

##### **3.9.1.1 Material Properties**

Among the most important mechanical properties of composite materials (which are orthotropic) required in constructing the model in this research are:

1 - Modulus of elasticity, its value can be obtained through a tensile test.

2 - The shear modulus, that was determined using rule of mixtures rule.

3- The Poisson's ratio, it can be calculated from the rule of mixtures as well.

### 3.9.1.2 Geometry

The dimensions must be determined to create the geometry of the prosthetic pylon and know at any stage of the walking cycle to determine the angle of its inclination with the ground. Figure (3.12) shows that of the prosthetic pylon model the thickness, outer diameter, and length were (2.5 mm), (30 mm), and (210 mm) respectively, while it was at an angle of (30°) with the ground at the heel strike of the gait cycle.

### 3.9.1.3 Modeling

The pylon's finite element model was developed using globally agreed diameters for the metallic prosthetic pylons and the actual geometrical length of an amputee person (a male amputee below the knee 80 Kg and 55 years old). These measurements were later used to draw the model in ANSYS (version 17.2), as shown in figure (3.12).

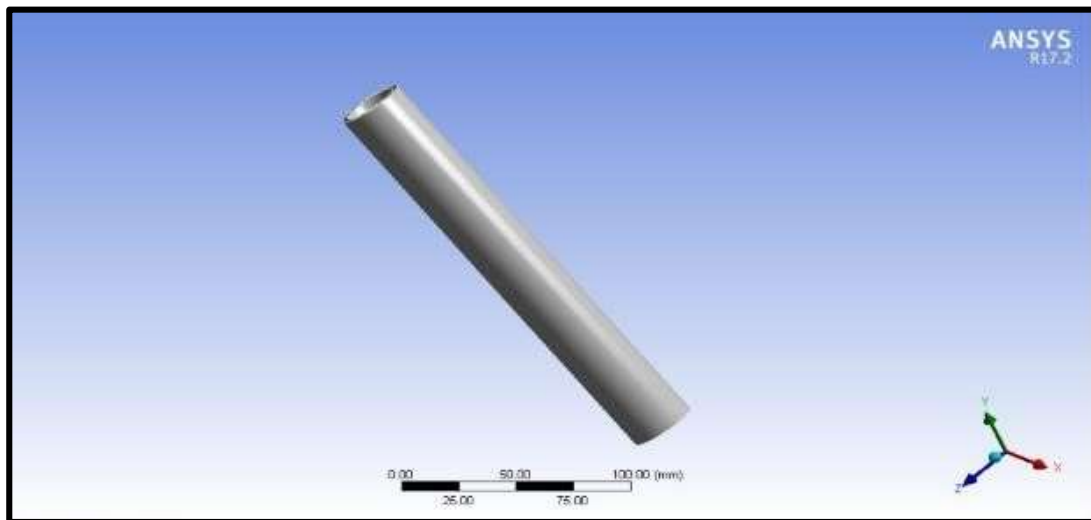


**Figure (3.12)** The geometry of prosthetic pylon.

**3.9.1.3.1 Meshing**

Whenever the mesh density was fine, this led to making the results more accurate, while if the mesh density is coarse, the results are contained an error. Therefore, determining the type of mesh density for the pylon is an essential factor in the accuracy of the results. The (ANSYS 17.2) program determines the mesh density automatically generated by using a meshing tool with the ability to change that according to the required accuracy as shown in figure (3.13), as well as it contains a feature through which you can know the number of elements in each mesh.

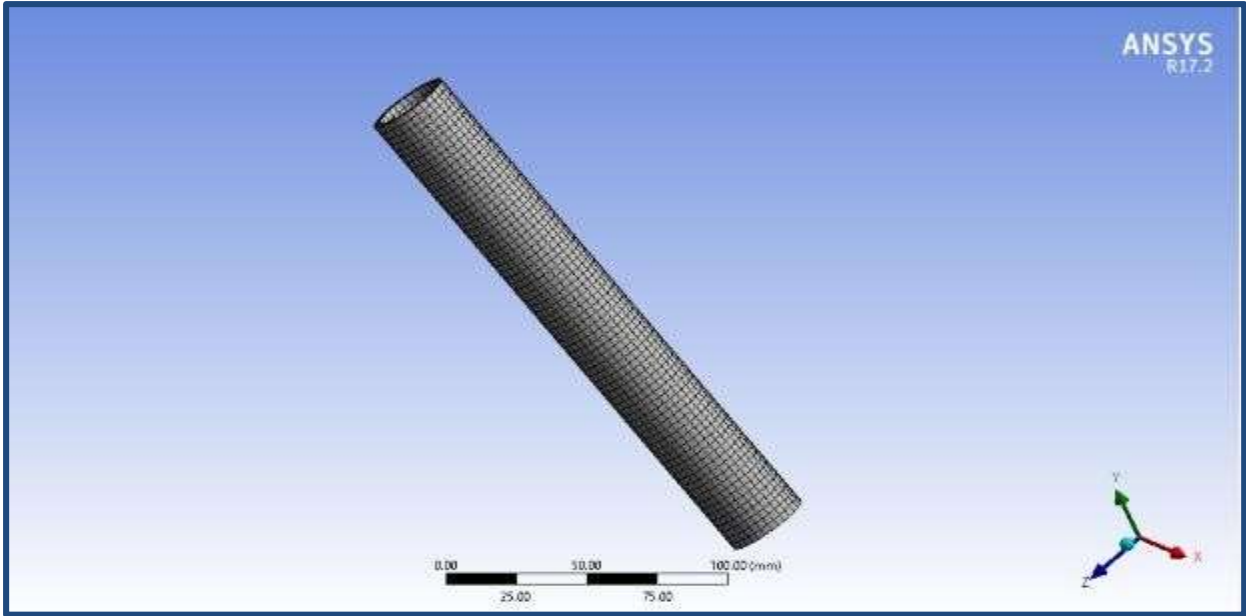


**Figure (3.13)** Meshing the prosthetic pylon.

**3.9.1.3.2 Convergence Test**

A convergence test was conducted to decide whether the final model's uniform mesh size produced correct results and whether mesh refinement or coarser meshes could be used to minimize computation time during research. The total number of mesh elements essential and buckling stress ( $\sigma_{cr}$ ) obtained from the ANSYS are



shown in figure (3.14). It can be seen that when the coarser mesh, the critical buckling stress is unstable. It becomes more stable when the mesh is fine, that means for a pylon, the model that consisting of the number of elements was (750) give adequate precision; where the geometry of the fine mesh of the component provides the correct geometry and, as a result, stable critical buckling stress.

The critical buckling stress is unstable, but it becomes more stable when the mesh is fine. That means the model of a pylon (that consists of 750 elements) has given adequate accuracy. The geometry of the fine mesh of the component provides the correct geometry. As a result, the critical buckling stress becomes more stable.

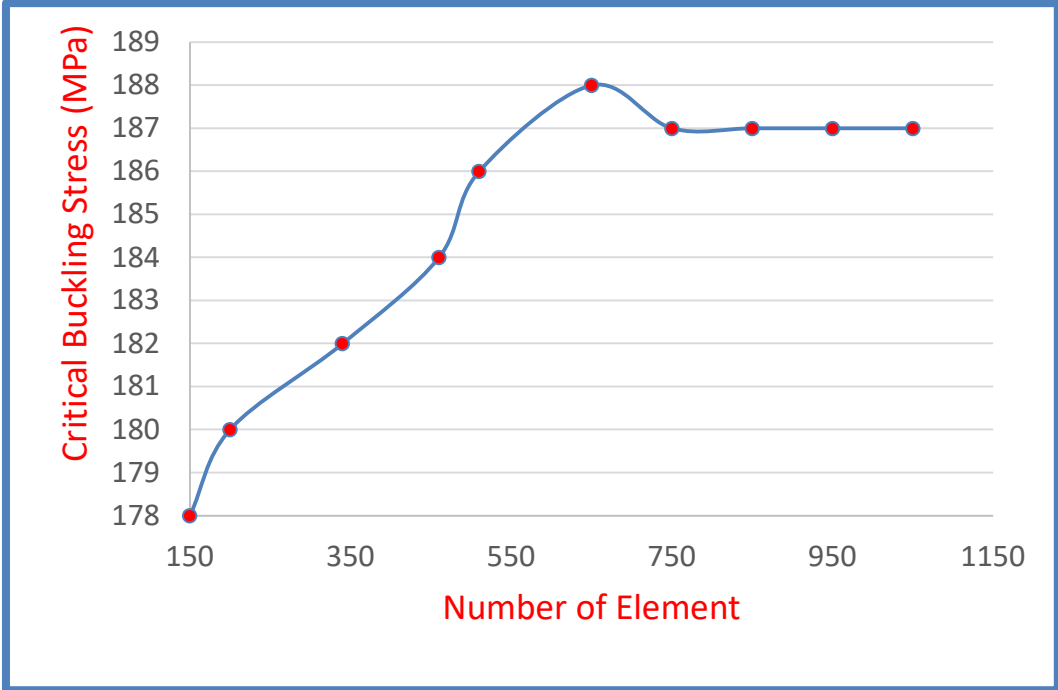


Figure (3.14) The critical buckling stress and number of elements.

**3.9.1.3.3 Boundary Conditions**

This step must show the boundary conditions for two ends of the prosthetic pylon by defining the loads and type of support (it was displacements in this case), as shown in figure (3.15). The conditions of pylon ends will be studied as fixed-pin

[36]. The upper end is fixed at the adapter of the socket, while the lower end is attached to the adapter of the ankle joint.

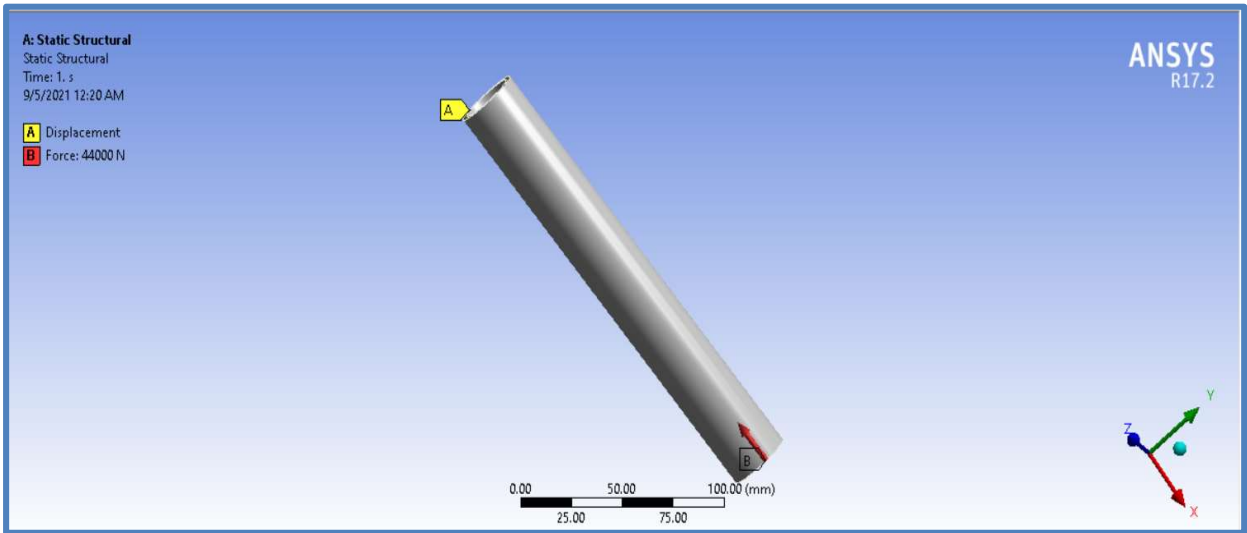


Figure (3.15) Boundary conditions for the prosthetic pylon.

### 3.9.2 The Static Analysis Solution

The effect of steady loading conditions on the composite prosthetic pylon was quantified using static analysis, which neglected the impact of time-varying loads. The form of study (static) should be specified before solving the problem to obtain pre-stress, which is transferred to the buckling analysis solution.

### 3.9.3 Buckling Analysis Solution

Eigenvalue buckling analysis was used to describe the prosthetic pylon in this study and predict the theoretical buckling stress of an ideal elastic structure. This study indicates the "bifurcation point," representing the critical buckling tension before the system collapses. For the specified unit loading and constraints, it calculates the eigenvalues of the prosthetic pylons.

Figures (3.16) and (3.17) show the flow chart of analysis steps by FEM for a static solution and buckling analysis solution, respectively.

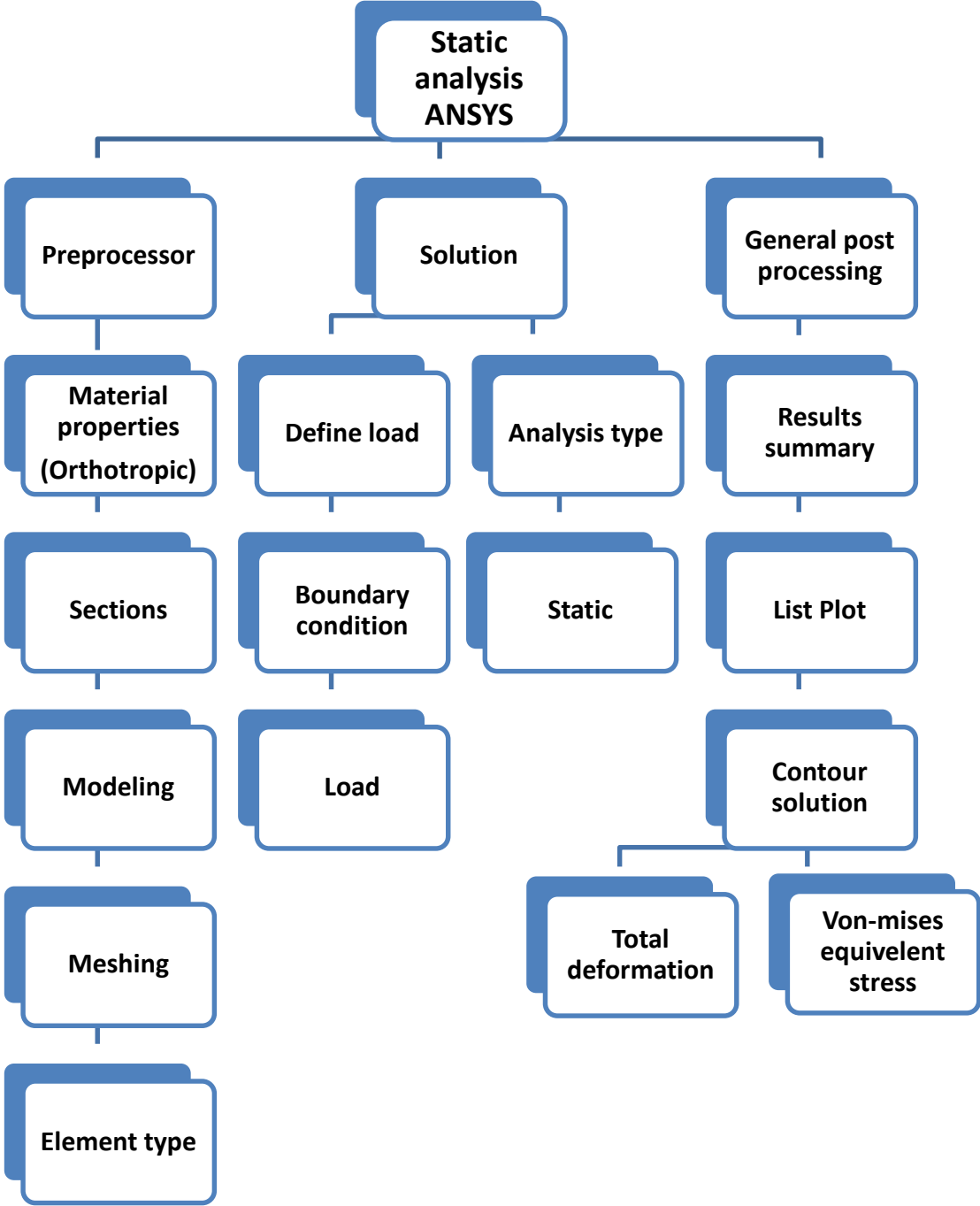


Figure (3.16) Flow chart of static analysis .

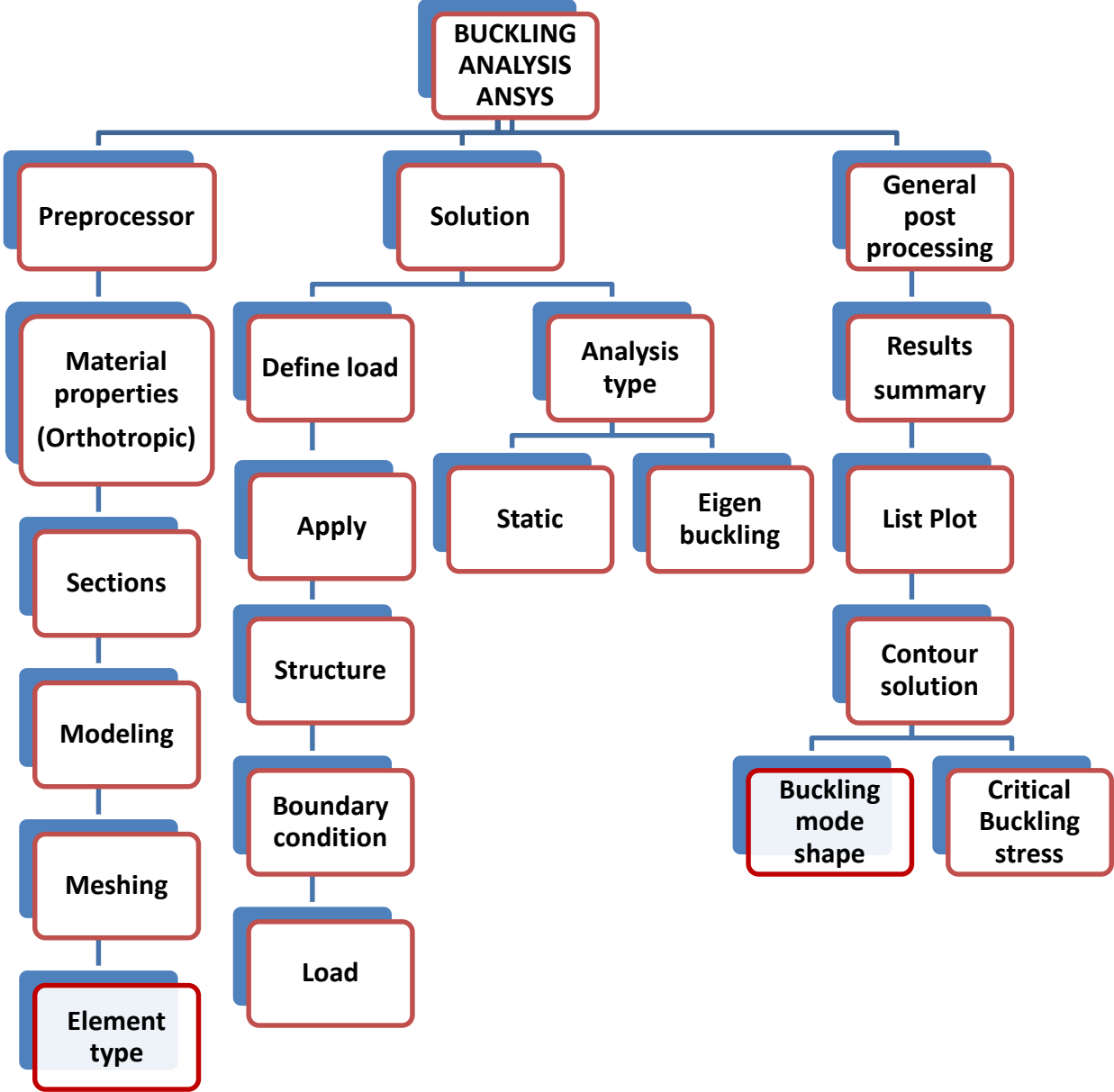


Figure (3.17) Flow chart of buckling analysis .

## **CHAPTER FOUR**

### **EXPERIMENTAL WORK**

#### **4.1 Introduction**

The work in this chapter is divided into two main stages. The first stage focuses on preparing samples, where terms of raw materials, the choice were made of (lamination 617H19) as a matrix and (carbon, glass, and perlon) fibers as reinforcing layers. Also, this stage involves the equipment needed to prepare the samples using the vacuum bagging technique. Then it is done carrying out automated cutting of composite samples under the applicable standards specifications of American Society for Testing and Materials (ASTM) for tensile and bending tests which performed to obtain the mechanical properties of each sample.

The second stage of this chapter explains how to design and manufacture the pylon for the artificial limb according to International Standard Specifications and Dimensions, employing a metal mold made of stainless steel specially manufactured for this purpose. These pylons were manufactured from the samples with the best mechanical properties; after performing the required tests on the produced pylons, it was used in a prosthetic limb for an amputated person below the knee, a walking test passed by the amputee was taken successfully. Figure (4.1) shows the experimental path of this research.

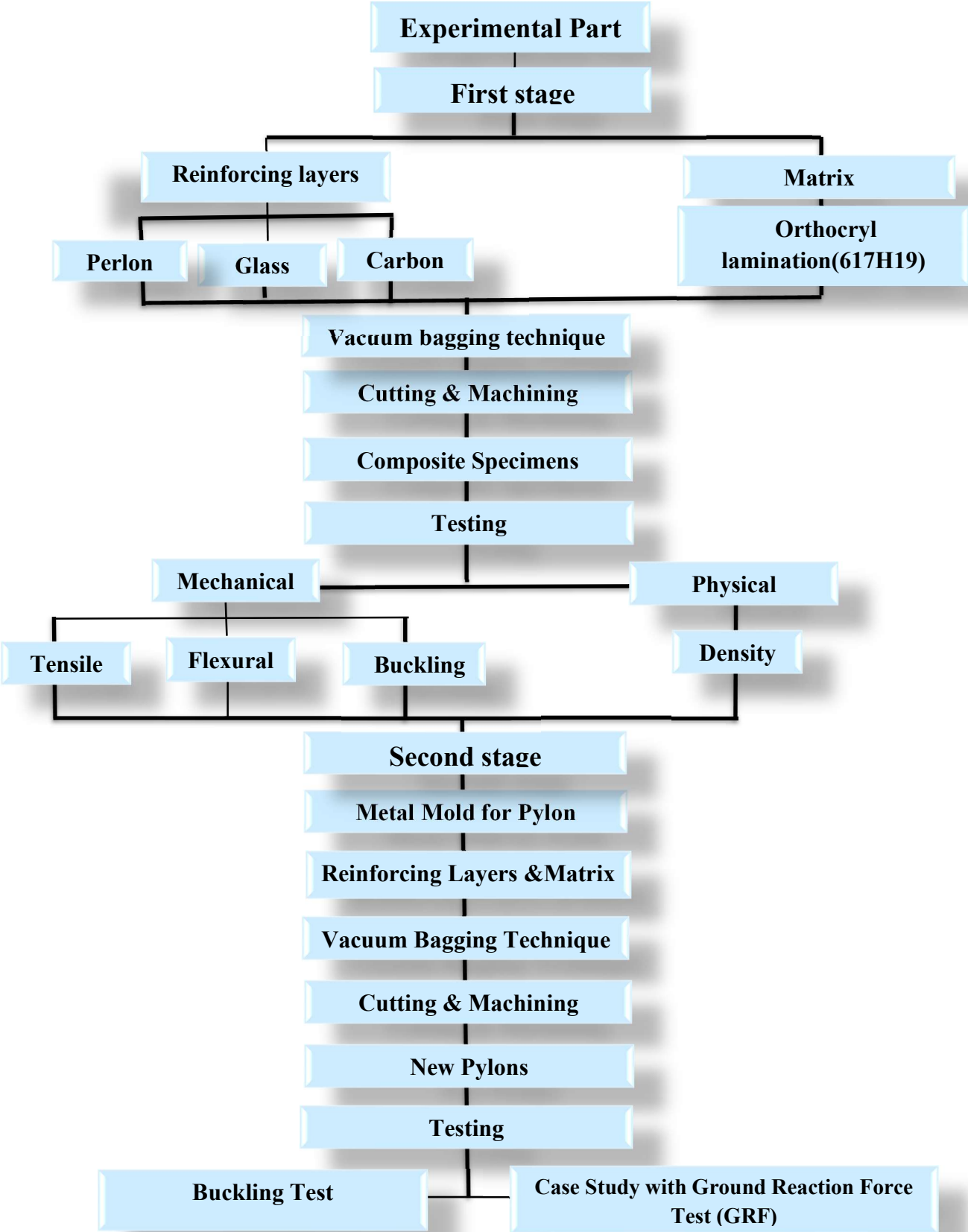


Figure (4.1) Technical path of this study.

## 4.2 Specimens Preparation

Specimens manufacturing and preparation include many stages: choosing the suitable raw materials, mold manufacturing, and completing the machining of models and cutting it, as illustrated in the following paragraphs.

### 4.2.1 Raw Materials

Samples that were made from composite (polymer) materials in this work consisted of (the orthocryl lamination 617H19) as (resin), and (perlon, carbon, and glass) fibers as (reinforcement layers) to produce a composite material with acceptable specifications as detailed in the following points and shown in Table (4.1). The materials that used in the manufacturing of specimens in this thesis are as follows:

1 - Polyvinylalcohol (PVA) bag (otto bock health care 99B71). Two PVA layers were used; the first layer was applied on the outer surface of the gypsum mold to prevent resin adhesion to the mold. The second plie was placed on top of the last layer of the fibers that have been fixed on the mold to achieve vacuum technology and complete the sample molding process successfully. Figure (4.2) shows a PVA bag.

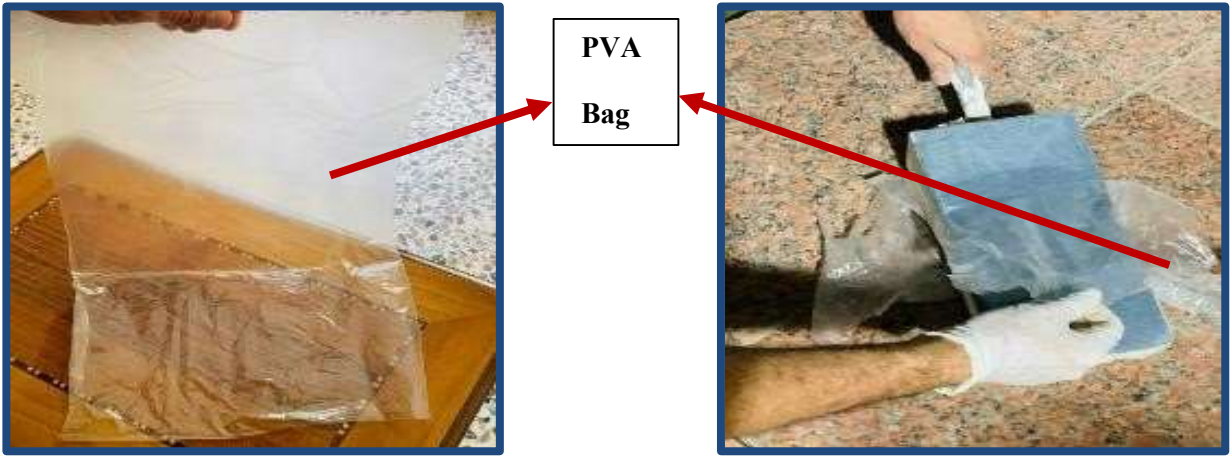


Figure (4.2) Polyvinylalcohol (PVA) bag

2- Perlon stockinet white or (polyamide 6) (otto bock health care 623T3) is distinguished by its high strength and sleek shape, making it ideal for final laminations. It is compatible with a wide range of resins and is simple to saturate. Figure (4.3) shows the perlon fiber, while its mechanical properties are shown in Table (4.1).

**Table (4.1)** Mechanical properties of perlon as obtained from the company

Young's modulus (GPa)	Tensile strength (MPa)	Elongation (100%)	Poisson's Ratio	Density (gm/cm <sup>3</sup> )	State
2.6 - 3	78	1 - 30	0.39	1.13	Knit



**Figure (4.3)** Perlon fiber (polyamide 6) layers.



3- Glass fiber (with orientation (0°/90°) is relative to the applied load on layers in composite specimens) is the most common material used for fiber-reinforced polymer composite, which for over (90 %) of the fiber used in reinforced plastics due to comparatively good and cheap. Figure (4.4) shows the glass fiber's mechanical properties are shown in Table (4.2).

Table (4.2) Mechanical properties of Glass fiber as obtained from the company

Young's modulus (GPa)	Tensile strength (MPa)	Elongation (%)	Poisson's Ratio	Density (gm/cm <sup>3</sup> )	State
72	3450	2.9	0.21	2.58	Woven

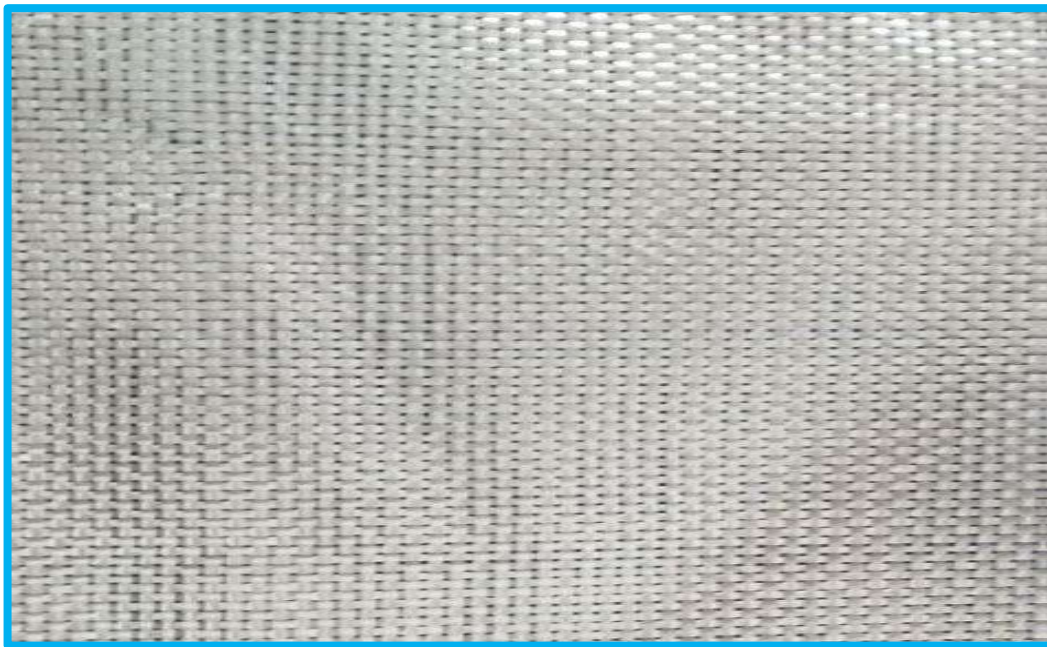
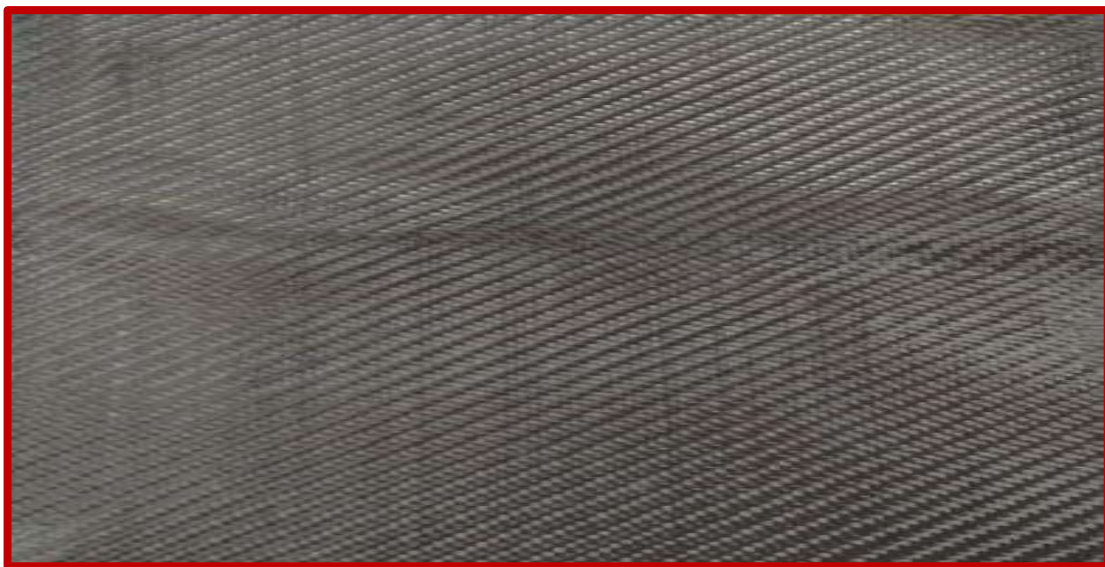


Figure (4.4) Glass fiber.

4- Carbon fiber (otto bock health care 616 G15) with orientation ( $0^{\circ}/90^{\circ}$ ) is relative to the applied load on layers in composite specimens). Carbon fibers are characterized by a high damping ratio, good resistance to acids and moisture, and low density. Also, it is characterized by the highest elastic modulus and strength to weight ratio compared with the other reinforcing fibers even at high temperatures. Carbon fibers are used in the promotion of advanced polymer composites. They are widely used in high-performance applications such as aero planes, rocket casings, space, and sports, in addition to it used in the manufacture of golf clubs, fishing rods, etc. [67]. The mechanical properties are shown in Table (4.3), while figure (4.5) shows the carbon fiber.

**Table (4.3)** Mechanical properties of carbon fiber as obtained from the company

Young's Modulus (GPa)	Tensile strength (MPa)	Elongation (%)	Poisson's Ratio	Density (gm/cm <sup>3</sup> )	State
230	3800 – 4200	0.6 - 2	0.2	1.78	Woven



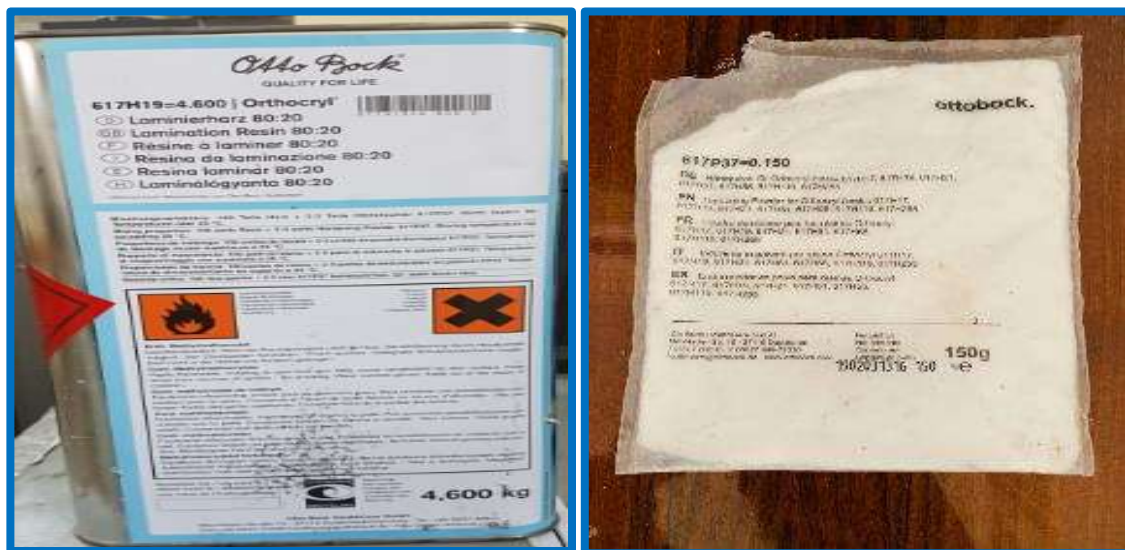
**Figure (4.5)** Carbon fiber.

5- Orthocryl 617H19 Lamination (80:20) resin has a smoother feel than other resins, its thermoplastic properties are good, as it is easy to modify and reshape after being heated. Also, it provides a high strength that allows a thinner, lightweight, delicate surfacing lamination, and low viscosity options led to increased penetration do not cause sensitivity to the skin. It is used in prosthetic centers. Where it enters in the manufacture of the socket of the lower limb, for this, it was chosen in the current study. Figure (4.6-a) shows the orthocryl (617H19) (80:20) lamination, while its mechanical properties are shown in Table (4.4).

**Table (4.4)** Mechanical properties of orthocryl lamination as obtained from the company

Young's Modulus (GPa)	Tensile strength (MPa)	Elongation (%)	Poisson's Ratio	Density (gm/cm <sup>3</sup> )	State
2.15 - 3.54	54.6	2.8	0.34	1.04	Liquid (resin)

6 - Hardening powder (otto bock health care) is added to the resin with a percentage (80:20) at room temperature to prepare the matrix. Figure (4.6-b) shows the hardening powder.



(a) Orthocryl lamination (617H19)

(b) Hardening powder

**Figure (4.6)** Lamination 617H19 and hardener.

### 4.2.2 The Used Equipment

1- A parallel-surface gypsum mold is manufactured, where it is poured into a glass mold whose dimensions are  $(30 * 20 * 5) \text{ (cm)}^3$ , as shown in figure (4.7). The edges must be adjusted and smoothed with a particular file and softened paper. The outer surface of the gypsum mold must be downy because it represents the inner surface of the samples. Two smooth thin panels of composite materials with dimensions  $(30 \text{ cm} * 20 \text{ cm})$  will be obtained, and thickness based on the volume fraction of each sample.

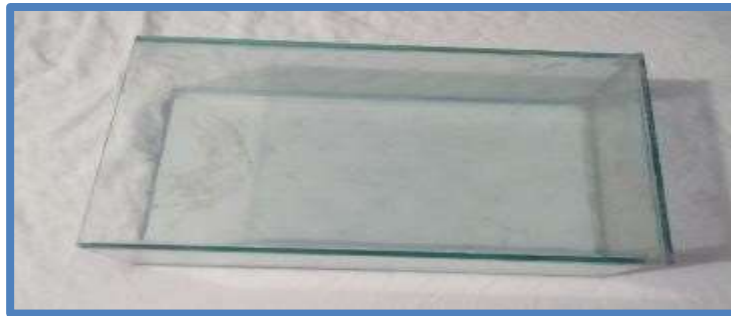


**Figure (4.7)** Glass mold used in this study.

2- Vacuum forming system including a vacuum pump reach to (5MPa) and different tubes, as shown in figure (4.8).



**(a) Vacuum Machine**



**(b) Vacuum processing**

**Figure (4.8)** Vacuum system.

3- Electronic sensitive balance for measuring the weight of fibers, hardener, resin, and specimens as shown in figure (4.9).



**Figure (4.9)** Electronic sensitive.

4- Digital vernier for measuring the inner and outer diameter of the pylon and thickness of specimens, as shown in figure (4.10).



**Figure (4.10)** Digital vernier.

5- Universal instrument test machines (available in the Materials Engineering Department /University of Technology laboratories) for tensile, flexural, and buckling tests. Table (4.5) shows the materials and the number of layers of fibers used to manufacture the eight proposed samples to manufacture the prosthetic pylon.

**Table (4.5)** Type of the composite specimens in this study

Sample name	Type of material	Fiber stockinet layers	Total No. of layers
Sample 1 (S1)	Lamination 617H19 + Glass layers at (0°/90°) + Perlon layers	(2 perlon+ 1 glass fiber + 2 perlon)	5
Sample 2 (S2)		(2 perlon+ 2 glass fiber + 2 perlon)	6
Sample 3 (S3)		(2 perlon+ 3 glass fiber + 2 perlon)	7
Sample 4 (S4)	Lamination 617H19 + Carbon layers at (0°/90°) + Perlon layers	(2 perlon+ 1 carbon fiber + 2 perlon)	5
Sample 5 (S5)		(2 perlon+ 2 carbon fiber + 2 perlon)	6
Sample 6 (S6)		(2 perlon+ 3 carbon fiber + 2 perlon)	7
Sample 7 (S7)	Lamination 617H19+ Carbon layers at (0°/90°) + Glass layers at (0°/90°) + Perlon layers	(2 perlon+ 1 glass fiber+1 carbon fiber + 1 glass fiber + 2 perlon)	7
Sample 8 (S8)		(2 perlon +1 carbon fiber 1 glass fiber + 1 carbon fiber + 2 perlon)	7

### 4.2.3 Preparation of Composite Specimens

The following steps explain the sample fabrication procedure:

1- First, the gypsum mold is installed in the stand, then preparing it, where the gypsum mold edges are smoothed by sanding paper to be ready for applying the inner PVA layer, where this layer is placed on the gypsum mold directly. Then, it is connected to the vacuum system through a tube installed with a hole inside a pipe. Subsequently, the PVA ends are closed, and the vacuum system is operating to allow the trapped air between the gypsum mold and the PVA to escape through a hole was made near the lower end of the mold. The advantage of this stage is showing the samples without bubbles and the ease of separating the samples from the gypsum mold. Figure (4.11) shows these stages.

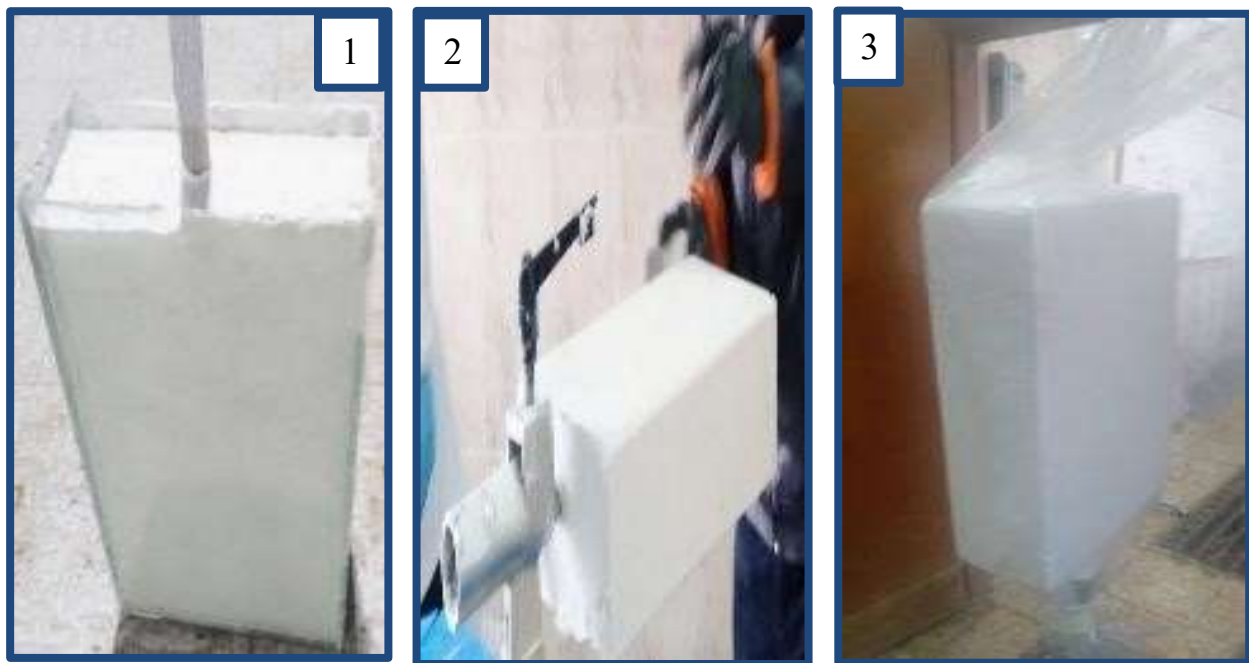


**Figure (4.11)** The stage of casting, adjusting, and smoothing the gypsum mold.

2- The masses of the perlon, carbon, and glass fibers are measured according to each sample's dimensions and volume fraction. The type and number of these fibers were fixed for each sample, as shown in Table (4.5). Figure (4.12) illustrates this step.



**Figure (4.12)** The stage of measuring the fiber mass & its installation on the gypsum template .



3 - The second (outer) PVA layer is placed to cover all fiber layers that have been installed. The upper end of this PVA layer is opened to add the resin through it, as shown in figure (4.13).

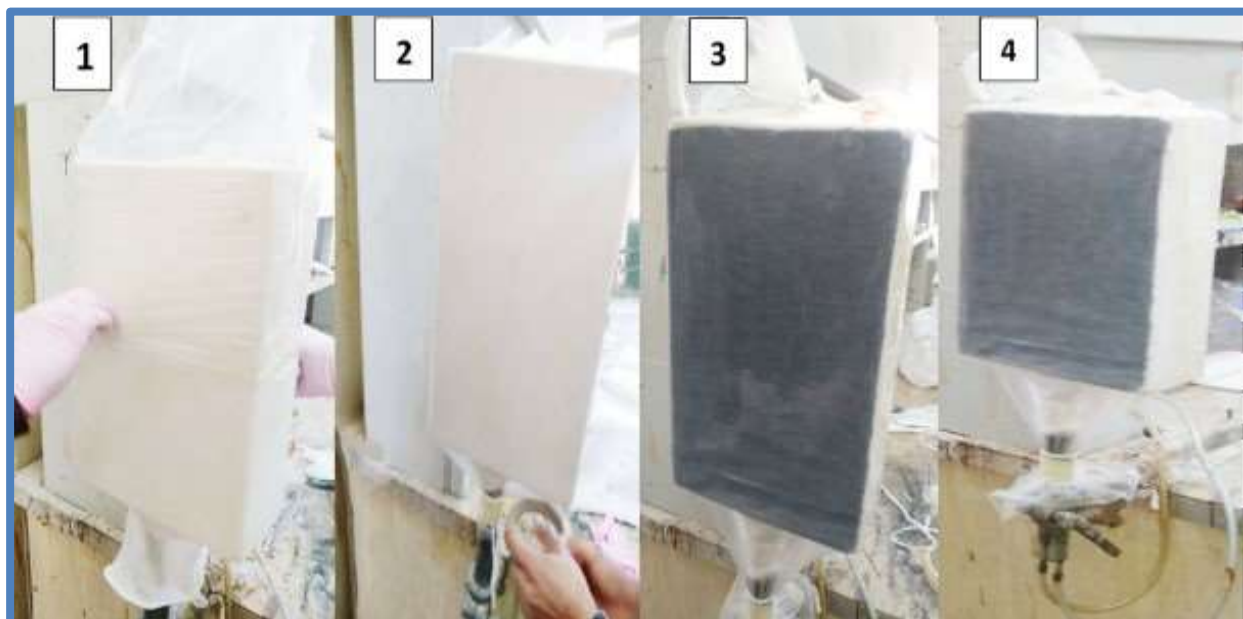


**Figure (4.13)** A second (external) PVA is applied to cover all fiber.

4 – The resin required amount must be known according to each sample's volume fraction and dimensions before adding it. Then the hardener is added to the resin in a ratio of (80: 20) slowly with continuous stirring for about ten minutes to make the resin homogeneous. The high temperature of the resin will be observed, which is evidence for the onset of the reaction.

5- The resin is added to the mold and distributed correctly to all the mold ends with the continued vacuum processing for about an hour. The temperature rises and the resin becomes solid; then the vacuum device is stopped. Now, the samples can be separated from the gypsum mold by a cutting machine. Figure (4.14) illustrates the steps (4 and 5).



**Figure (4.14)** Adding the resin to the mold& separated samples from the gypsum mold.

6 -The edges of the samples are modified by the Belt Grinding Machine (located in the Babylon Center for Prosthetics), as illustrated in figure (4.15), to make them ready for cutting by CNC machines as shown in figure (4.16), where It cut according to the orientation of fiber and the standard dimensions of each test.



**Figure (4.15) Belt Grinding Machine.**



**Figure (4.16) CNC Machine.**

## 4.3 Tests Conducted in This Research

### 4.3.1 Tensile Test

The tensile test was carried out in the laboratories of the Materials Engineering Department at the University of Technology. The (LARYEE) type test machine was used, as shown in figure (4.17). This test is performed at room temperature on samples which is cut according to the American Society for Testing and Materials (ASTM) (D-638 standards) as shown in figure (4.18) [56]. The velocity of the test machine was about (1mm/min), and the capacity load reached (50 KN). The tensile test provides the mechanical properties of the samples produced (percentage elongation at break, Young's modulus, and tensile stress) through the stress-strain curve as shown in figure (4.19). The specimens before and after the tensile test are shown in figure (4.20). Three samples were tested for each model and took the average of the results.

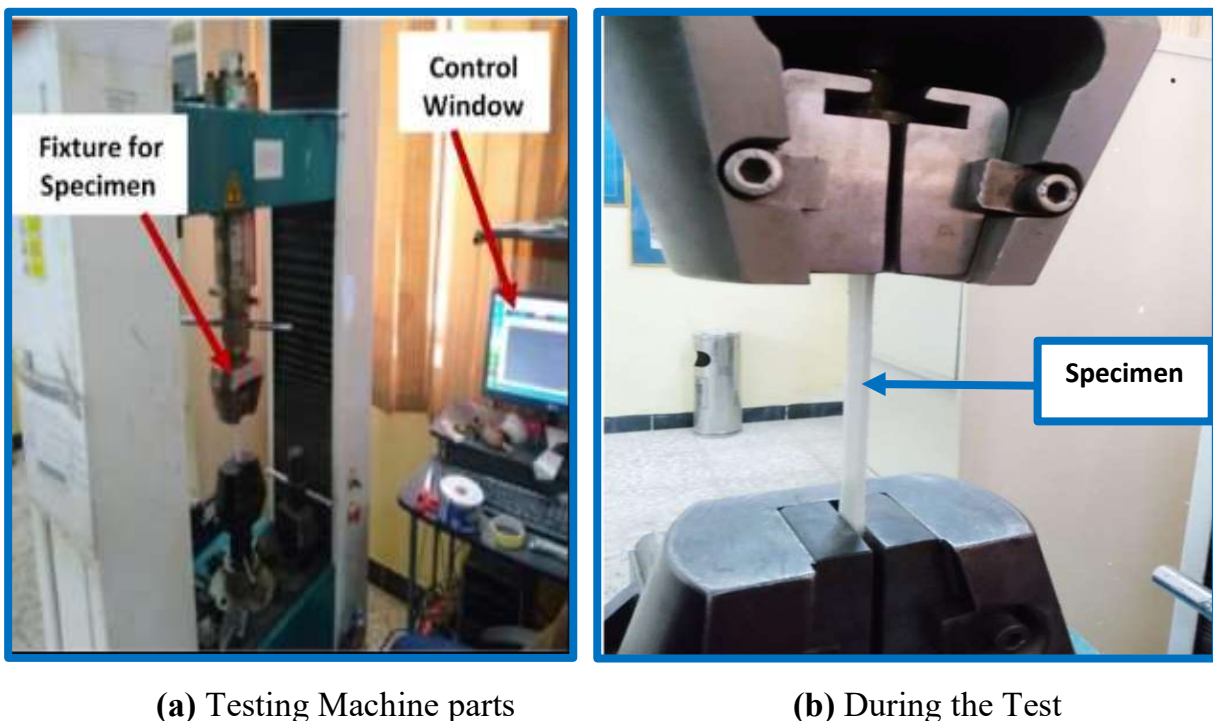


**Figure (4.17)** Tensile testing machine.

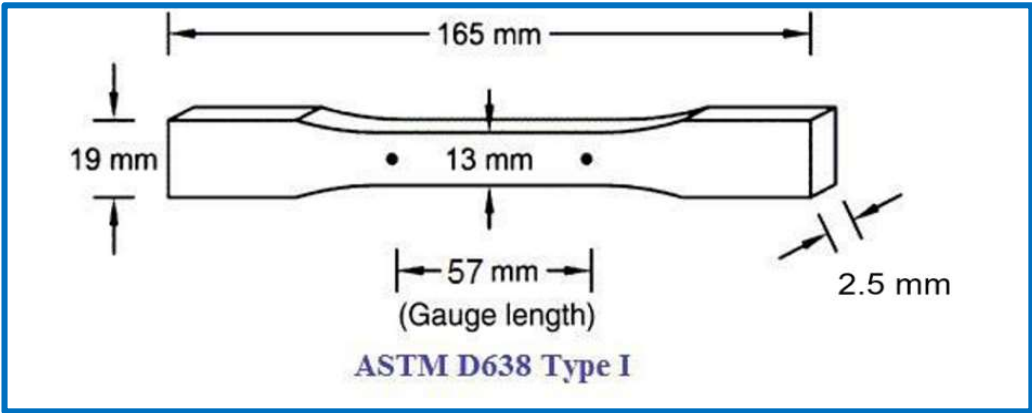


Figure (4.18) The dimensions of the standard specimen for the tensile test [56].

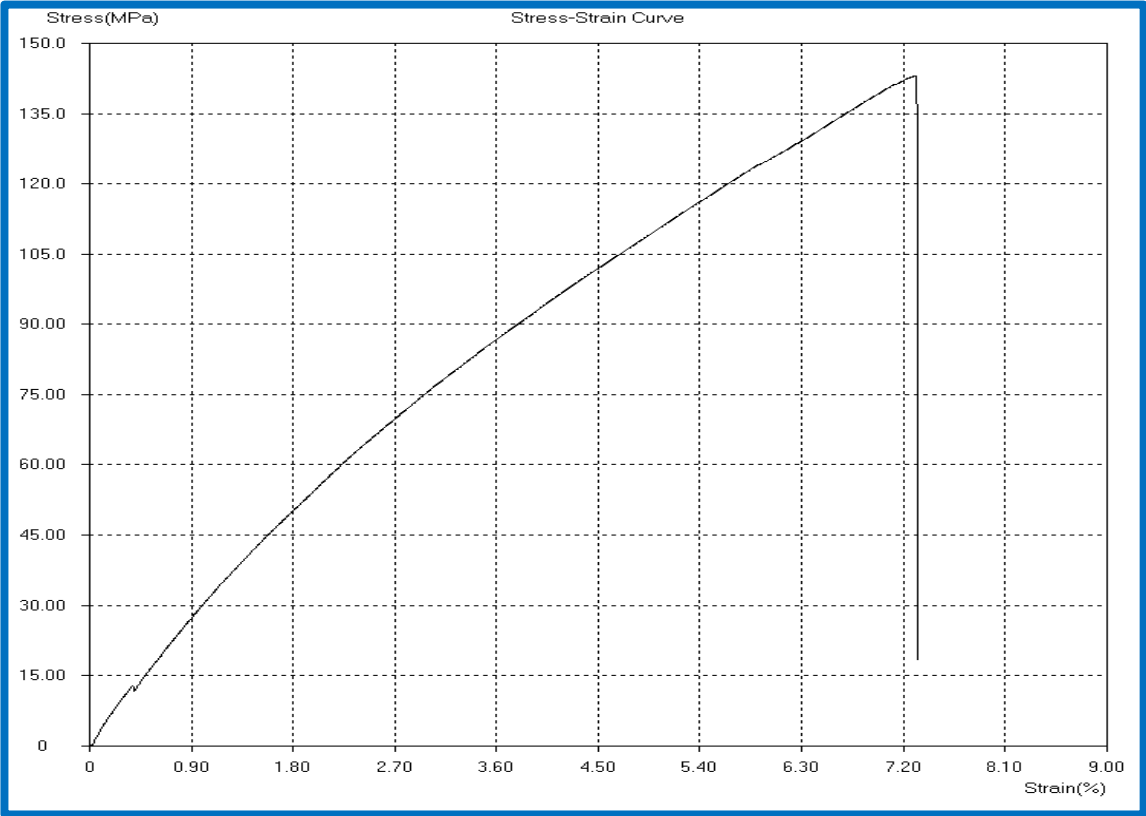
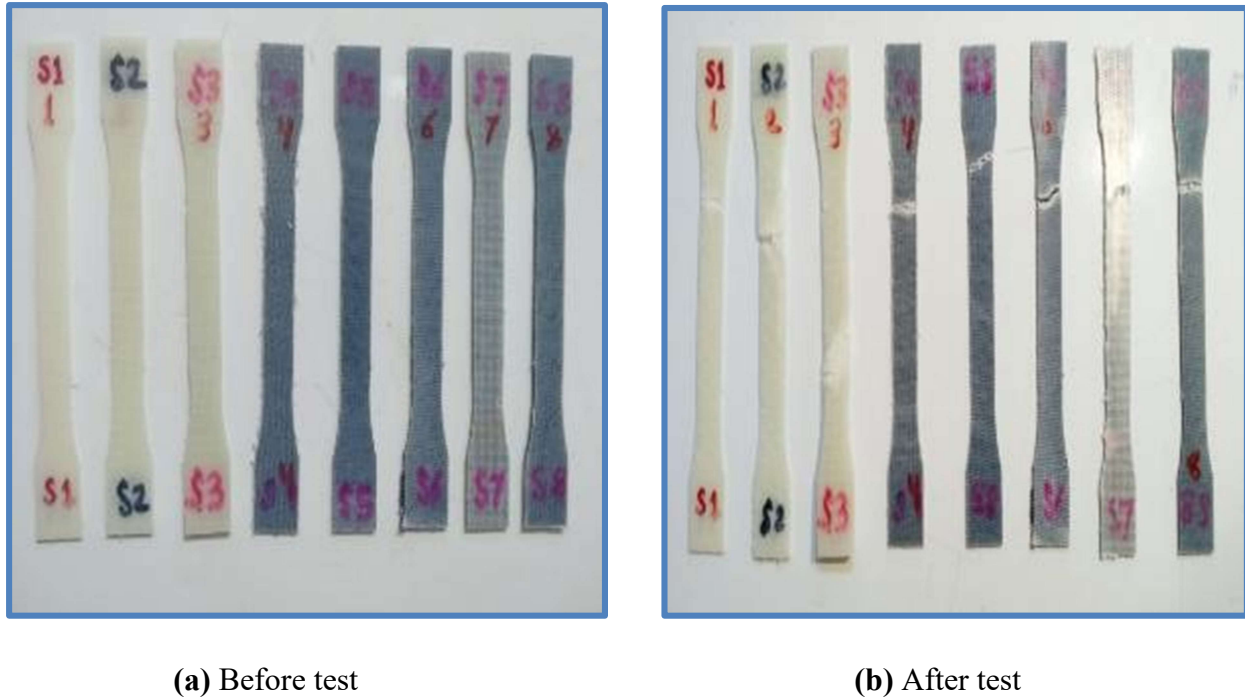


Figure (4.19) Stress-Strain Curve for the sample (3) with three Glass fiber layers.



(a) Before test

(b) After test

**Figure (4.20)** Specimens for tensile test

### 4.3.2 Flexural Test

The load-deflection curve can be obtained in this test for each sample (which average thickness is around 2.5mm) was cut according to (ASTM-D790) [58], as shown in figure (4.21).

This test was performed in the laboratories of the Materials Engineering Department at the University of Technology by a universal test machine with the three-point bending test head flexural test shown in figure (4.22). The samples were supported on two cylindrical bars (100 mm). The vertical applied load was increased gradually with velocity (1.25 mm/min) to feed this head, which pressurizes the center of samples until it failed (the outer fibers of the sample were torn apart). Figure (4.23) shows the samples before and after the bending test, and the average results of the bending modulus and bending strength were taken for two samples tested for each model.

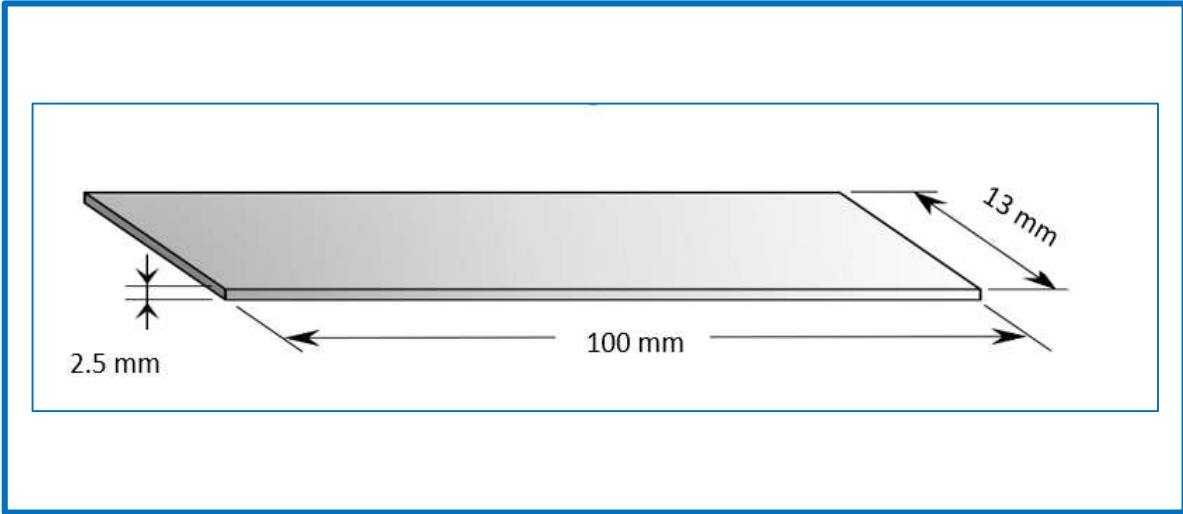


Figure (4.21) The dimension of the standard specimen for the flexural test

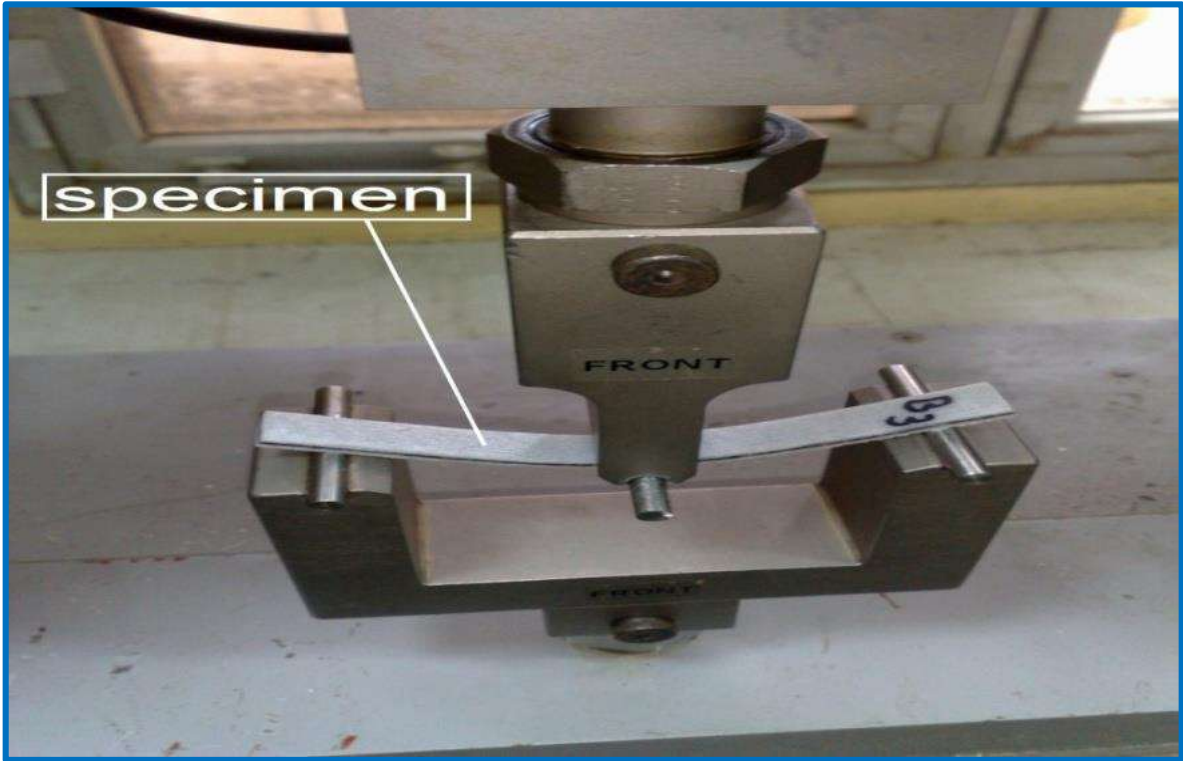
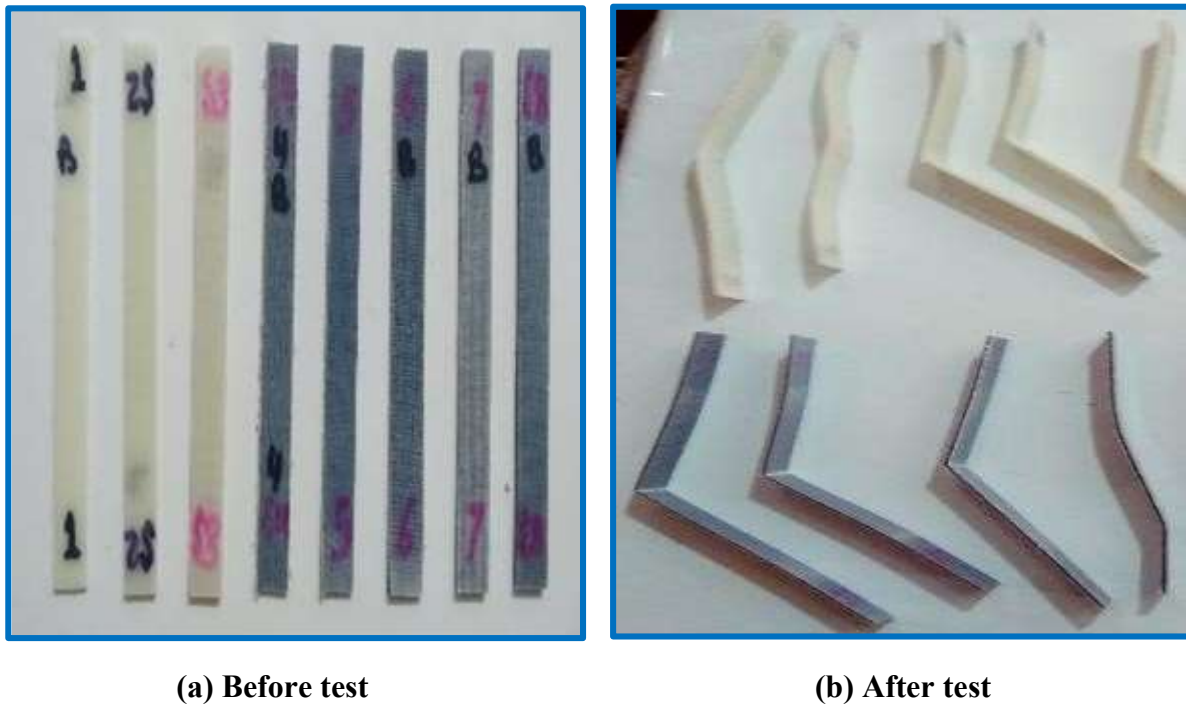


Figure (4.22) Three-point flexural test machine.



**Figure (4. 23)** Specimens of the bending test.

### 4.3.3 Buckling Test

It is the third test that was conducted in this work. This test is used to investigate the critical load at which the buckling occurs by drawing the deflection-load curve. In this test, the volume fraction of the fibers, the aspect ratio, and the effect on the critical buckling load will be studied. The samples were examined with width and thickness are (20 mm) and (2.5 mm) respectively, as shown in Table (4.6).

**Table (4.6)** Specimens specifications prepared for buckling test

No. of sample	Angle of fiber	The volume fraction of fiber100%	Length (mm)	Aspect ratio L/T %	No. of layers
S1	(0°/90°)	25	175	70	5
			200	80	



			225	90	
<b>S2</b>	(0°/90°)	28.4	175	70	5
			200	80	
			225	90	
<b>S3</b>	(0°/90°)	32	175	70	6
			200	80	
			225	90	
<b>S4</b>	(0°/90°)	22.7	175	70	6
			200	80	
			25	90	
<b>S5</b>	(0°/90°)	26.2	175	70	7
			200	80	
			225	90	
<b>S6</b>	(0°/90°)	28.4	175	70	7
			200	80	
			225	90	
<b>S7</b>	(0°/90°)	30.7	175	70	7
			200	80	
			225	90	
<b>S8</b>	(0°/90°)	29.5	175	70	7
			200	80	
			225	90	

The sample (the column is a suggested composite material for making pylon) was fixed by special jaws in the tensile test machine, loaded in axial compression shown in figure (4.24). The two short edges of the sample (the top and bottom

edges) were fixed in the jaws. In comparison, the other two edges remain free, and to measure the deflection, the dial gauge type (MITUTOYO) is fixed at the middle of the sample and in contact with it. By moving the lower part of the testing machine upwards by a hydraulic cylinder, with the upper head of the test machine remaining stationary, the sample begins to deflect. The deflection load curve is drawn, where the greater the applied load, the greater the deflection until it reaches the critical buckling load. It begins to decrease and then begins to increase again with the increase of the deflection until the sample fails. Figure (4.25) shows the samples before and after the test.

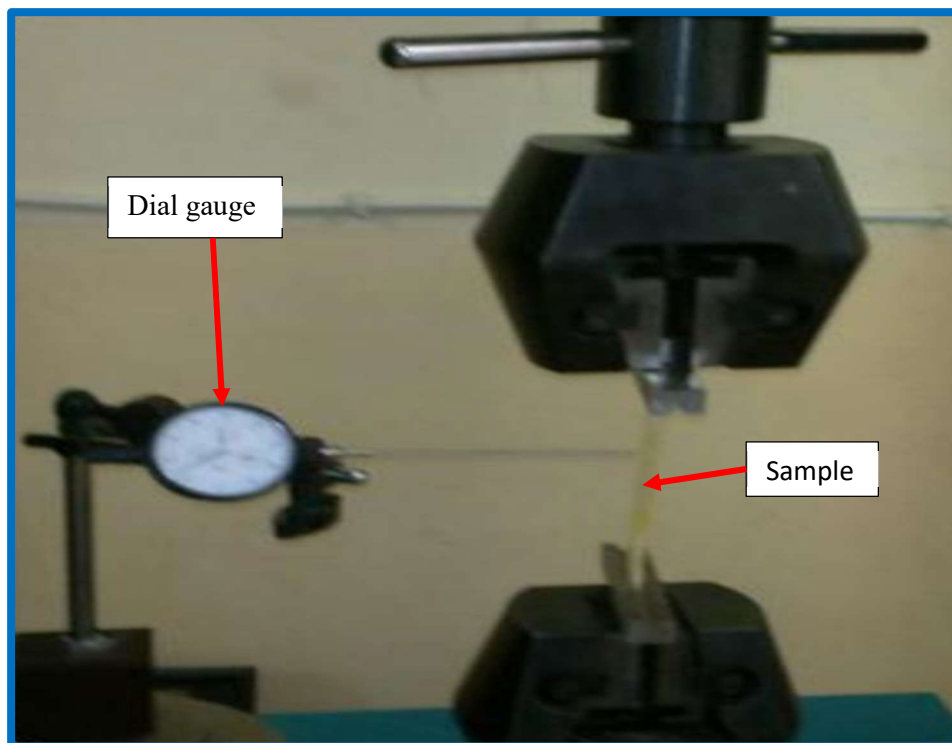
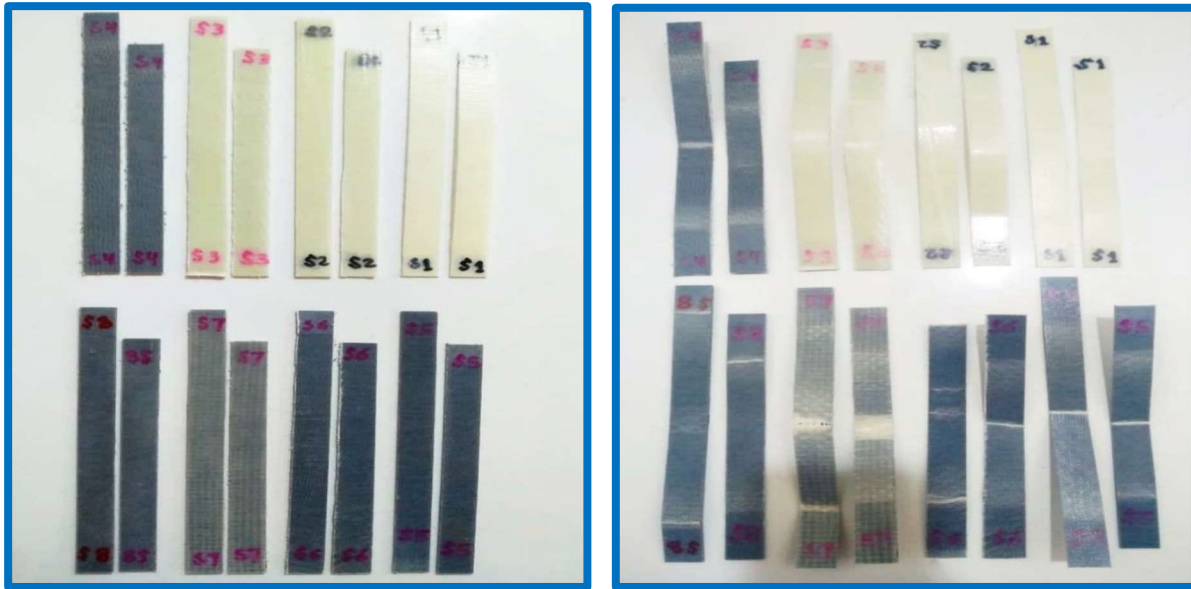


**Figure (4.24)** The sample during the buckling test.



(a) Before test

(b) After test

**Figure (4. 25)** Specimens of the buckling test.

#### 4.3.4 Density Test

The density of suggested composite specimens affords innuendo to know the pylon lighter weight. Also, it was included in the calculation stiffness to weight ratio in the current study. This test was carried out in the laboratories of the Ministry of Science and Technology, Department of Materials. The samples were cut according to ASTM (D-792) standard [68]. Density measuring device consists of a balance, a closed room, suspended (to suspend the sample), and a container filled with a certain liquid whose density is known, like water, for example, as shown in figure (4.26). The density calculation process is carried out according to Archimedes' rule by measuring the mass of the sample in the air and measuring its mass is in the water (which is completely submerged), according to the following law:

$$\frac{\text{Density of sample}}{\text{Density of water}} = \frac{\text{Mass of the sample in the air (m}_1\text{)}}{\text{Mass of the sample in water(m}_2\text{)}}$$



**Figure (4.26)** Measuring of the density of samples.

## 4.4 Pylon Manufacturing

### 4.4.1 Equipment

- 1- The body of the mold, firstly, designing the pylon mold according to the internationally applicable standard dimensions and manufacturing it from stainless steel. This mold consists of two symmetrical halves, as shown in figure (4.27 a).
- 2- A cylindrical rod made of stainless steel to install the fiber layers on it, as well as to give the inner shape of the produced pylon, as shown in figure (4.27 a).
- 3-Two valves were used to enter the matrix and remove air by the vacuum process, as shown in figure (4.27 b).
- 4- Vacuum system including a vacuum pump reach to (5MPa) and different tubes, stance, as shown in figure (4.27 c).

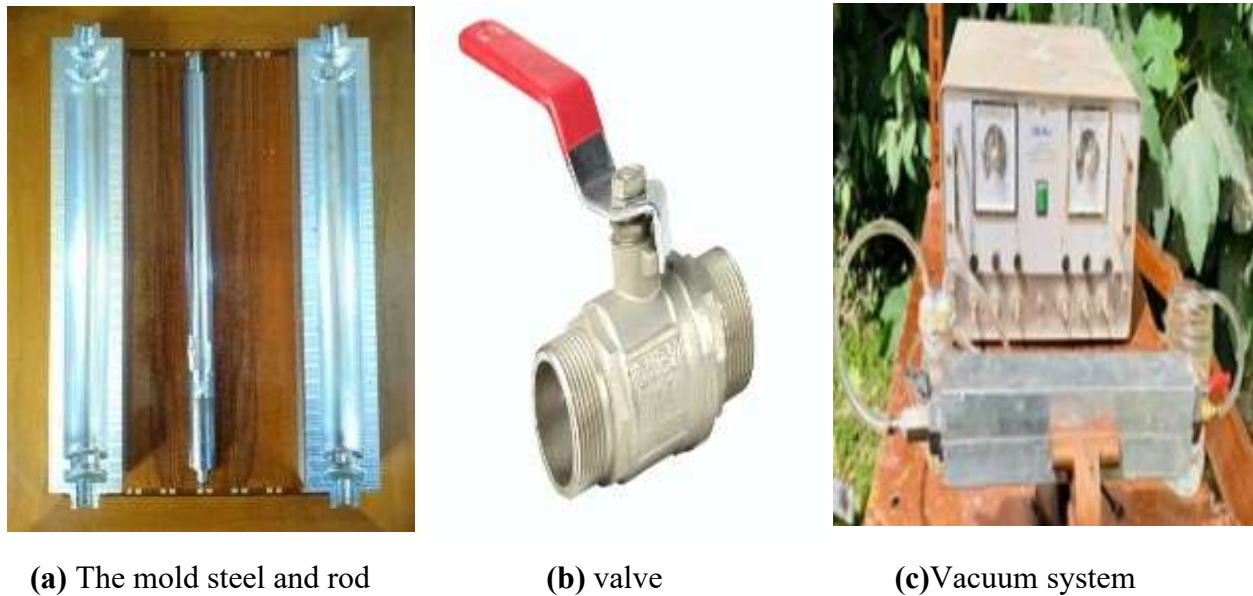


**Figure (4.27)** Equipment is used in pylon manufacturing.

#### 4.4.2 Procedure of Pylon Manufacturing

Two types of pylons were manufactured with dimensions, as shown in figure (4.28). The first pylon (pylon I) was made of the sixth sample, consisting of (2 perlon and 3 carbon fibers and 2 perlon) layers. The other pylon (pylon II) was made of the third sample with (2 perlon and 3 glass fibers and 2 perlon) layers, as shown in Table (4.2).

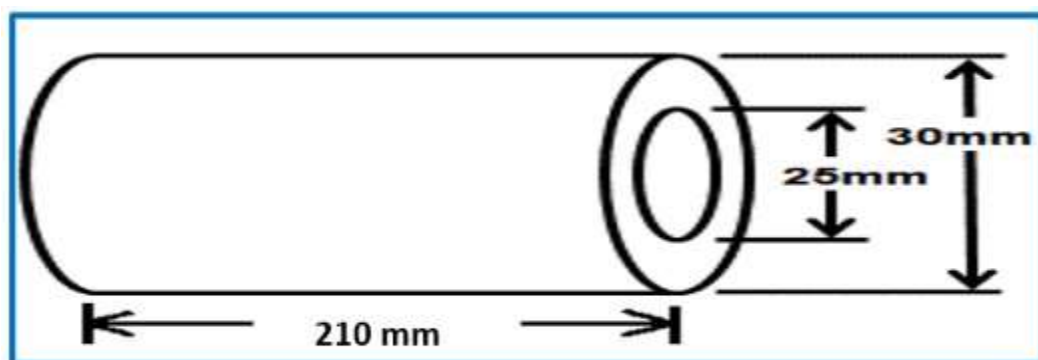


**Figure (4.28)** A sketch of the prosthetic pylon.

The pylon manufacturing process is explained in the following steps:

- 1-Covering the cylindrical rod made of stainless steel by PVA (polyvinyl acetate)
- 2- Install two layers of the perlon fiber.
- 3- Install three layers of the carbon fiber when manufacturing the (pylon(I) or three layers of the glass fiber when manufacturing the pylon (II).
- 4-Two layers of the perlon were installed again.
- 5- Covering the cylindrical rod (with all layers which arrangement on it) with the second layer of PVA (polyvinyl acetate)
- 6- Putting the stainless -steel rod on which the fiber is fixed in the metal mold made of stainless steel and closing the mold tightly.
- 7- Installing valves on both ends of the mold. The first one was connected to the vessel in which the resin is placed (which the harder is added to the resin in a ratio of (80:20)). The other valve is connected to the vacuum device through transparent tubes.
- 8- After operating the vacuum device, the air from inside the mold will be drawn, and the resin will be inserted into the mold. The vacuum device will continue operating for about an hour.
- 9-The mold is opened, then the resulting pylon is separated from the metal rod.

Figures. (4.29-4.31) illustrates the steps for manufacturing the two pylons.



Figure (4.29) Arranging( PVA),perlon, and (carbon or glass) fibers for the new pylons.



**Figure (4.30)** Stages of casting pylons with vacuum technique.





Figure (4.31) Separating the pylons produced from the metal mold and cutting it.

### 4.5 The Pylons Buckling Test

The manufactured pylons made of composite materials were tested in the buckling test with the same procedure the samples were tested. This test is used to know the critical load at which the buckling occurs by drawing the curve of the maximum deflection - critical buckling load. Also, the currently used metallic pylon made of stainless steel was tested for comparison. Figure (4.32) shows the pylons during the test, and figure (4.33) shows the pylons before and after the buckling test. Two pylons were tested for each model.

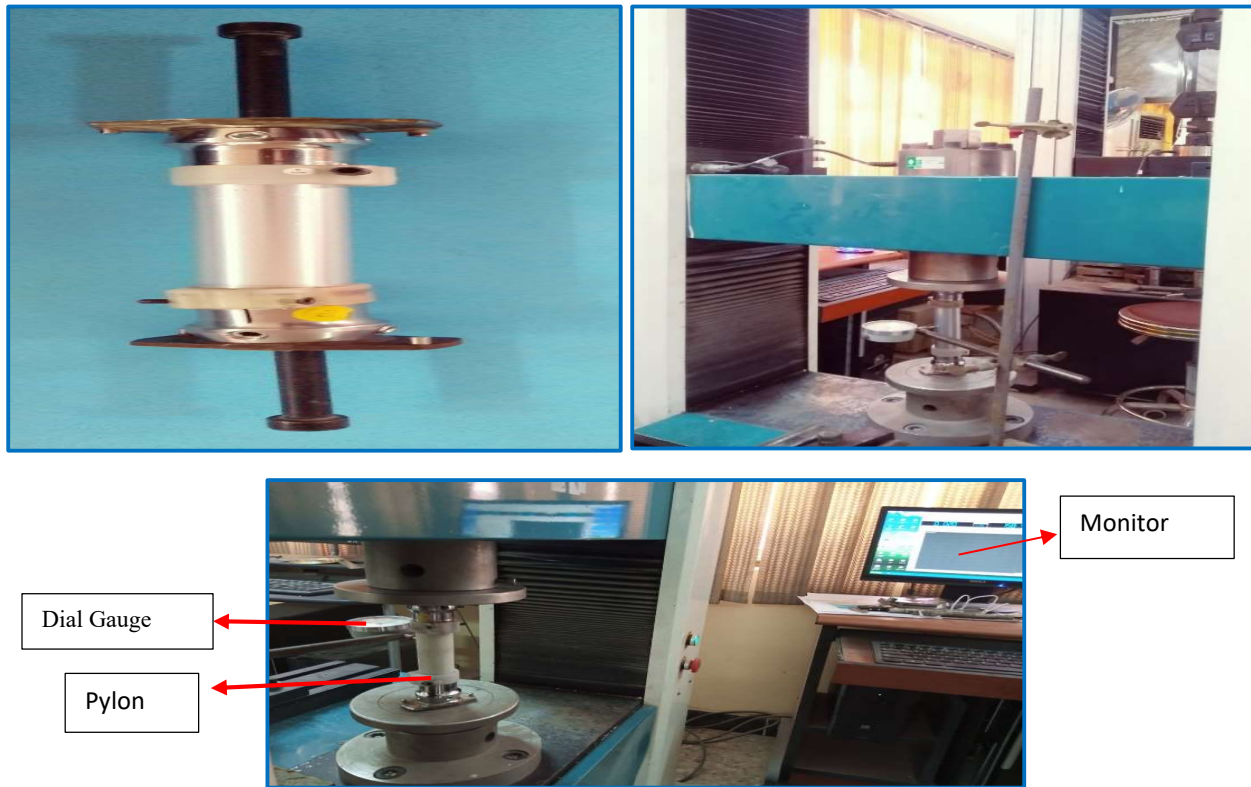
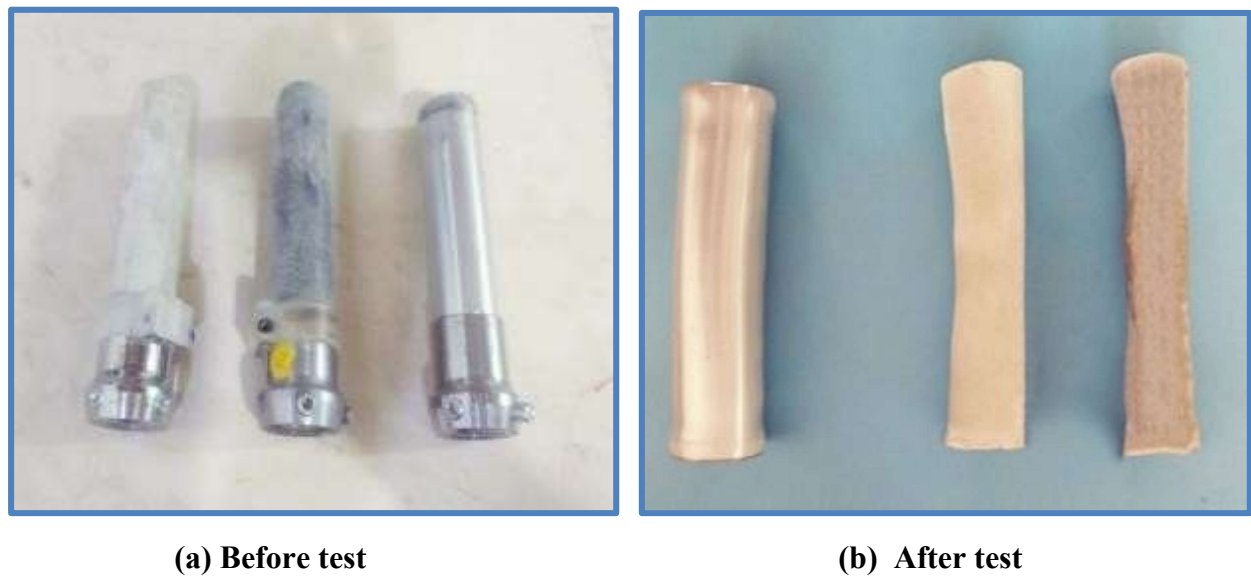


Figure (4.32) Pylons during the buckling test.



(a) Before test

(b) After test

Figure (4.33) The pylons before and after the buckling test.

#### 4.6 The New Pylons in the Lower Limb for an Amputee (Case Study)

To verify the durability of the manufactured pylons proposed in the current study and compare them with the metallic pylons used in terms of strength, weight, flexibility, and user comfort. A case study was considered, where one of the patients at Babylon Center for Artificial Limbs was chosen for this purpose. The patient had an (80 kg) mass and has a height (1.7 m) and (55) years old. His left leg was amputated below the knee, as shown in figure (4.34), due to complications from diabetes. After completing the pylon manufacturing process, the machining processes were performed on them and cut to suit the condition of an amputated person below the knee. Figures (4.35 and 4.36) show the stages of installing the new pylon(I) and pylon (II) in the prosthesis lower limb for the amputated person, respectively.

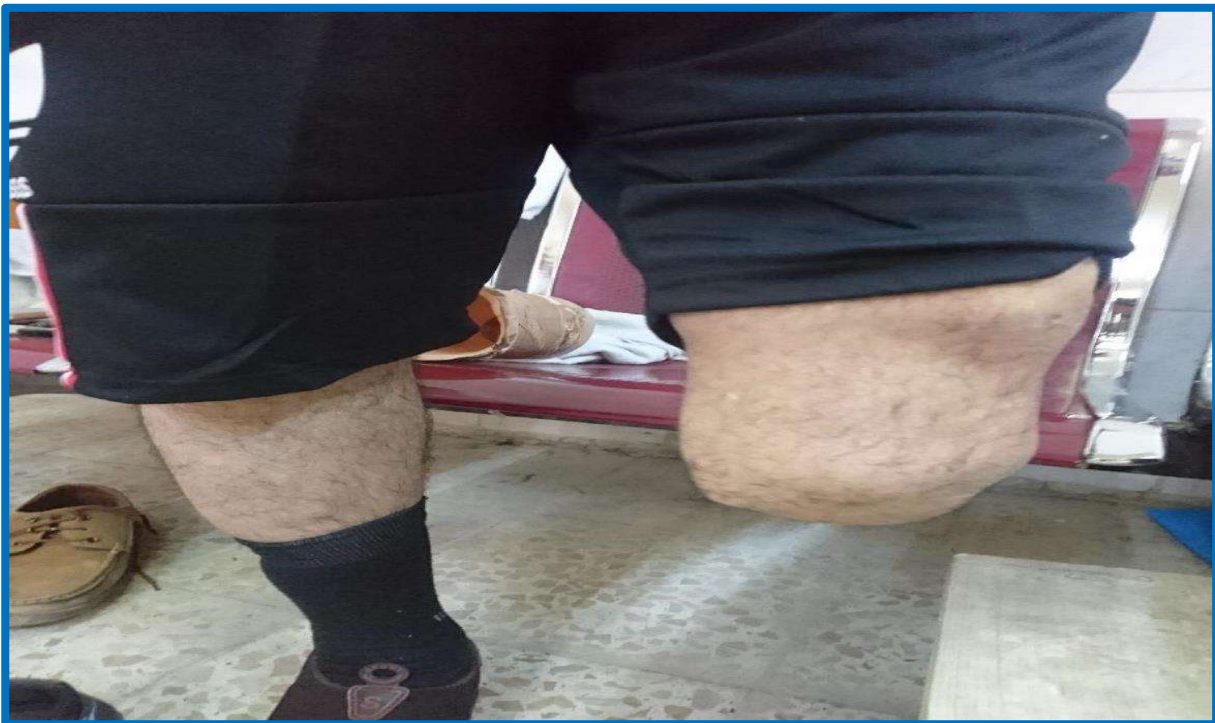


**Figure (4.34)** Trans Tibial amputation BK for the patient had (80 kg and 55 years old).



Figure (4.35) Stages of installing the new pylon(I) in prosthesis for the amputated person.



**Figure (4.36)** Stages of installing the new pylon(II) in prosthesis for the amputated person.

## 4.7 Biomechanical Test

### (Ground Reaction Force Test (GRF) and Measurements of Gait Cycle)

The primary force acting on the human body in vertical direction components is the ground reaction force during walking. To measure this force generated when the amputee person is walking with the new suggested pylons, the ground reaction force GRF test was conducted in the Faculty of Physical Education laboratories at the University of Kerbala, the (Zebris) type test machine was used, which contain of a force plate and monitor shown in figure (4.37). A force plate is a device put on the ground to analyze the gait cycle and provides data about it, such as (gait velocity, step length, number of strikes, step velocity, cadence, etc.). It is also used for measuring the forces imposed on it. A monitor connected to the force plate shows all the data related to the gait cycle.

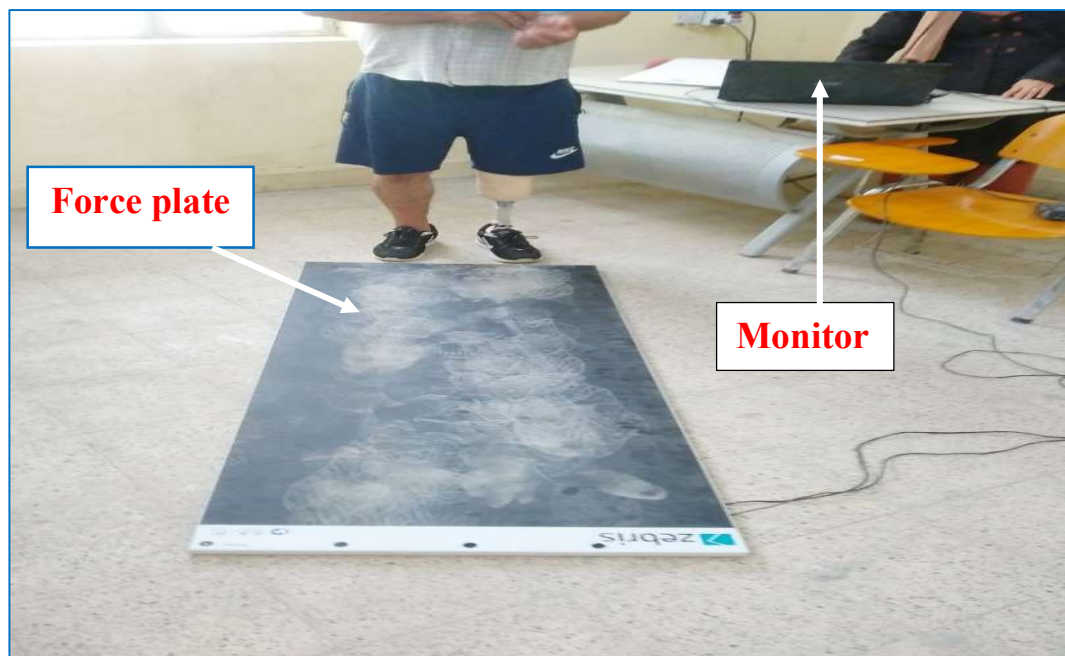


Figure (4.37) Ground reaction force test.

The first GRF test for the amputated person was walking on a force plate using the lower limb containing an available metallic (stainless steel) pylon. The amputated person used the suggested pylon (I) and pylon (II) through walks on a force plate in the second and third GRF tests respectively, as shown in figures (4.38) to (4.40). He was instructed to walk over the device about two minutes in all tests, to ensure that the walk condition was stable.



**Figure (4.38)** The amputated person walks on a force plate using an available metallic pylon.



**Figure (4.39)** The amputated person walks on a force plate using suggested pylon (I)



**Figure (4.40)** The amputated person walks on a force plate using suggested pylon (II).



---

## CHAPTER FIVE

### RESULTS AND DISCUSSION

#### 5.1 Introduction

The theoretical, experimental, and numerical results were listed and discussed in this chapter. The theoretical results were obtained through the governing equations for each case. whilst, the experimental results included the tensile, flexural, and buckling tests for the different lamination composite materials as mechanical properties. As well, the density test was done as physical properties. Also, experimental results presented the results of the buckling test of two types of manufactured pylons, besides the stainless-steel pylon, as well as the results of the gait cycle for the case study through GRF test. This chapter presented the numerical results were obtained by employing the (ANSYS WORKBENCH 17.2) software program in modeling of buckling test for the new pylons, which contain:

- 1- Determine (total deformation, elastic strain (Von- Mises), and equivalent stress (Von-Mises)) by static analysis of the composite pylon.
- 2-Determine (critical buckling stress, critical deflection, and buckling mode shape) by buckling analysis of the composite pylon to compare it with that got experimentally and verified the models' accuracy.

#### 5.2 Experimental Results

##### 5.2.1 Physical Properties

Table (5.1) shows the results of the density test for all composite samples, experimentally using Archimedes' rule and theoretically using the equation (3.11)

as mentioned in chapter three. These results were very similar, with a difference of only (2.49%). At the same time, the **thickness** was determined with unit digital vernier, and **volume fraction** was determined using the equation (3.1). Table (5.2) displays these results for the samples with thickness (2.5mm).

**Table (5.1)** Density theoretical and experimental for the samples suggested for the pylon

No. of samples	Theoretical Density (g/cm <sup>3</sup> )	Experimental Density (g/cm <sup>3</sup> )	$= \left  \frac{\text{Difference}100\%}{\text{Theoretical}} * 100\% \right $
S1	1.350	1.368	1.33
S2	1.454	1.471	1.169
S3	1.533	1.565	2.08
S4	1.214	1.238	1.97
S5	1.280	1.298	1.4
S6	1.323	1.356	2.49
S7	1.450	1.479	2
S8	1.285	1.305	1.55

**Table (5.2)** Volume fraction for the samples suggested with a thickness (2.5mm)

No. of sample	The volume fraction of fiber (100%)	The volume fraction of the matrix (100%)
<b>S1</b>	25	75
<b>S2</b>	29.4	70.6
<b>S3</b>	34	66
<b>S4</b>	21.7	78.3
<b>S5</b>	25.2	74.8
<b>S6</b>	28.4	71.6
<b>S7</b>	32.7	67.3
<b>S8</b>	30.5	69.5

## 5.2.2 Mechanical Properties Results

### 5.2.2.1 Tensile Test Results

The tensile test was performed to get the stress-strain curves, as shown in figure (5.1), which are paramount to know the modulus of elasticity, yield stress, tensile strength at break, and percentage elongation for each sample. Appendix (A) The report of the Ministry of Higher Education and Scientific Research- University of Technology- Laboratories of Department of Materials Engineering, shows the tensile test results.

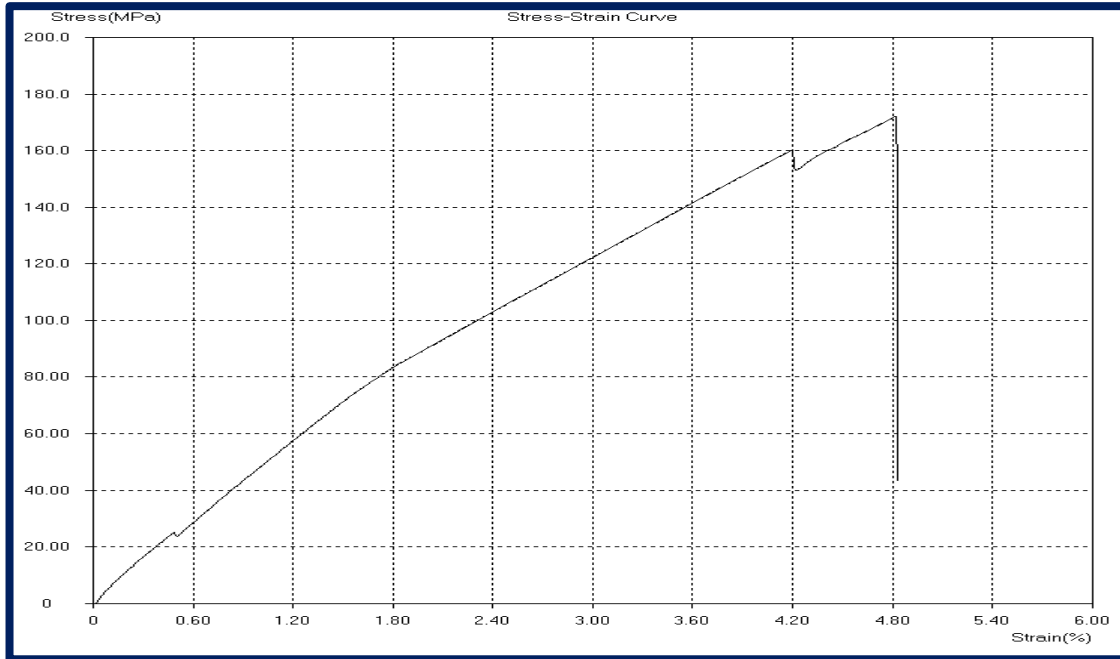


**Figure (5.1)** The stress -strain curve for the sample 6 with three carbon fiber layers

Table (5.3) illustrates the tensile test results for all suggested samples that the stress increases with the increment number of reinforcing layers for (Carbon or Glass) fibers. Also, the tensile strength (ultimate stress) increases when the fiber volume fraction is increased in all samples. The specimens with three Carbon layers have maximum tensile strength and the maximum value of the modulus of elasticity than all specimens, reaching (175 MPa), (4.63 GPa) respectively at ( $V_f = 28.4\%$ ). Also, the tensile strength and the modulus of elasticity obtained for specimens with three Glass fibers layers is (143 MPa), (3.78 GPa) respectively at ( $V_f = 34\%$ ). The comparing all samples that contain a certain number of carbon fibers with samples that have the same number of glass fibers, the percentage of increase in the tensile strength, and modulus of elasticity for specimens with Carbon fibers were (18-22%), (16-20%) respectively.

The difference in strength for these specimens is because of the variation in properties for carbon and glass fibers. It is worth noting that the values of mechanical properties of the composites increase with the number of fiber layers.

This is because the fibers are usually stiffer and more robust than the matrix. After all, the elasticity modulus of a matrix is less than fiber. Therefore, the increase in the number of fiber layers in the matrix will mean that Young's modulus of the composite samples will be increased.

**Table (5.3)** Tensile test results (Mechanical properties for all suggested samples)

No. of Sample	Ultimate stress (MPa)	Average Ultimate tensile stress (MPa)	Modulus of elasticity (GPa)	Average modulus of elasticity (GPa)	Maximum elongation (mm)
S1 - 1	65.5	71	0.96	1.18	4.8
S1 - 2	72.5		1.25		
S1 - 3	75		1.35		
S2 - 1	87	93	1.92	2.10	4
S2 - 2	91		2.16		
S2 - 3	101		2.24		
S3 - 1	138	143	3.59	3.78	3.6
S3 - 2	144		3.76		
S3 - 3	147		3.99		
S4 - 1	84	88	1.79	1.85	4.1
S4 - 2	87		1.87		
S4 - 3	93		1.91		
S5 - 1	123.5	127	3.21	3.46	3.5
S5 - 2	127		3.42		
S5 - 3	130.5		3.77		
S6 - 1	171.5	175	4.25	4.63	2.4
S6 - 2	174.5		4.68		
S6 - 3	179		4.97		
S7 - 1	161.5	163	3.95	4.13	3.2
S7 - 2	165.5		4.17		
S7 - 3	164		4.28		
S8 - 1	166.5	168	4.21	4.41	3
S8 - 2	168		4.36		
S8 - 3	169.5		4.66		

### 5.2.2.2 Flexural Test Results

Most of the specimens were fractured on the two sides (compression and tensile) during the flexural test. This has been proven through visual inspection for specimens during the trial. This indicates that the material has a brittle behavior under flexure, especially with carbon fiber samples. This is consistent with the researcher's findings [69].

Table (5.4) illustrates that the flexural strength values for the specimens are variable according to the type of reinforcement fiber and the volume fraction for it. This difference led to the betterment of the flexural properties of the orthocryl lamination(617H19) resin. All listed results of the flexural test refer to the sample (6) with three carbon-fiber layers more flexible than other samples. The flexural modulus and ultimate stress of this sample reach (6.38 GPa), (230.769 MPa) respectively, while the flexural modulus and ultimate stress equal to (4.654 GPa), (166.153 MPa) respectively in a sample (3) with three glass fiber layers.

The flexural (load-deflection) curves of a sample (6) with three carbon layers and sample (3) with three glass fibers layers are shown in figures (5.2 and 5.3) respectively. Sample (6) has a brittle behavior in flexural and tensile tests where the stress-strain curve for the tensile test showed that the fracture strain is less than (0.05); Therefore, it is considered a brittle material. In contrast, sample (3) has ductile behavior in failure [70]. Table (5.5) shows a comparison of the results of tensile and flexural tests.

**Table (5.4)** Flexural ultimate stress and the flexural modulus of all samples

No. of Sample	Flexural strength (MPa)	Average flexural strength (MPa)	Flexural modulus ( $E_b$ ) (GPa)	Average flexural modulus (GPa)
S1 - 1	85.7	92.307	2.4	2.6
S1 - 2	99.497		2.8	
S2 - 1	135.25	138.461	3.14	3.44
S2 - 2	141.67		3.74	
S3 - 1	162.155	166.153	4.54	4.654
S3 - 2	170.150		4.768	
S4 - 1	109.4	110.769	3.114	3.195
S4 - 2	112.138		3.276	
S5 - 1	150.726	156.923	3.98	4.12
S5 - 2	159.120		4.244	
S6 - 1	228.758	230.769	6.220	6.38
S6 - 2	232.78		6.54	
S7 - 1	207.115	212.307	5.19	5.310
S7 - 2	217.5		5.43	
S8 - 1	218.786	221.538	5.648	5.785
S8 - 2	224.29		5.922	

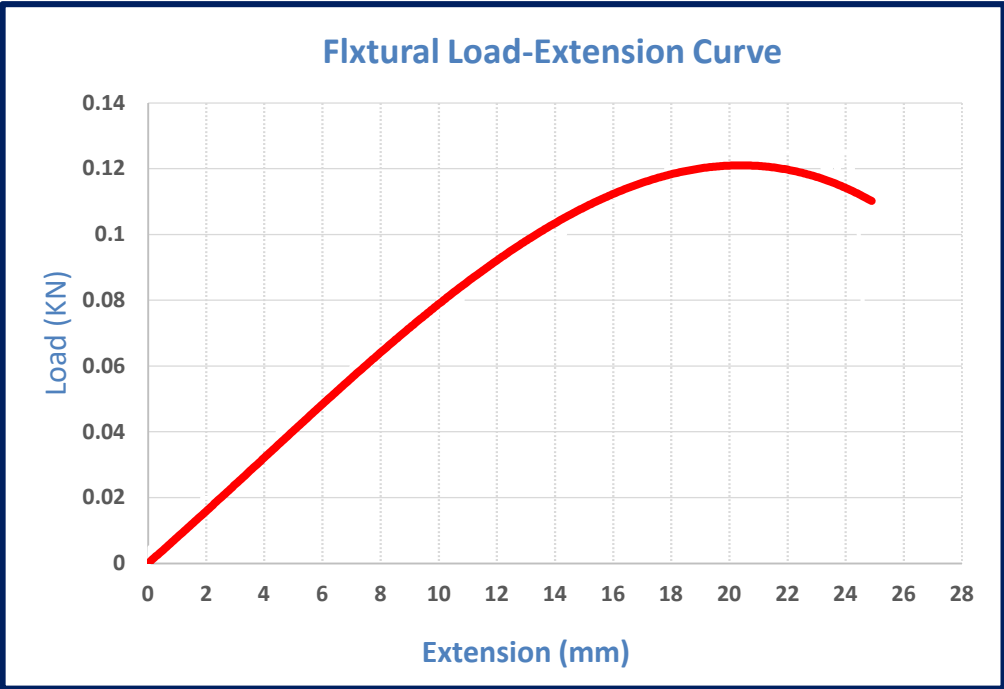


Figure (5.2) Flexural Load-Extension curve for sample 6.

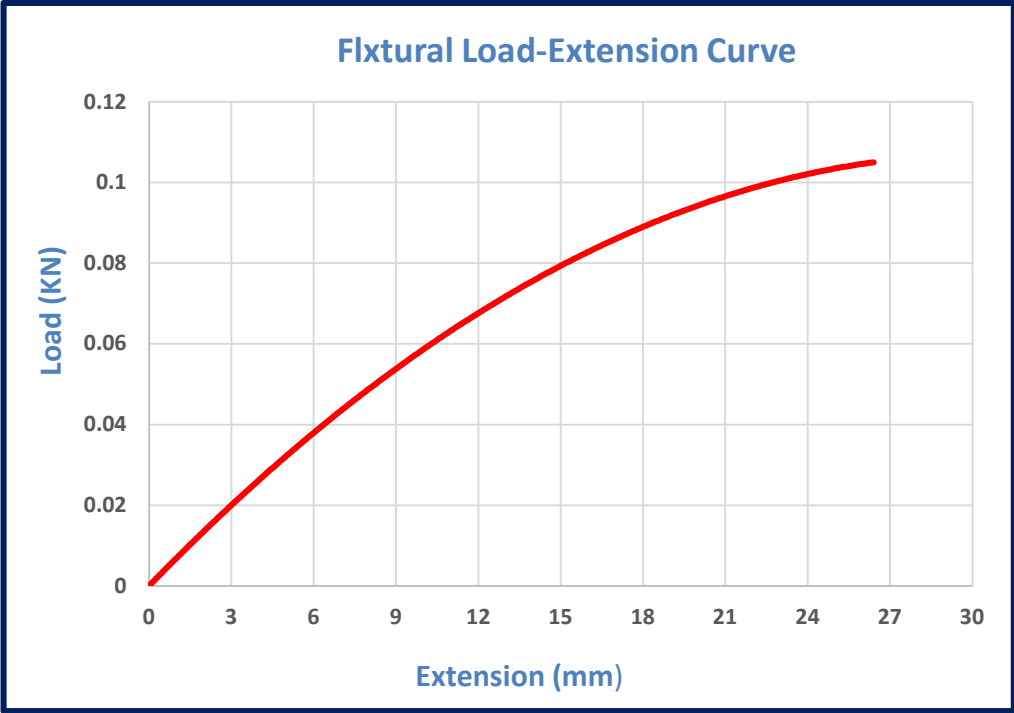


Figure (5.3) Flexural Load-Extension Curve for sample 3.



**Table (5.5)** Comparison the results of tensile and flexural tests

No. of sample	Tensile Strength (MPa)	Tensile Young's Modulus (GPa)	Flexural Strength (MPa)	Flexural Modulus (GPa)
<b>S 1</b>	71	1.18	92.3	2.6
<b>S 2</b>	93	2.10	138.4	3.44
<b>S 3</b>	143	3.78	166.1	4.65
<b>S 4</b>	88	1.85	110.7	3.19
<b>S 5</b>	127	3.46	156.9	4.12
<b>S 6</b>	175	4.63	230.7	6.38
<b>S 7</b>	168	4.13	212.3	5.31
<b>S 8</b>	171	4.41	221.5	5.78

### 5.2.2.3 Buckling Test Results

#### 5.2.2.3.1 Critical Buckling Load and Maximum Deflection for Samples

It took the buckling test results at room temperature (24 °C) for eight types of suggested samples composite materials, where three specimens for each sample are tested. It was noted that all specimens were buckled until the complete failure occurred.

The load-deflection curve determines the experimental critical load, where determines the point where the straight line leaves the graph(curve). The value of projecting this intersection point on the y-axis is called the buckling load [71], as shown in figure (3.8) in Chapter three. Also, figure (5.4) shows the critical buckling load for the sample (6).

Table (5.6) shows the results of a test for critical buckling load and deflection. It is noticeable that when the applied load increases, the buckling deformation increases as well. The essential buckling loads appear to change experimental results according to the aspect ratio and the fiber volume fraction. Where can be noticed that under constant thickness, when the aspect ratio increases, the buckling load at a critical point decreases, but the maximum deflection values increase. Also, the critical buckling load depends on the aspect ratio when the stresses change along the length of the specimen; at constant, the aspect ratio and thickness have broad resistance to compression and are suitable for buckling. Also, the fiber volume fraction represents a significantly important factor in improving buckling resistance due to stiffness fibers. It was found that when the volume fraction increases, the critical load increases, increasing the stiffness of composite specimens and improving buckling resistance.

The maximum critical load can be observed in the sample (6) at  $V_f = 28.4\%$ , and  $L/T = (70)$  was (204.5N), while the minimum value of critical load can be seen in a sample (1) at  $V_f = 25\%$ , and  $L/T = (90)$  is (49.5N). Figure (5.5) shows the experimental critical buckling load and aspect ratio for samples with the thickness (2.5 mm) and width (20 mm).

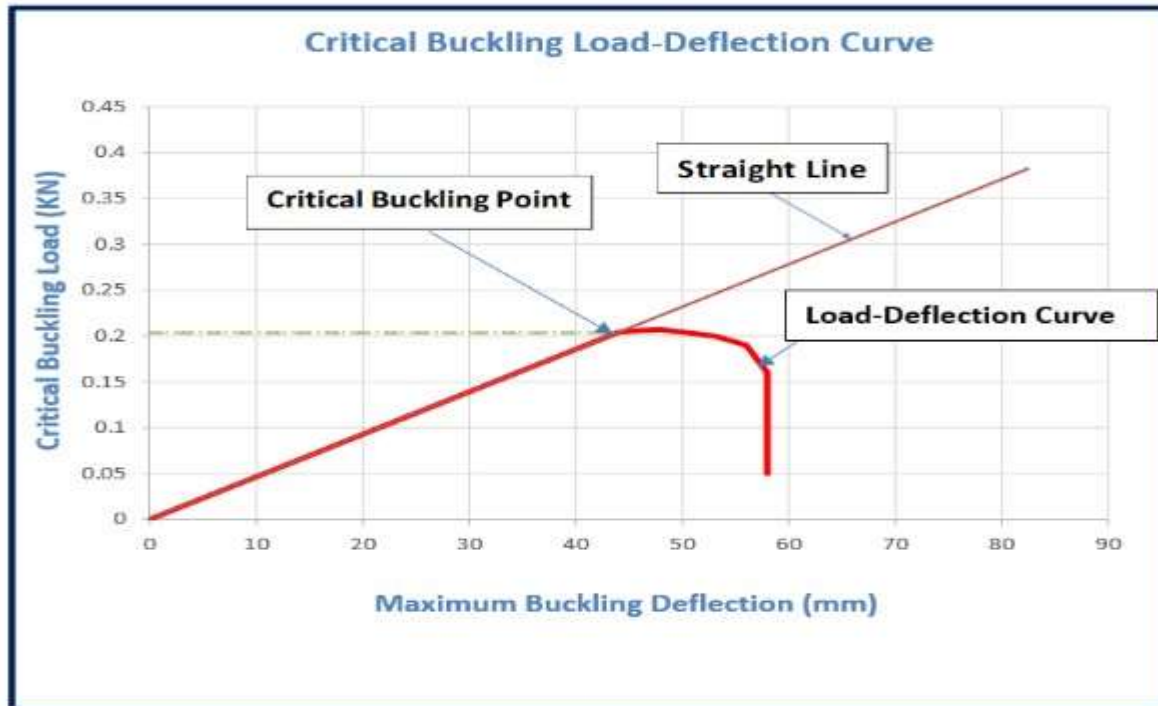


**Figure (5.4)** Critical buckling load against maximum deflection for sample (6)

**Table (5.6)** Critical buckling load and maximum deflection for the buckling test

No. of sample	Angle of fiber	Volume fraction 100%	Length (mm)	Aspect Ratio L/T	Critical Load(N)	Deflection (mm)
S1	(0°/90°)	25	175	70	82	31
			200	80	62.5	38
			225	90	49.5	44
S2	(0°/90°)	29.4	175	70	110	33
			200	80	83.5	41
			225	90	65.5	48
S3	(0°/90°)	34	175	70	150	37
			200	80	113.5	45
			225	90	89	51
S4	(0°/90°)	21.7	175	70	101.5	35
			200	80	77	41
			25	90	61.5	47
S5	(0°/90°)	25.2	175	70	134	40
			200	80	101	48

			225	90	79.5	52
S6	(0°/90°)	28.4	175	70	204.5	44
			200	80	156	53
			225	90	123.5	56
S7	(0°/90°)	32.7	175	70	171	39
			200	80	130.5	45
			225	90	102.5	50
S8	(0°/90°)	30.5	175	70	186	37
			200	80	139.5	44
			225	90	113	48

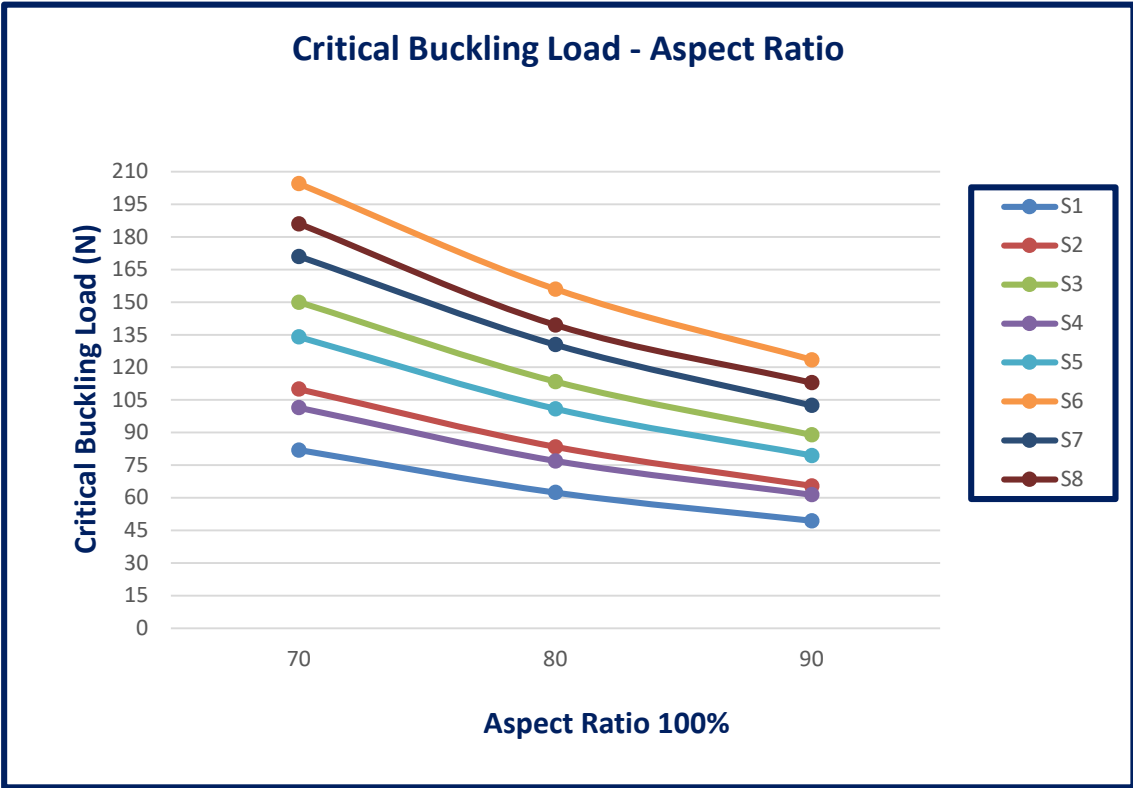


Figure (5.5) The experimental critical buckling load and aspect ratio for samples

The theoretical critical load values for all samples were obtained through equation (3.32) described in chapter three. While the experimental critical load was determined by projecting the intersection onto the load-deflection curve through the crucial point. The maximum difference between them reaches (6.4%) it was in

a sample (1). Table (5.7) shows the experimental and theoretical values of critical load for all samples.

**Table (5.7)** Critical buckling load theoretically and experimentally for all samples

No. of sample	Volume Fraction of Fiber 100%	Aspect ratio L/T	Theoretical Critical Load(N)	Experimental Critical Load(N)	Difference =
					$\left  \frac{\text{Theoretical-Experimental}}{\text{Theoretical}} * 100\% \right $
S1	25	70	87.2	82	5.9
		80	66.8	62.5	6.4
		90	52.7	49.5	6
S2	28.4	70	115.4	110	4.6
		80	88.4	83.5	5.5
		90	69.8	65.5	6.1
S3	32	70	156.2	150	3.9
		80	119.6	113.5	5.1
		90	94.5	89	5.8
S4	22.7	70	107.2	101.5	5.3
		80	82.1	77	6.2
		90	64.8	61.5	5
S5	26.2	70	138.3	134	3.1
		80	105.8	101	4.5
		90	83.6	79.5	4.9
S6	28.4	70	213.5	204.5	4.2
		80	163.4	156	4.5
		90	129.1	123.5	4.3
S7	30.7	70	178.2	171	4
		80	136.4	130.5	4.3
		90	107.8	102.5	4.9
S8	29.5	70	194.1	186	4.1
		80	148.6	139.5	6.1
		90	117.4	113	3.7

---

### **Material test results evaluation in terms of mechanical properties**

The results of all tests (tensile, flexural, and buckling) indicated that samples containing a certain number of carbon fibers had mechanical properties highest than the samples containing the same number of glass fibers. The percentage increase in tensile strength, Young's modulus, flexural strength, and critical buckling load were (22.3%), (37.2%), (38%) and (36%) respectively for the sample (6) with three carbon-fiber layers higher than the sample (3) with three Glass-fiber layers. Tables (5.3 to 5.7) showed these results.

The choice of materials to be used for pylon fabrication depends entirely upon the patient's weighing, the activity level, whether inactive or active (heavy-duty or super-duty), and the total weight of the pylon so that it is comfortable for the user (patient), besides the total cost of the prosthesis.

#### **5.2.2.3.2 Critical Buckling Load and Maximum Deflection for Pylons**

The buckling test was performed for new pylons. The first (pylon I) was manufactured from the sixth sample, while the second (pylon II) was made from the third sample. Likewise, the currently used metallic pylon made of stainless steel was tested too, to comparison. All pylons with thickness and outer diameter (with standard dimensions) were (2.5 mm, 30 mm), respectively, While the length of the pylons was (210 mm) and in proportion to the length of the amputee (case study); therefore, the aspect ratio for all pylons was (84).

From the findings in Table (5.8), it can be noted that the type of pylon influenced the critical buckling load, critical deflections critical buckling stress for each prosthetic pylon. These results show that the critical buckling load of the metallic pylon was (46.5 KN) while the critical load was equal to (44 KN) (41 KN) for the pylon (I) and pylon (II), respectively. Whereas the results are recorded for the maximum deflection of the metallic pylon was (1.2 mm). In contrast, the maximum

deflection was equal to (1.3 mm) (1.5 mm) for the pylon (I) and pylon (II), respectively. Appendix (C).

The reason for these results is that the stainless steel has higher properties (ultimate tensile strength and Young's modulus) than (carbon or glass) fibers that were reinforcing orthocryl lamination (617H19) (80:20) resin. Still, the metallic pylon has very high stiffness and is heavier, which usually causes discomfort for the patient. In addition, it is costly because it is imported from international companies. Besides the way it is manufactured, which does not need an air vacuum system and does not contain fibers that need to be arranged. The pylon (I) has good properties and is less rigid, which helps absorb impact compared with the stainless-steel pylon. Also, it is lighter and more comfortable for the patient when compared to the second pylon (II). This is because carbon fibers have higher properties (ultimate tensile strength and Young's modulus), and are lighter than glass fibers. The deflection was in pylon (II) is more than pylon (I) because the glass fiber has more flexibility, and the carbon fiber does not bend much before failing.

**Table (5.8)** Critical buckling load and maximum deflection in buckling pylons test

Type of Pylon	Materials	$P_{cr}$ (KN)	Crit. Deflection (mm)	$\sigma_{cr}$ (MPa)
<b>Metallic Pylon</b>	Stainless steel	46.5	1.2	207
<b>Pylon I</b>	Sample (6)	44	1.3	195
<b>Pylon II</b>	Sample (3)	41	1.5	181

#### 5.2.2.4 Results of Ground Reaction Force (GRF) Test

The test carried out on the patient (case study) when wearing the prosthesis with the two new composite pylons, besides the standard pylon, is the ground reaction force (GRF) test. This test aims to measure gait cycle parameters with two

new composite pylons and contrast them with gait parameters with standard pylon to improve the kinematic style of the gait so that the amputee walks better much as possible. The force plate uses to measure these parameters and gives the gait data as Tables and figures. These parameter results were classified into two groups:

- 1- The temporal (time) parameters like step time, stride time, swing time, stance time, stride velocity, cadence, and gait cycle time.
- 2- The spatial (distance) parameters, like stride length, step length, step width, toe-out rotating (foot angle), etc.

The two parameters (temporal and spatial) differ from one person to else according to the old and gender of this person. Usually, the cycle time, foot angle, cadence, stride length, and stride velocity in the gait cycle for healthful men with old (50-64) years are (0.95-1.46) sec, ( $4^{\circ}$ - $7^{\circ}$ ), (82-126) steps/min, (1.22-1.82) m and (0.96-1.68) m/s respectively [72].

The resulted data for the three tests (for the standard pylon and with new suggested pylons) are summarized in Tables (5.9) to (5.11) and figures (5.7) to (5.9). The comparison of the prosthetic leg with the new pylons (I) and pylon (II) regarding the foot rotation, step length, and step time, with their counterparts of the prosthetic leg with standard pylon through the gait cycle tests show that there are differences in the specification of the step-strip. These differences between the injured leg and regular leg can be observed in the foot rotation angle for the suggested pylon (I), and pylon (II) were (0.1 deg) and (1.3 deg), respectively. In comparison, it was (2.1 deg) for the prosthetic leg with standard pylon.

This means it is having been enhanced (95%) and (38%) respectively. The differences in step length with the suggested pylon (I) and pylon (II) were (2 cm), (4 cm) respectively, while it was (8 cm) for the prosthetic leg with standard pylon, these improved by (75%), and (50%) respectively. Also, the step time differences were (0.01 sec) and (0.03 sec) for the suggestion pylons (I) and pylon (II)



respectively, while it was (0.09 sec) for the prosthetic leg with standard pylon these led to give improvement by (88%), and (66%).

In Tables (5.9) to (5.11), the results of the gait cycle showed the difference in stance phase between the injured leg and regular leg does not override (2%), and (2.1%) for the two new suggested pylons (pylon (I) and pylon (II)) respectively. In comparison, it was equal to (4.2%) for the standard pylon. Likewise, the difference through the swing phase was (-1.9%) and (2%) for the pylon (I) and pylon (II), respectively; however, for the standard pylon was (-4.2), this means that the center of mass (COM) of the patient with new pylons was nearer to the normal state [73], which resulted in increased stability and equilibrium during locomotion.

**Table (5.9)** Results of step-stride and gait cycle of the amputee with stainless steel

<b>Parameters</b>	<b>Left Leg</b>	<b>Right Leg</b>	<b>Difference</b>
<b>Foot rotation(deg)</b>	7	9.1	2.1
<b>Step length (cm)</b>	49	41	-8
<b>Step time (sec)</b>	0.73	0.82	0.09
<b>Stance phase %</b>	69.5	73.7	4.2
<b>Load response %</b>	19.3	16.8	-3.5
<b>Single support</b>	27.7	30.2	2.5
<b>Pre – swing</b>	16.5	20.6	4.1
<b>Swing phase</b>	30.5	26.3	-4.2
<b>Maximum force (N)</b>	894	884	-10

**Table (5.10)** Results of step-stride and gait cycle of the amputee with a pylon (I)

Parameters	Left Leg	Right Leg	Difference
Foot rotation(deg)	8.2	8.1	-0.1
Step length (cm)	50	48	-2
Step time (sec)	0.66	0.67	0.01
Stance phase %	66.5	68	1.5
Load response %	17.6	15.9	-1.7
Single support	30.3	32.2	1.9
Pre – swing	15.9	18.6	2.7
Swing phase	33.5	32	-1.5
The maximum force (N)	840	834	-6

**Table (5.11)** Results of step-stride and gait cycle of the amputee with a pylon (II)

Parameters	Left Leg	Right Leg	Difference
Foot rotation(deg)	7.8	9.1	1.3
Step length (cm)	48	52	4
Step time (sec)	0.72	0.69	-0.03
Stance phase %	70.9	73	2.1
Load response %	20	22.8	2.8
Single support	29.6	33	3.4
Pre – swing	20	16.2	-3.8
Swing phase	29.1	27	-2.1
Maximum force (N)	876	868	-6

As explained in figures (5.6) to (5.8), which represents the pressure distribution of the amputee subject in three dimensions with standard pylons, pylons I and pylons, (ii) respectively, the butterfly form indicates the adduction and abduction of feet during ambulation.

The center of pressure (COP) path is displayed in these figures for the right, left foot, and butterfly forms. These data show the attitude of the COP beneath the foot, beginning with the heel strike, the midst, and the toe-off stage. Thus, the maximum pressure value is established in each of these stages.

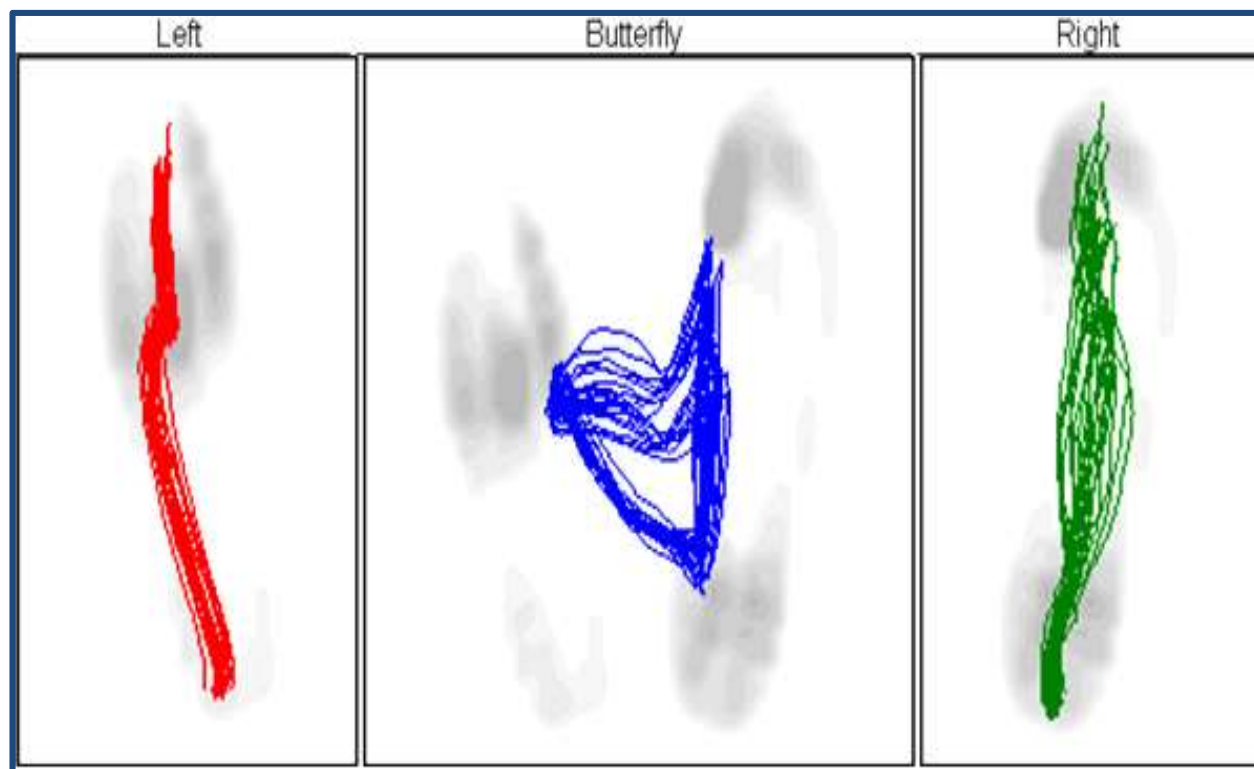
These curved lines in this figure follow the maximum pressure points to sketch the track of the COP.

The most important reasons why the GRF vector is directed more perpendicular to the prosthesis side are the increased weight and lack of flexibility, which reduces the propulsive forces needed to bring the patient's gait closer to the natural state.

Therefore, it can be said the suggestion pylon (I) shows best results where the COP in the amputee with a pylon(I) case approaches to be in the midst of the foot similar approximately to the normal case where the butterfly form appears clearly as shown in figure (5.7). This is due to the high adjust of a prosthetic pylon (I). The butterfly's symmetrical shape was determined using the data in Tables (5.12) to (5.14). The differences in gait line length and single support line were (9mm) and (4mm) respectively, while they equal to(14mm) and (8mm) respectively for the suggestion pylon (II). However, they were (21mm) and (15mm) for the standard pylon, respectively.

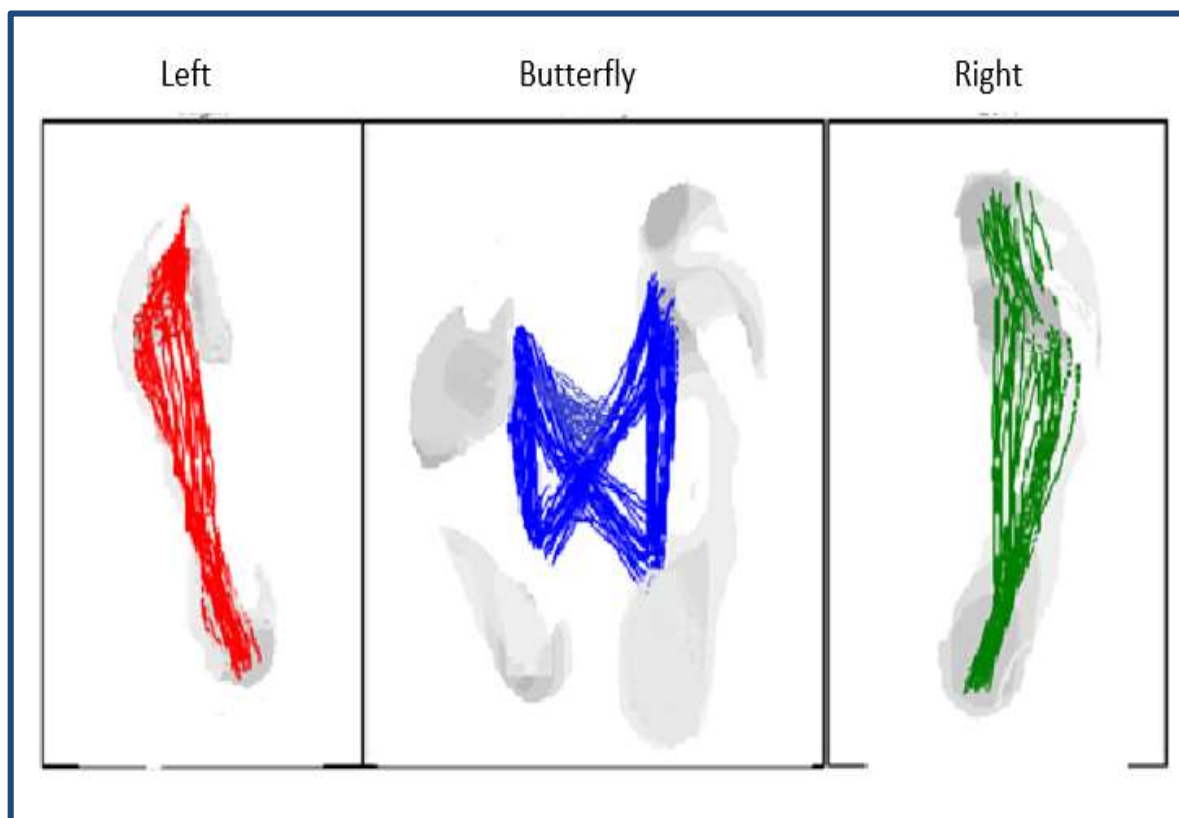
**Table (5.12)** Butterfly parameters for gait cycle of the amputee with standard pylon

Parameters	Left Leg	Right Leg	Difference
Gait cycle length (mm)	242±11	262±22	32±22
Single support line (mm)	119±25	134 ±36	76±9
Ant/post position (mm)	159		
Ant/post variability (mm)	9		
Lateral symmetry (mm)	-44		
Lateral variability (mm)	14		

**Figure (5.6)** The Butterfly parameters of center of pressure for an amputee with metallic pylon.

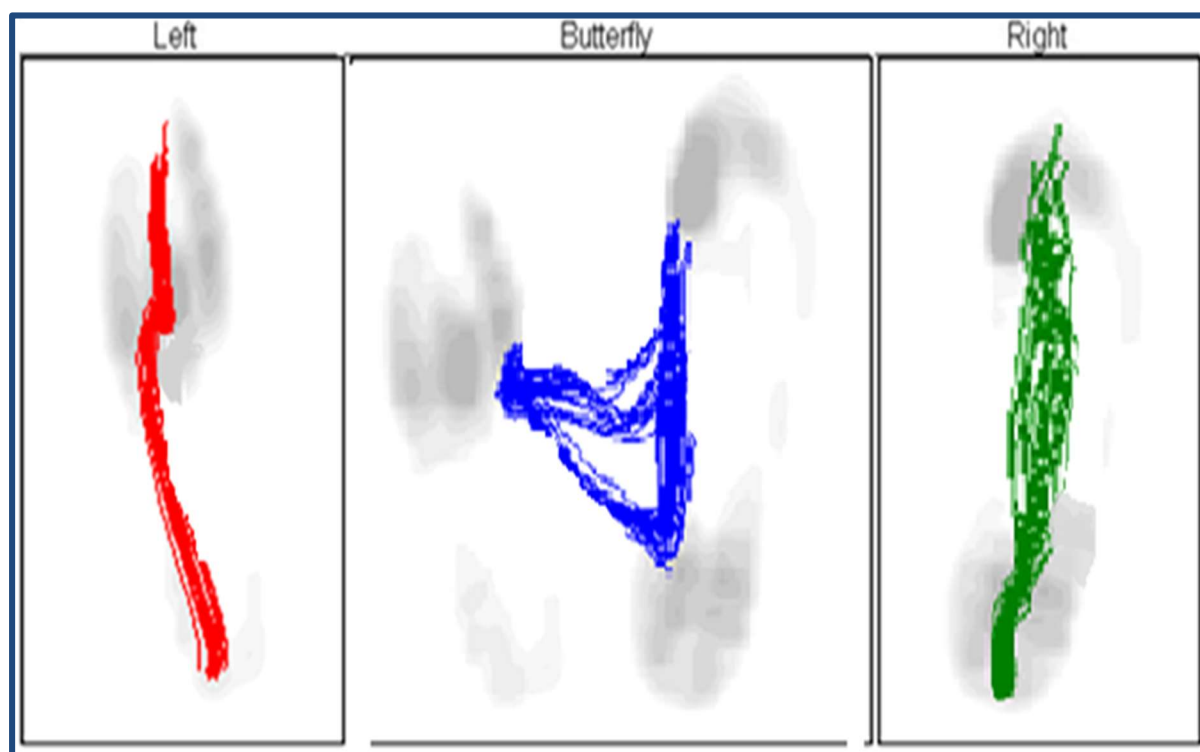
**Table (5.13)** Butterfly Parameters for gait cycle of the amputee with a pylon (I)

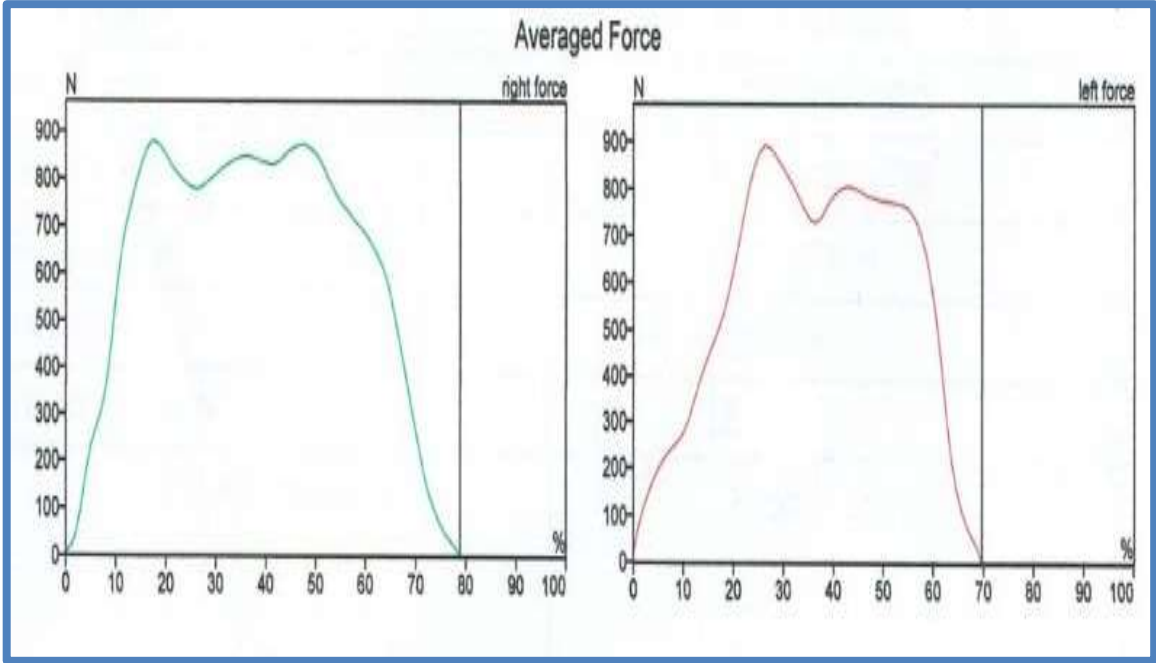
Parameters	Left Leg	Right Leg	Difference
Gait cycle length (mm)	233±7	242±16	9±9
Single support line (mm)	108±15	112 ±8	4±7
Ant/post position (mm)	134		
Ant/post variability (mm)	5		
Lateral symmetry (mm)	-30		
Lateral variability (mm)	14		

**Figure (5.7)** The Butterfly parameters of center of pressure for an amputee with a pylon (I).

**Table (5.14)** Butterfly Parameters for gait cycle of the amputee with a pylon (II)

Parameters	Left Leg	Right Leg	Difference
Gait cycle length (mm)	238±3	252±18	14±15
Single support line (mm)	105±23	115 ±11	8±12
Ant/post position (mm)	139		
Ant/post variability (mm)	12		
Lateral symmetry (mm)	-130		
Lateral variability (mm)	-39		

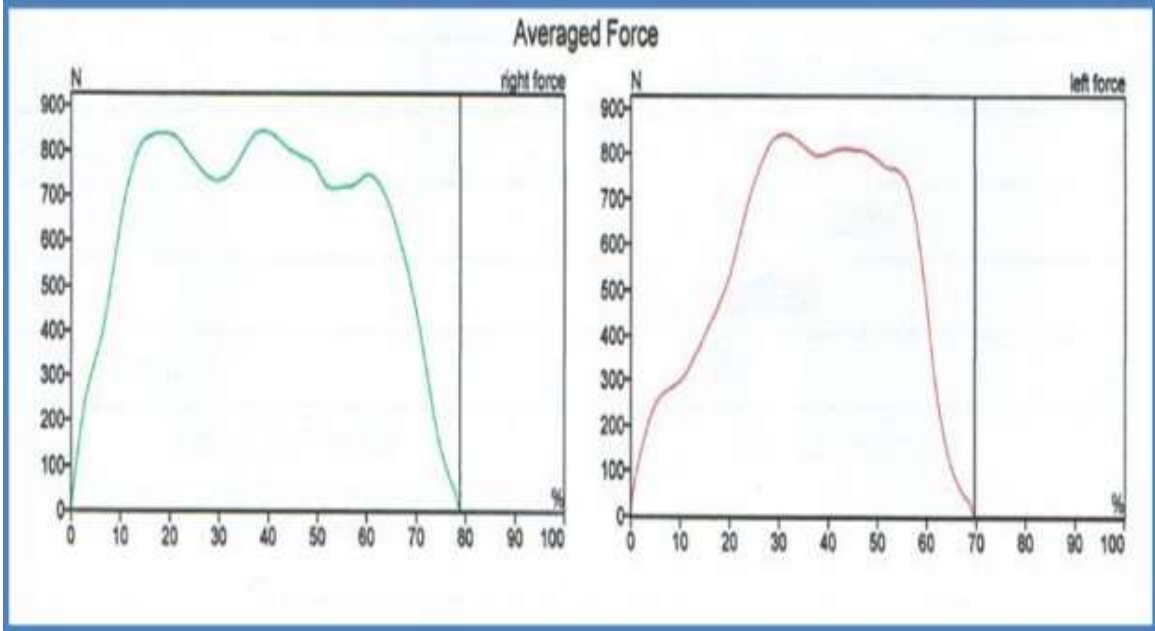
**Figure (5.8)** The Butterfly parameters of center of pressure for an amputee with a pylon (II).



(a) GRF for right( healthy) leg

(b) GRF of left(injured) leg

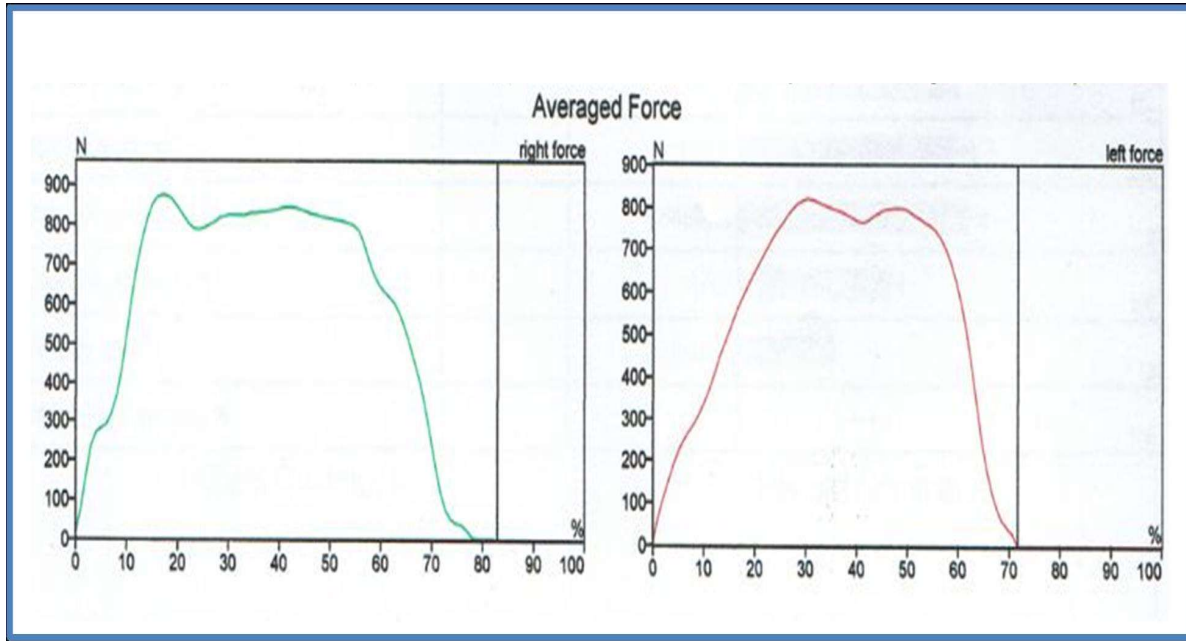
**Figure (5.9)** The GRF of the right (healthy) and the left (injured) legs with standard pylon.



(a) GRF for the right( healthy) leg

(b) GRF of the left(injured) leg

**Figure (5.10)** The GRF of the right (healthy) and the left (injured) legs with pylon (I)



(a) GRF for the right( healthy) leg

(b) GRF of the left(injured) leg

**Figure (5.11)** The GRF of the right (healthy) and the left (injured) legs with pylon (II).

During these tests, the left leg (injured leg) had recorded the GRF with the standard pylon (894 N) and (740 N) at heel strike and toe-off, respectively, as illustrated in Figure. (5.9 a), while in the second case with a pylon(I), the (GRF) became (840 N), and (710 N) at heel strike and toe off, respectively, as shown in figure (5.10 a). Also, it became (818 N) and (680 N) with a pylon (II), at initial contact and toe-off, respectively, as shown in figure (5.11 a).

As well, figure (5.9 b) shows the results of the GRF for the healthy right leg (during the prosthesis in the left leg with the standard pylon) are (884 N) and (770 N) at heel strike and toe off, respectively. Also, it was (837 N) at heel strike and (740 N) at toe off (during the prosthesis in the left leg with the pylon (I)) as shown in Figure (5.10 b). But it became (876 N) and (750 N) (during the prosthesis in the left leg with a pylon (II)), at initial contact and toe-off, respectively, as shown in



figure (5.11 b). This variation in these results is due to the difference in the pylon's weight and the properties of the materials used in its manufacture, such as flexibility.

These data showed that the suggested pylons can be considered a clear improvement, where they were within the required limits and specifications and met the requirements of the gait cycle. Besides their lightweight and low cost, the patient feels more comfortable using them, especially with a pylon (I), which the patient confirmed when asked.

### 5.3 Cost and Weight of Pylons

Compared with the standard pylon, the two new types of prosthetic pylons are lightweight since they are made from composite material, usually lighter than metals. In addition, new prosthetic pylons are less expensive than standard pylons. The weight reduction and the cost reduction percentages for each pylon are stated in Table (5.15).

**Table (5.15)** Percentages reduction of cost and weight for the suggested pylons relative to standard pylon

Pylon type	Percentage cost reduction % =	Percentage weight reduction %=
	$\frac{\text{Cost of Stander} - \text{Cost of New Pylon}}{\text{Cost of Stander}} * 100\%$	$\frac{\text{W of Stander} - \text{W of New Pylon}}{\text{W of Stander}} * 100\%$
<b>Pylon (I)</b>	78	82
<b>Pylon (II)</b>	86	79

## 5.4 Stiffness to Weight Ratio

A measure of an elastic body's resistance to deformation is called stiffness ( $k$ ); in other words, it is the ability of the material to resist the change in its shape that occurs because of the applied load and maintain its shape after the load is removed. Specific stiffness is a material's property composed of an elastic modulus per the material mass density and is also referred to as the specific modulus or stiffness to weight ratio.

Table (5.16) illustrates stiffness to weight ratio results for a unit load  $F_z = 1\text{N}$  [74]. This Table also contains the deflection, which is developed under the loads in the same direction. Figure (5.12) show the axial stiffness to weight ratio for all pylons. This figure shows that the stiffness of materials for the suggested pylon (I) is higher than that of the standard pylon and pylon (II) materials; this increase is because the pylon(I) materials have higher mechanical properties and lower density.

**Table (5.16)** Stiffness to weight ratio for all pylons when applied a unit load

Type of Pylon	Load (1N)	The deflection $\delta$ (m)	Axial stiffness $K=1/\delta$ (N/m)	Weight W (N)	The density $\rho$ (Kg/m <sup>3</sup> )	Stiffness to Weight Ratio $K/\rho$ (N. m <sup>2</sup> /Kg)
Stainless Steel Pylon	Fz	$6.9354 \cdot 10^{-9}$	$1.441 \cdot 10^8$	7.068	7850	$1.836 \cdot 10^4$
Pylon I	Fz	$5.7901 \cdot 10^{-9}$	$1.727 \cdot 10^8$	1.221	1356	$12.73 \cdot 10^4$
Pylon II	Fz	$5.6745 \cdot 10^{-9}$	$1.762 \cdot 10^8$	1.436	1565	$11.26 \cdot 10^4$

The above results indicate that the axial stiffness of the pylon is reasonably acceptable where the value of deflection is a measure of the stiffness that means high the deflection, low the stiffness; it is known that the axial stiffness is directly proportional to Young's modulus and according to the following relationship:

$K_{axial} \propto E \times A$

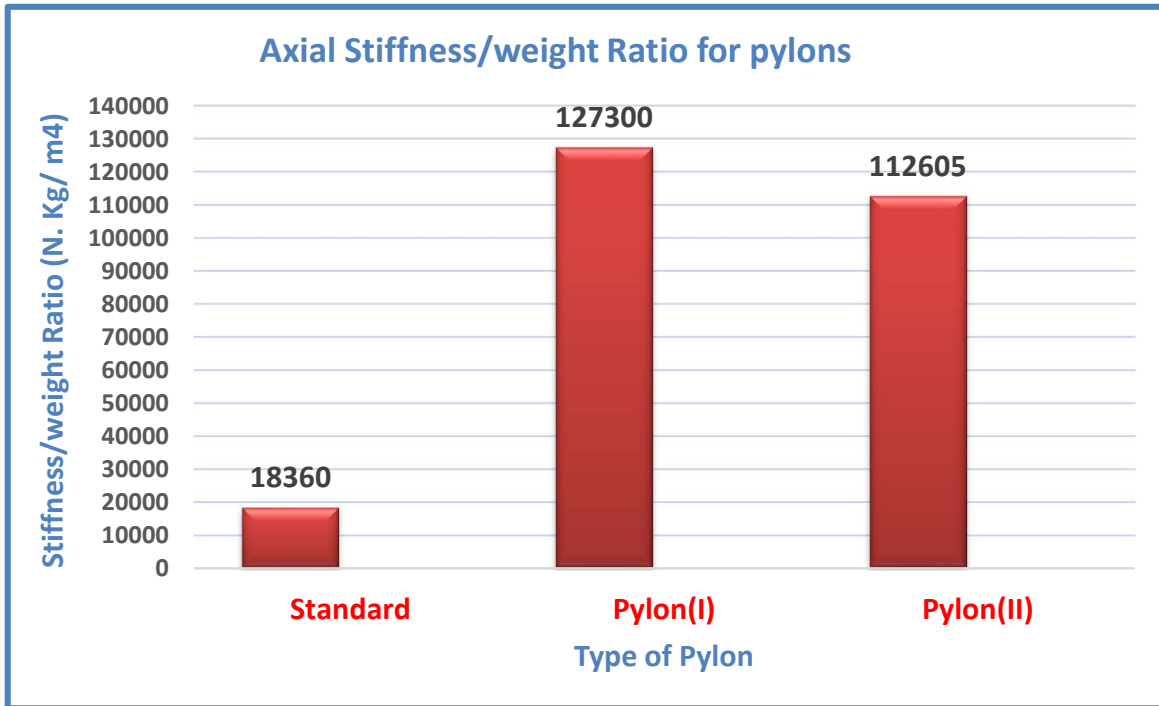


Figure (5.12) Axial stiffness to weight ratio for the prosthetic pylons.

## 5.5 Theoretical Results

The theoretical calculations of the Poisson's ratio, density and modulus of rigidity for all suggested samples were done using the equations from the third chapter. The theoretical results yielded the values of these parameters, as shown in Table (5.17). Also, figure (5.13) shows the modulus of elasticity for all samples.

Table (5.17) Mechanical properties of composite samples suggested for manufacturing pylon

Property	Sample1	Sample2	Sample 3	Sample 4	Sample5	Sample 6	Sample7	Sample 8
$E_1 = E_2$ (GPa)	2.6	3.44	4.654	3.195	4.12	6.38	5.310	5.785

$E_3$ (GPa)	1.4	1.4	1.4	1.4	1.4	1.4	1.4	1.4
$\nu_{12}$	0.338	0.326	0.318	0.345	0.330	0.336	0.322	0.326
$\nu_{23} = \nu_{13}$	0.34	0.34	0.34	0.34	0.34	0.34	0.34	0.34
$G_{12}$ (GPa)	1.075	1.153	1.236	1.008	1.093	1.147	1.075	1.029
$G_{23} = G_{13}$ (GPa)	0.923	0.923	0.923	0.923	0.923	0.923	0.923	0.923

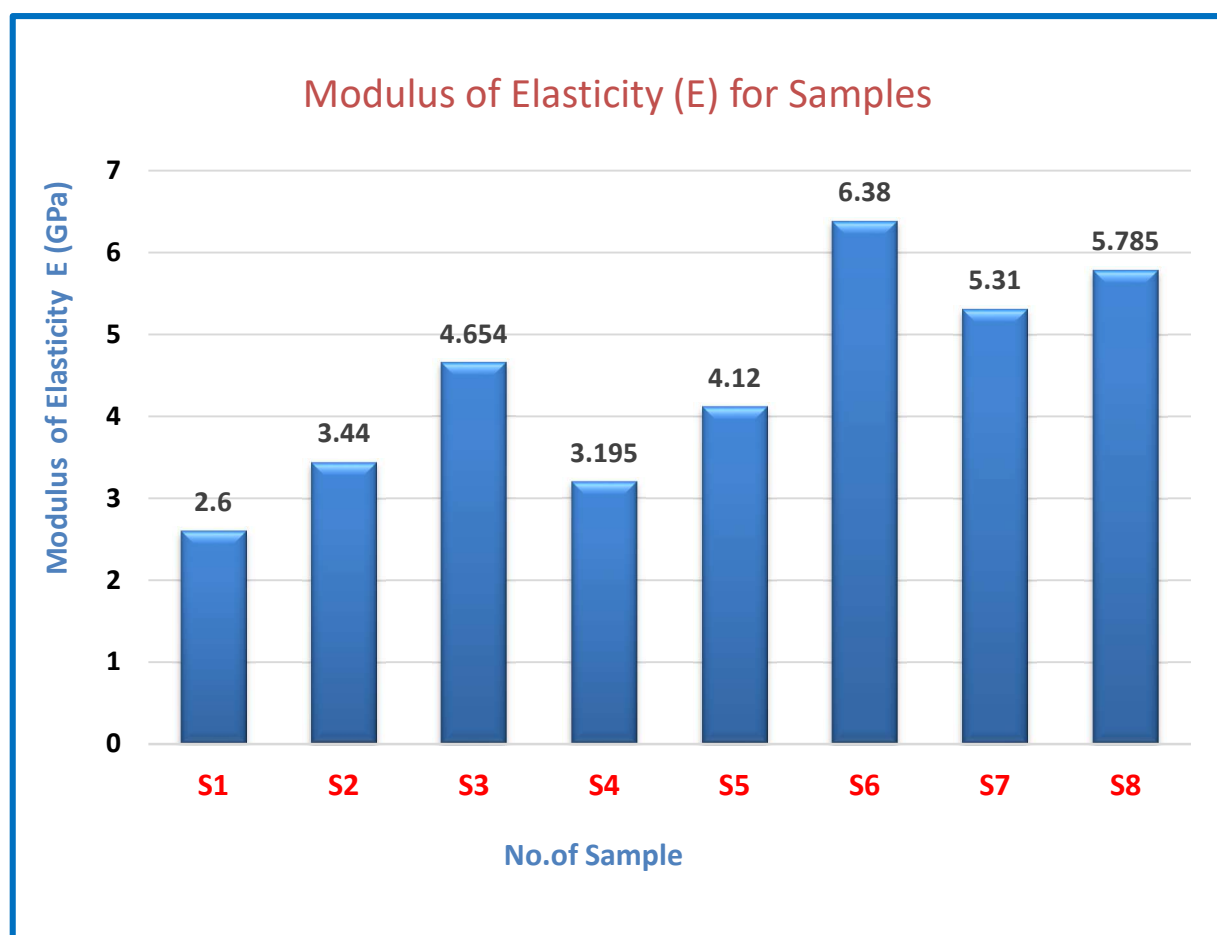


**Figure (5.13)** Modulus of Elasticity (E) for all samples.

### 5.6 Results of The Numerical Analysis

The results of the numerical analysis for the new composite prosthetic pylons (pylon I and pylon II), in addition to the standard prosthetic pylon, were obtained using the finite element method (ANSYS WORKBENCH 17.2) package program. In this study, numerical analysis is divided into static and buckling analysis for prosthetic pylons. When comparing these numerical results with the experimental results gave excellent agreement, as the percentage of difference was (2-4) only.

#### 5.6.1 Static Analysis Results

All pylons deformed when a compressive load was applied to them at touching the ground in the heel strike from the gait cycle. This load represents the maximum load applied on the pylon through walking. The highest deformation of the standard prosthetic pylon was (0.97 mm), as shown in figure (5.14).

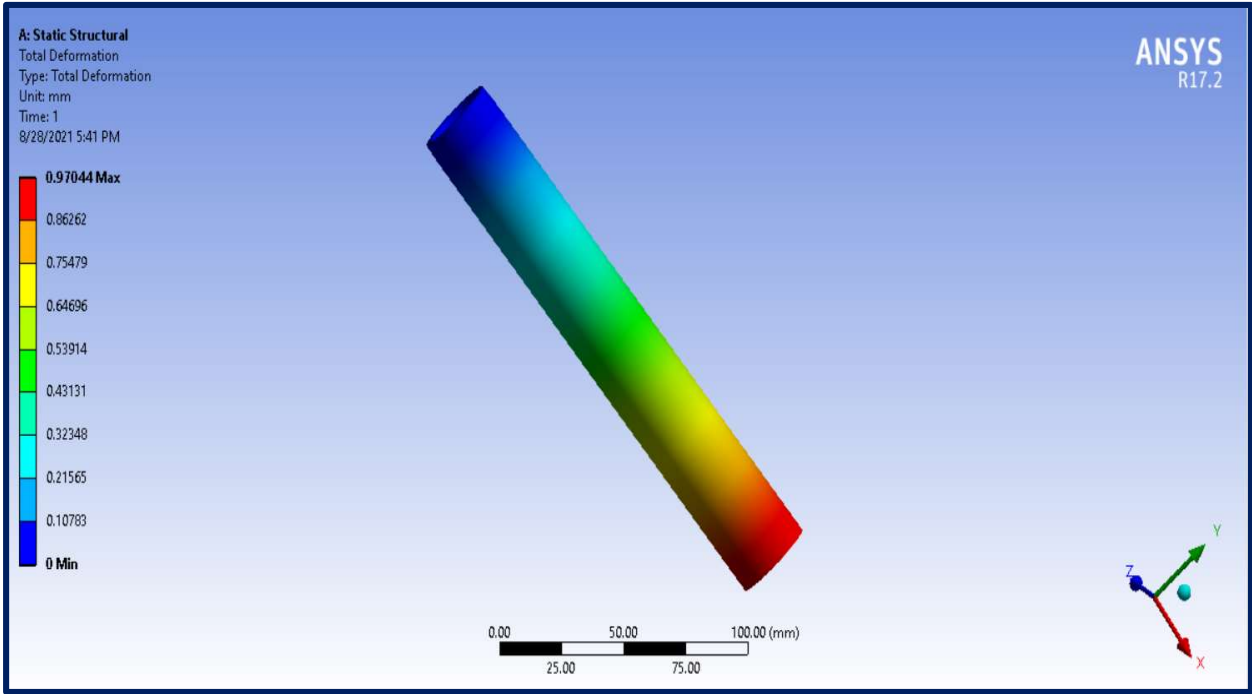


Figure (5.14) Total deformation for the standard prosthetic pylon.

While the pylon (I) and pylon (II) had total deformation equal to (1.067 mm) and (1.213 mm), respectively, as illustrated in figures (5.15) and (5.16). The carbon fibers are stiffer than glass fiber, which significantly resists the compression load applied to the prosthetic pylon. Also, it was clear from these figures, the maximum deformation has happened at the end of the prosthetic pylon near the ground in all pylon types. It has differed according to the reinforcing materials used; this is consistent with the results of the researcher (36).

It is worth mentioning, the length of the prosthetic pylon that has been studied represents the length of the prosthetic pylon used in the artificial lower limb for a person amputated below the knee (case study). Thus, these deformations that have been recorded in all the prosthetic pylons are only for this case. Figure (5.17) illustrates a comparison of total deformation for pylons.

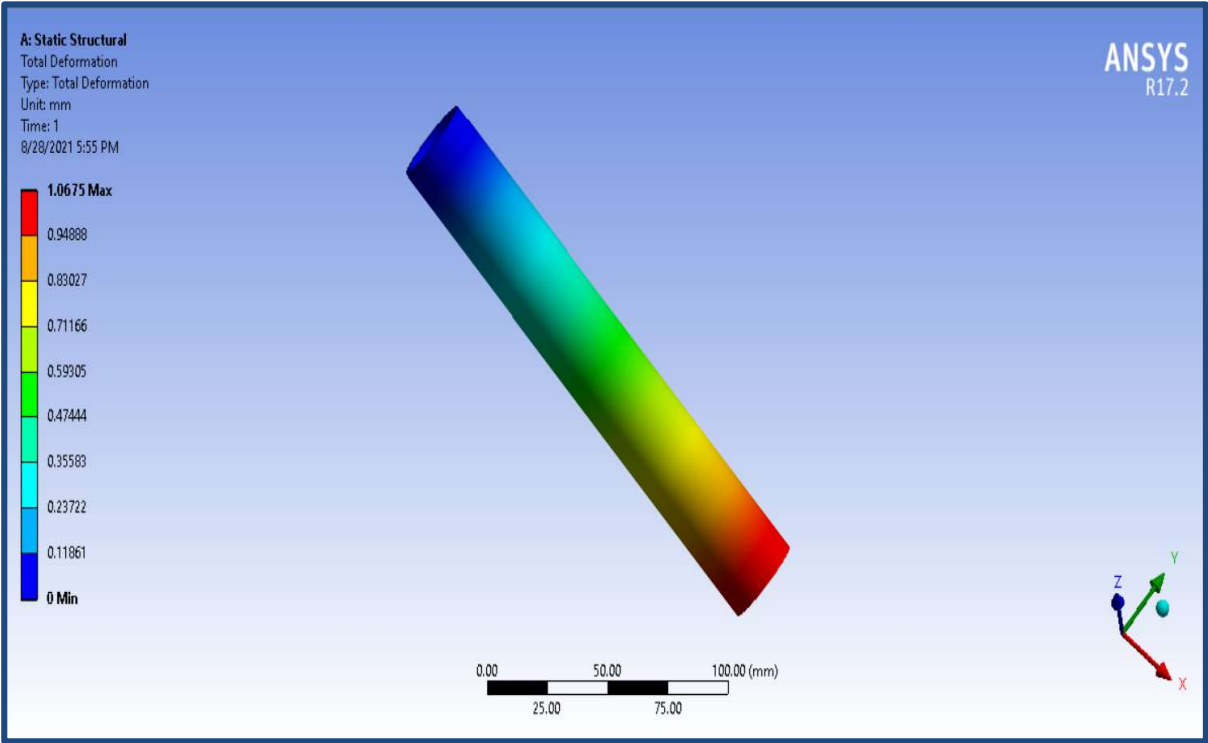


Figure (5.15) Total deformation for the prosthetic pylon (I).

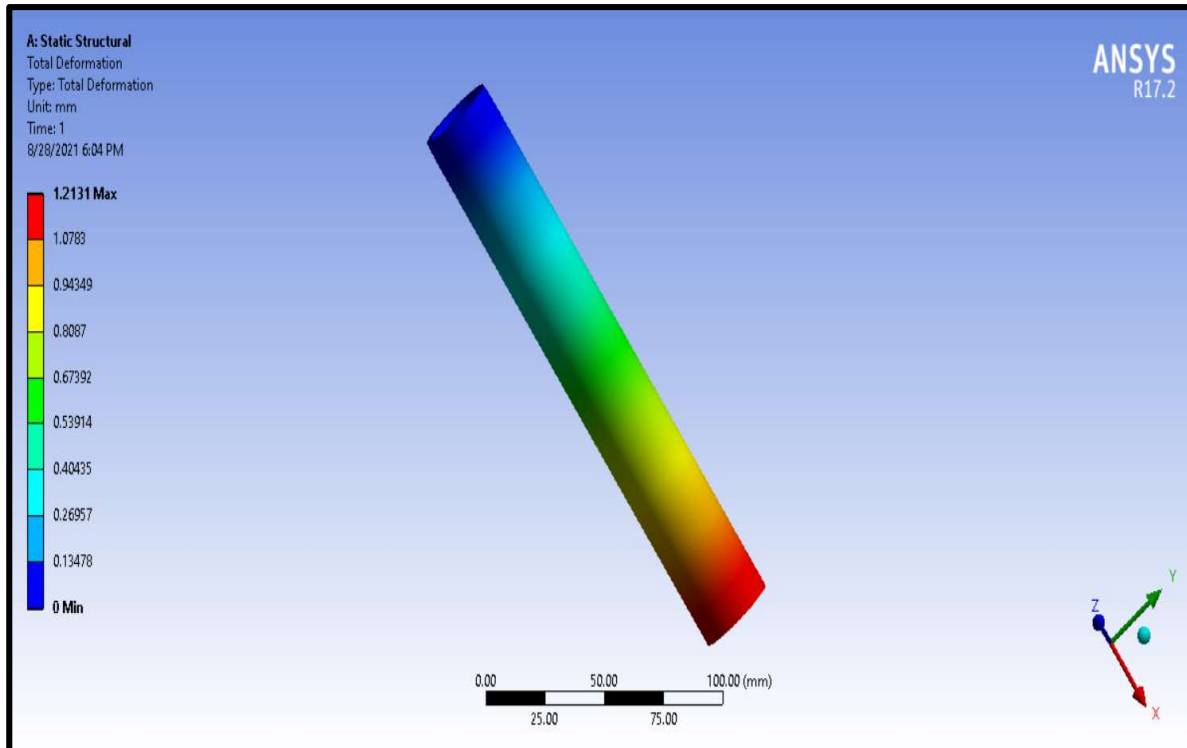


Figure (5.16) Total deformation for the prosthetic pylon (II).

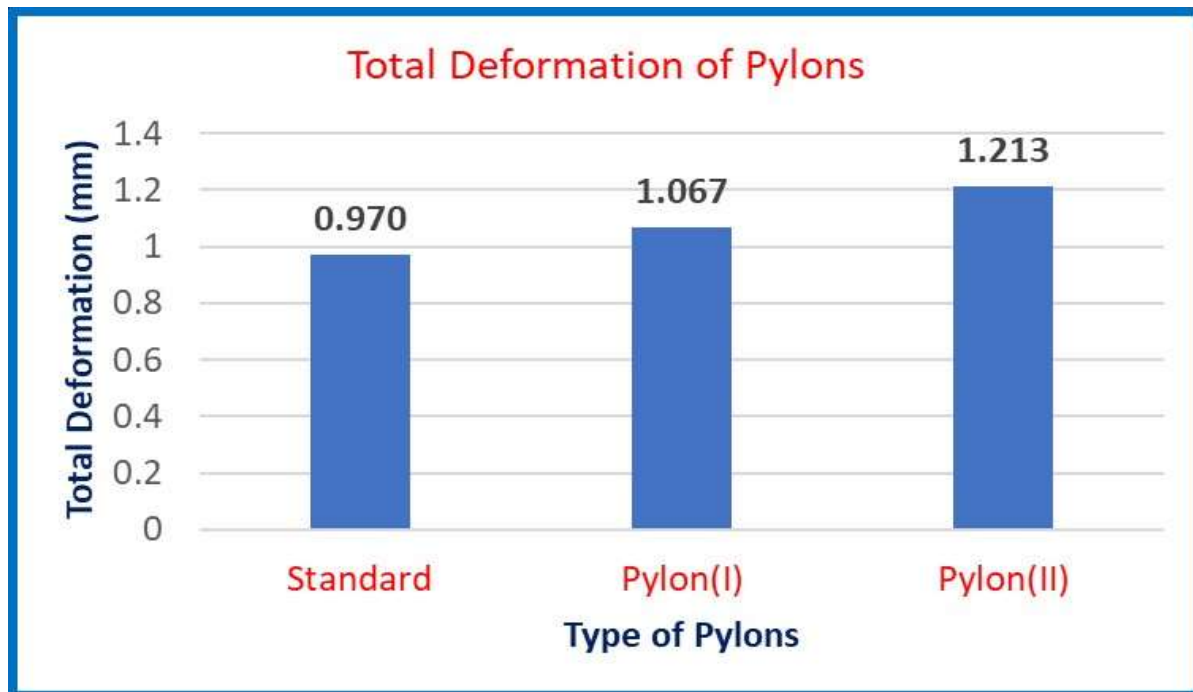
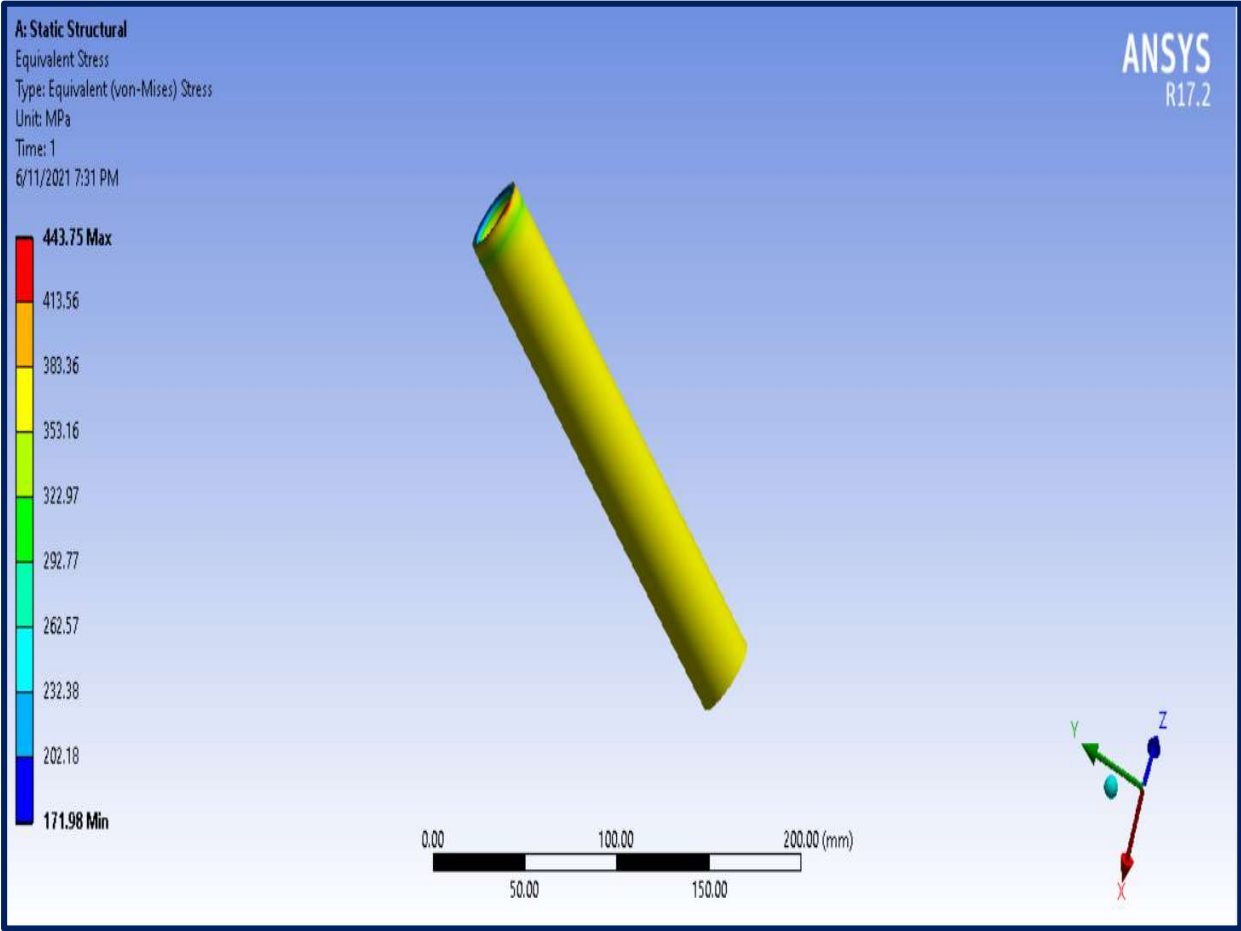


Figure (5.17) Comparison for total static deformation (numerically) of the prosthetic pylons.

The Von-Mises equivalent stress of prosthetics is a haven for prosthetic design engineers. The contour plot in figures (5.18) to (5.20) shows the Von Mises equivalent stresses were equal to (443.75 MPa), (405.01 MPa), and (341.96 MPa) for the standard pylon, pylon (I), and pylon (II), respectively.



**Figure (5.18)** Von-Mises equivalent stress for the prosthetic standard pylon.



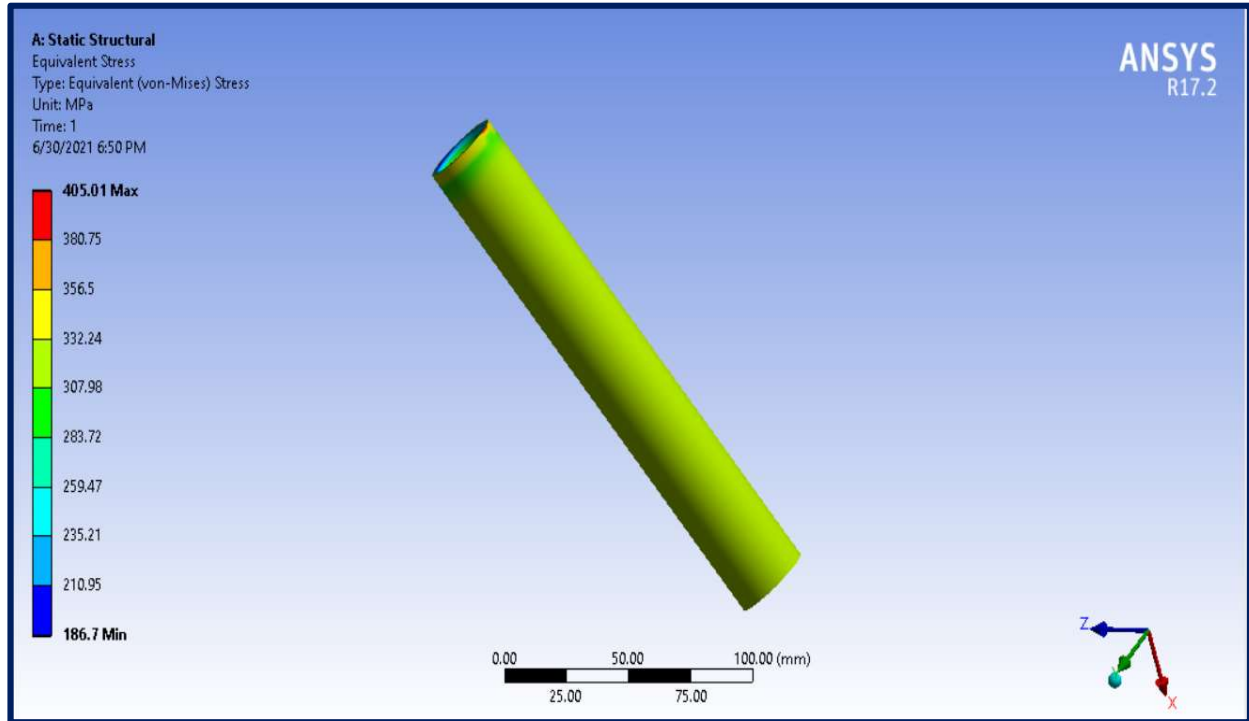


**Figure (5.19)** Von-Mises equivalent stress for the prosthetic pylon (I).

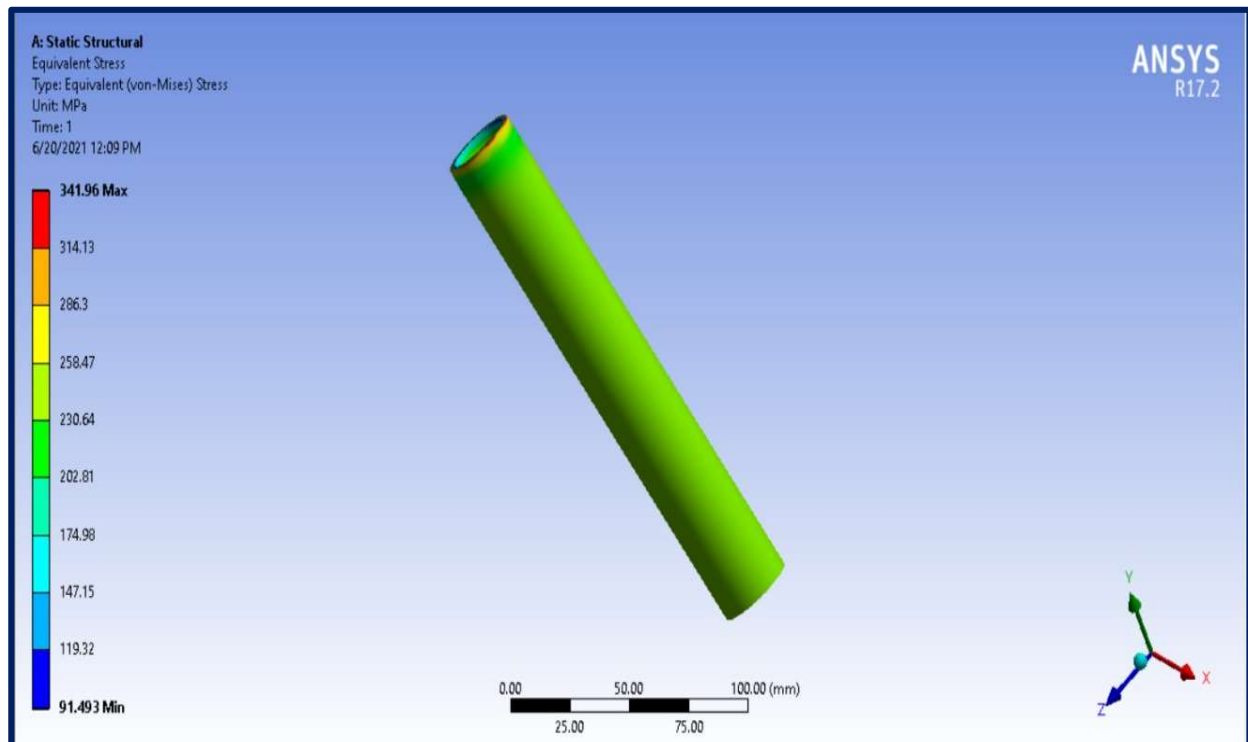


**Figure (5.20)** Von-Mises equivalent stress for the prosthetic pylon (II).

The contour plot in figures (5.21) to (5.23) shows the Von Mises equivalent strain was equal to (0.002246), (0.002396), and (0.002818) for the standard pylon, pylon (I), and pylon (II), respectively.

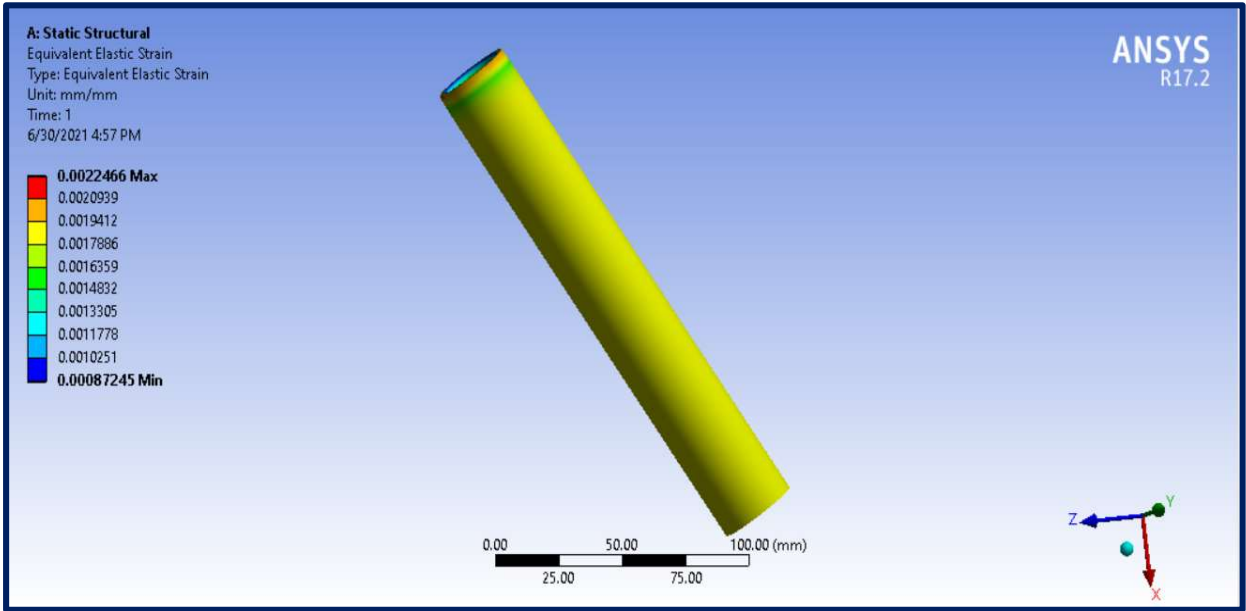


Figure (5.21) Von-Mises elastic strain for prosthetic standard pylon.

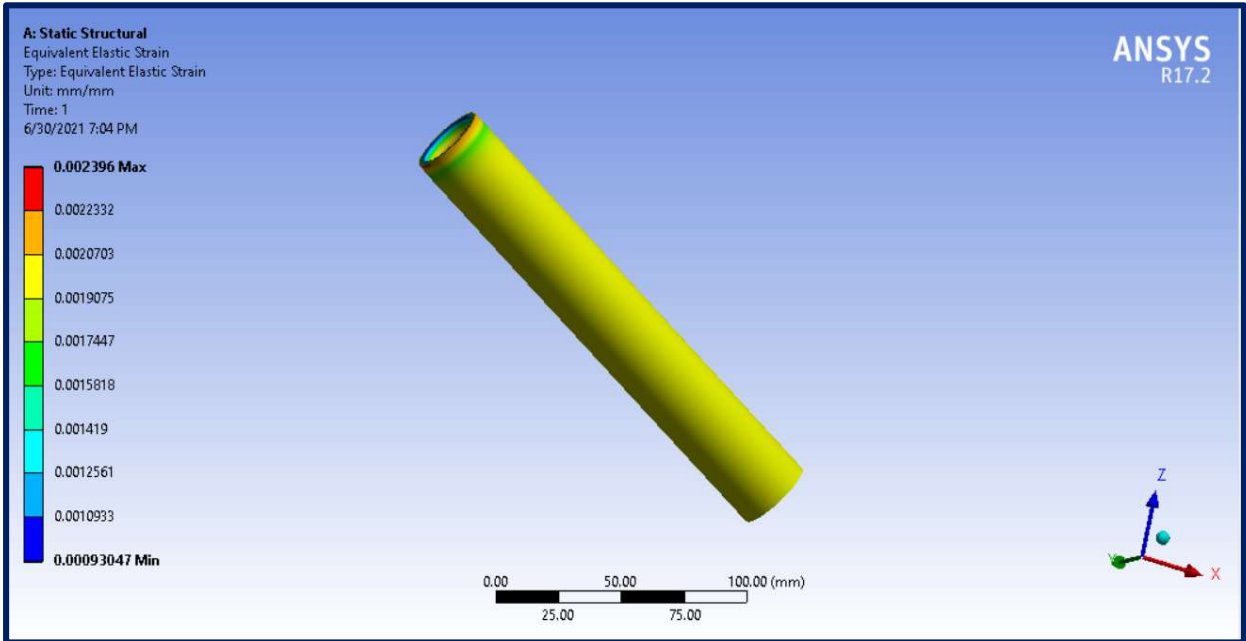


Figure (5.22) Von-Mises elastic strain for prosthetic pylon (I).

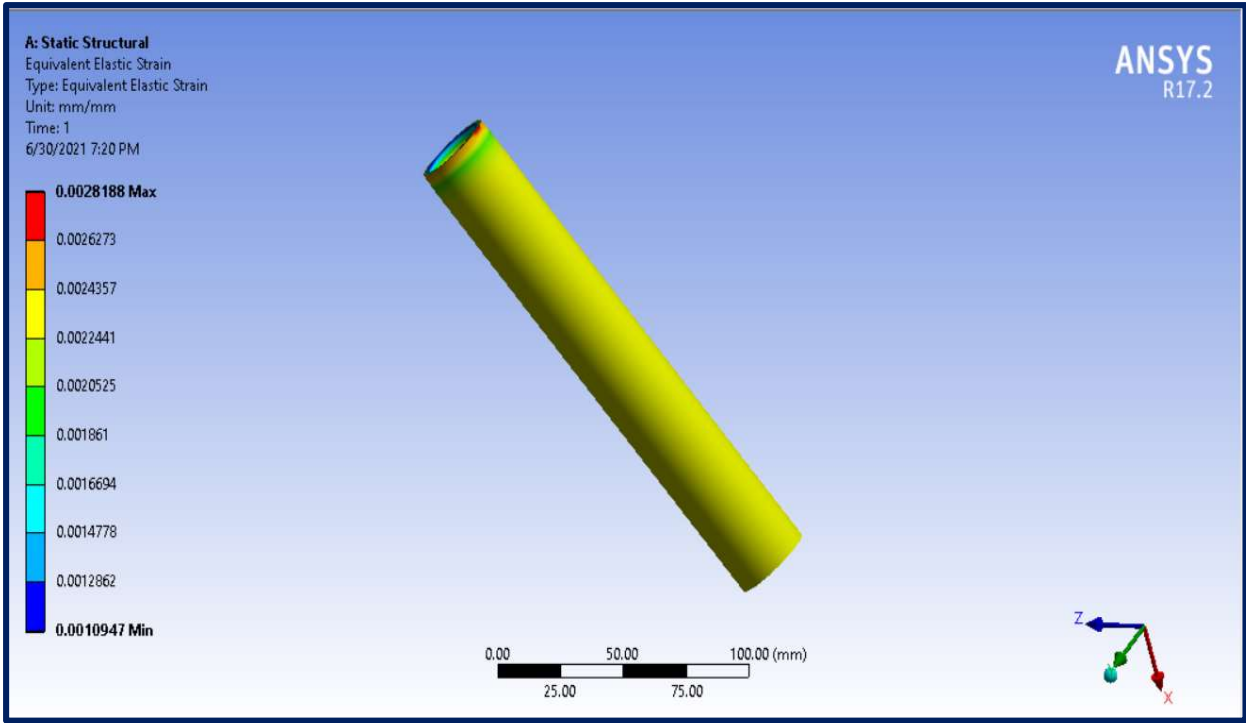


Figure (5.23) Von-Mises elastic strain for prosthetic pylon (II) .

### 5.6.2 Buckling Analysis Results

Using linear eigenvalues, buckling analysis reveals the prosthetic pylon's buckling shape mode and predicts the critical buckling stress. The contours of prosthetic pylons for all types of prosthetic pylons are shown in figures (5.24 to 5.26) for all types of prosthetic pylons. The critical buckling stress represents the critical point at which the prosthetic pylon begins to fail. The lowest value was found in prosthetic pylons made of orthocryl (617H19) lamination (80:20) reinforced three glass layers compared to prosthetic other prosthetic pylons. This is due to the properties of glass fiber being weaker than carbon fiber. Figure (5.27) shows the comparison of the total deformation for pylons.

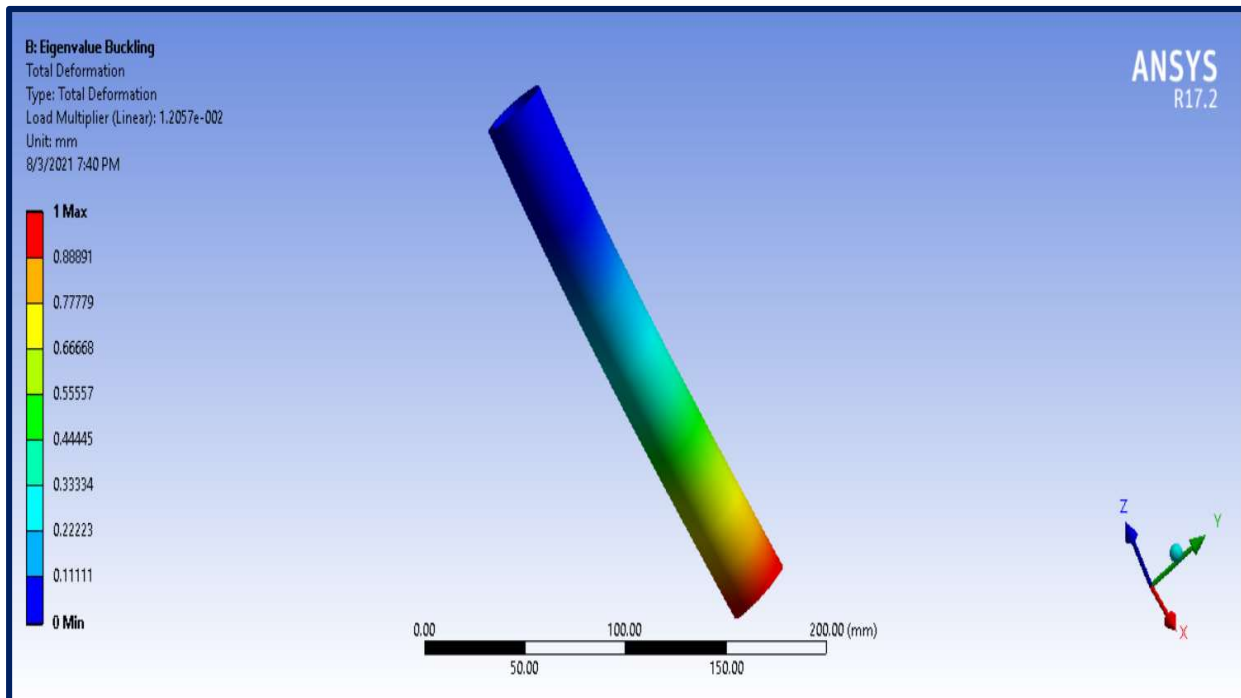


Figure (5.24) Buckling mode shape (1) for the standard prosthetic pylon.

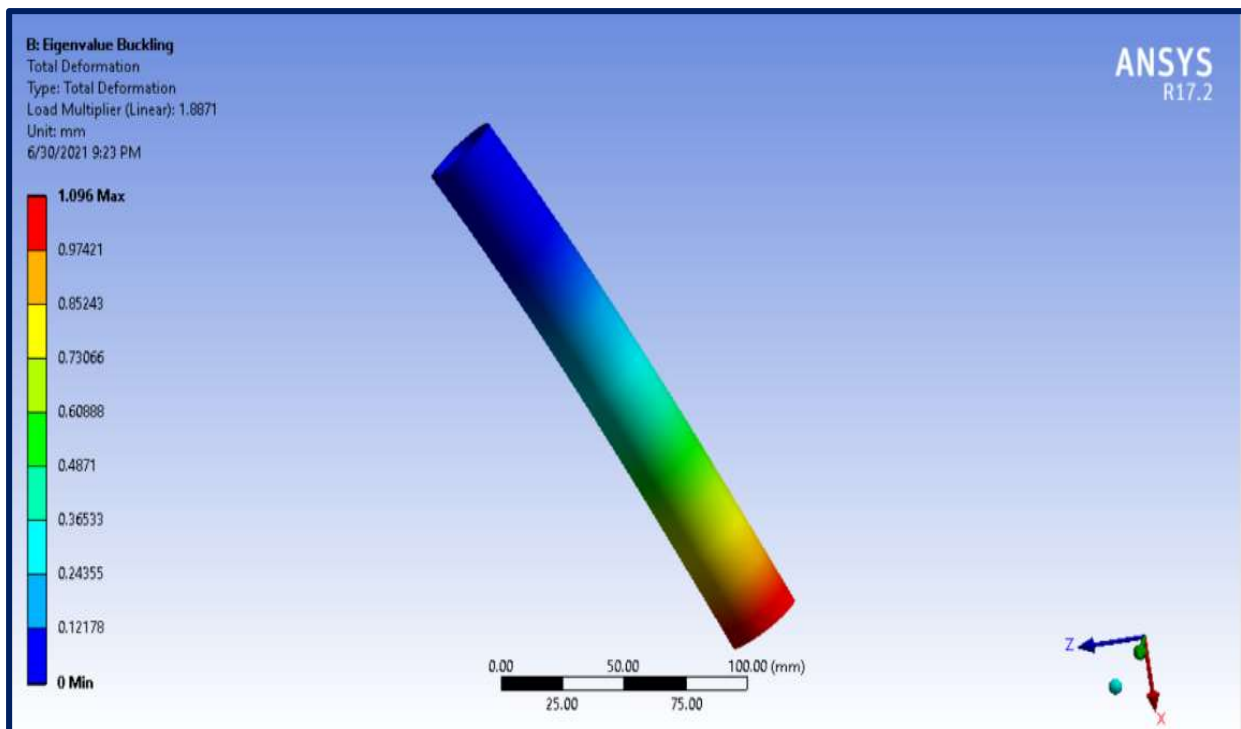


Figure (5.25) Buckling mode shape (1) for prosthetic pylon(I) with three carbon layers.

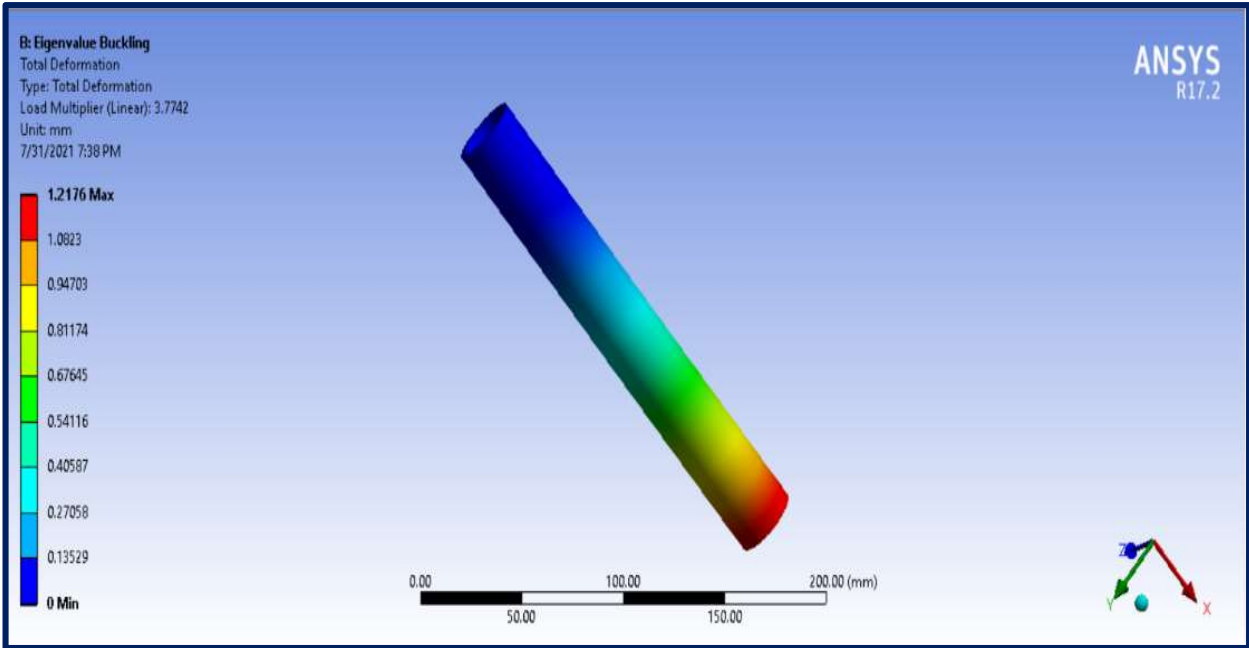


Figure (5.26) Buckling mode shape (1) for prosthetic pylon (II) with three glass layers.

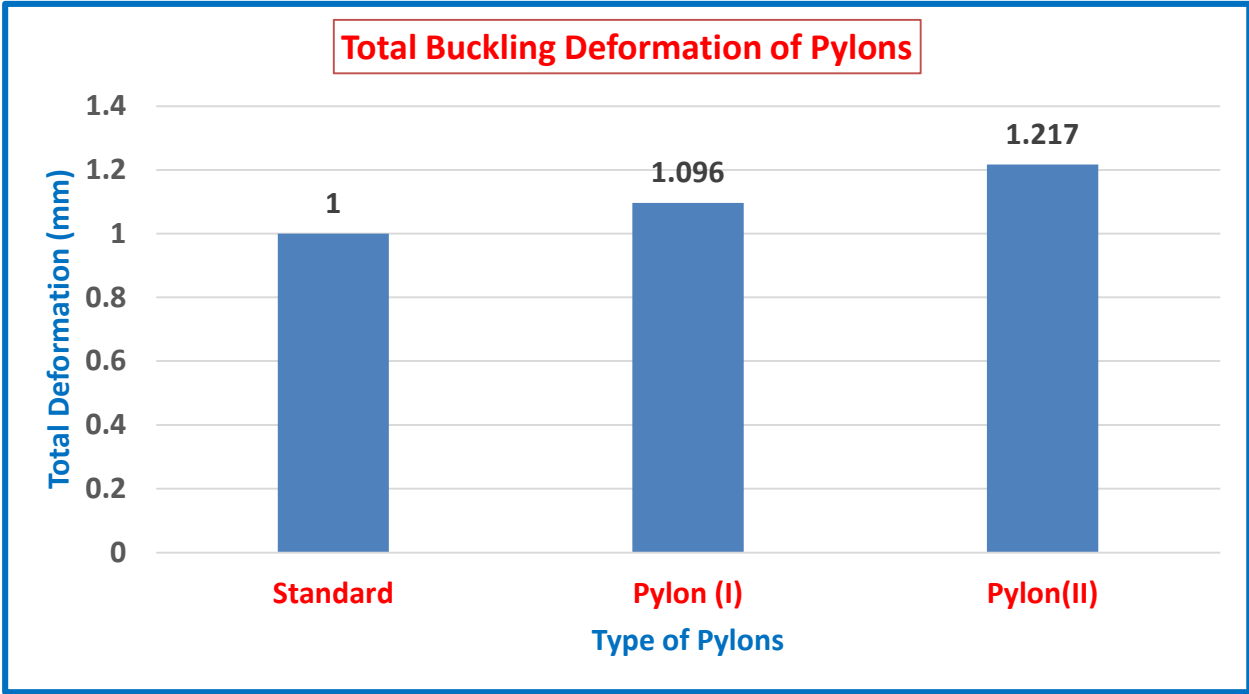


Figure (5.27) Comparison of the total buckling deformation (numerically) for pylons.

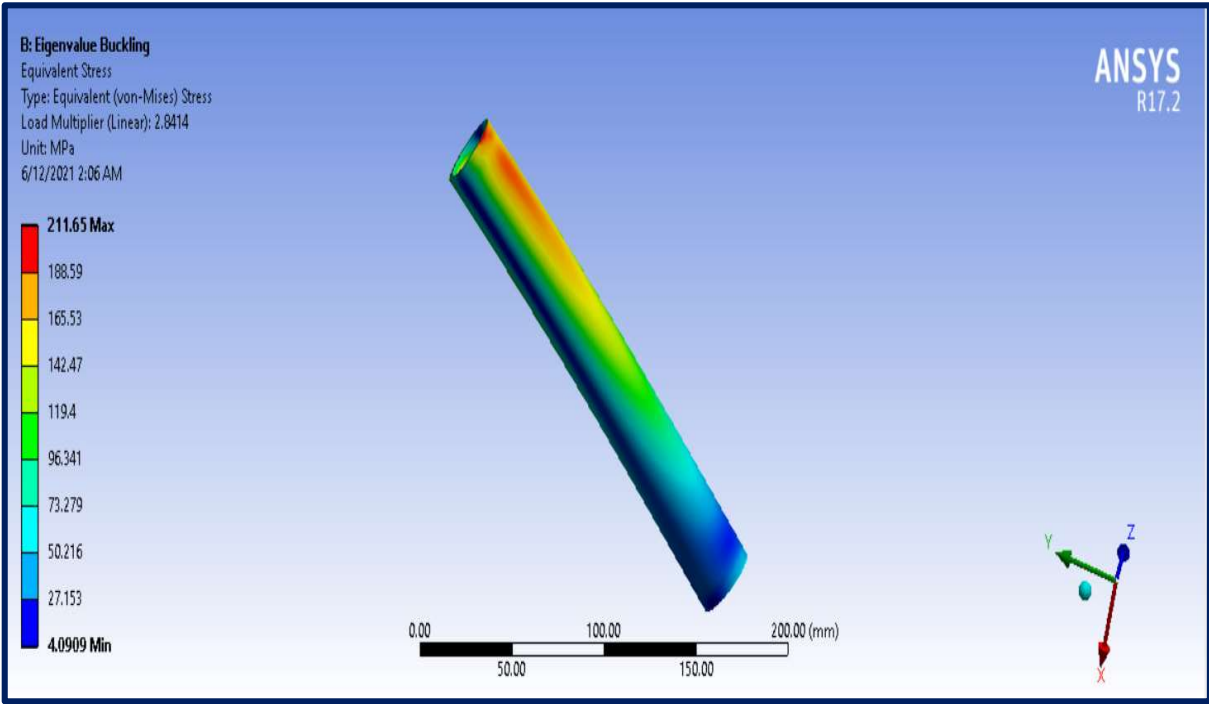


Figure (5.28) Max. Buckling stress for prosthetic standard pylon .

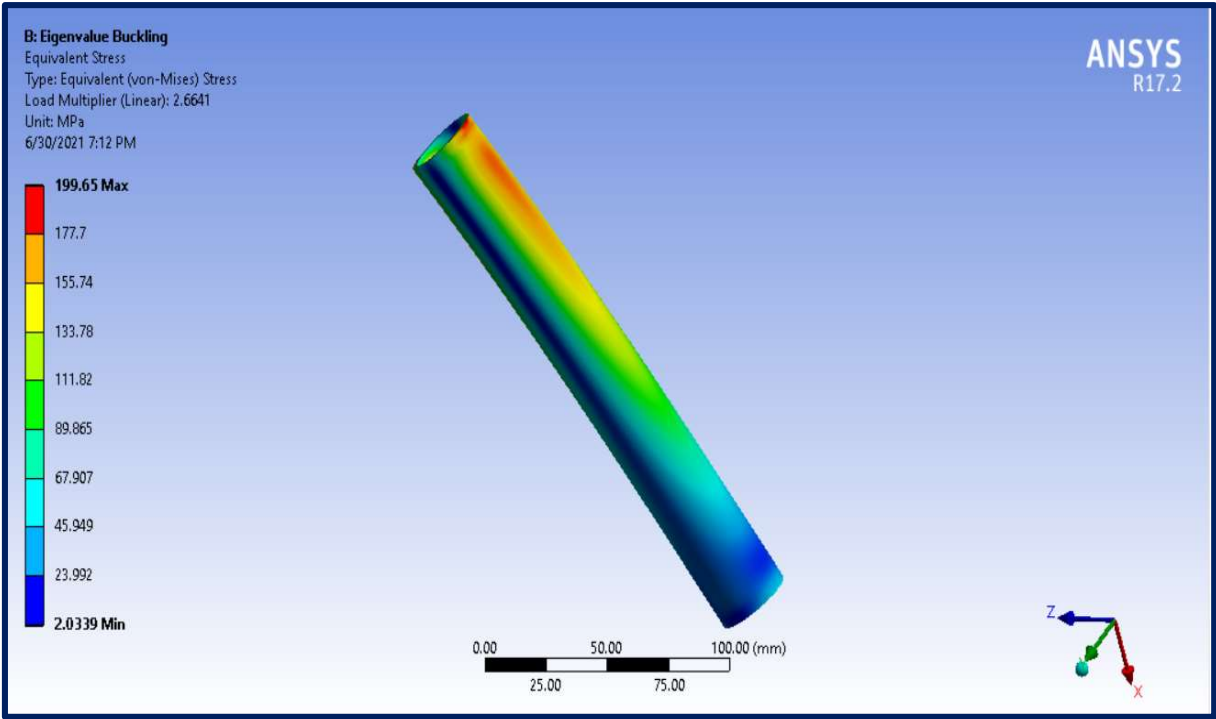
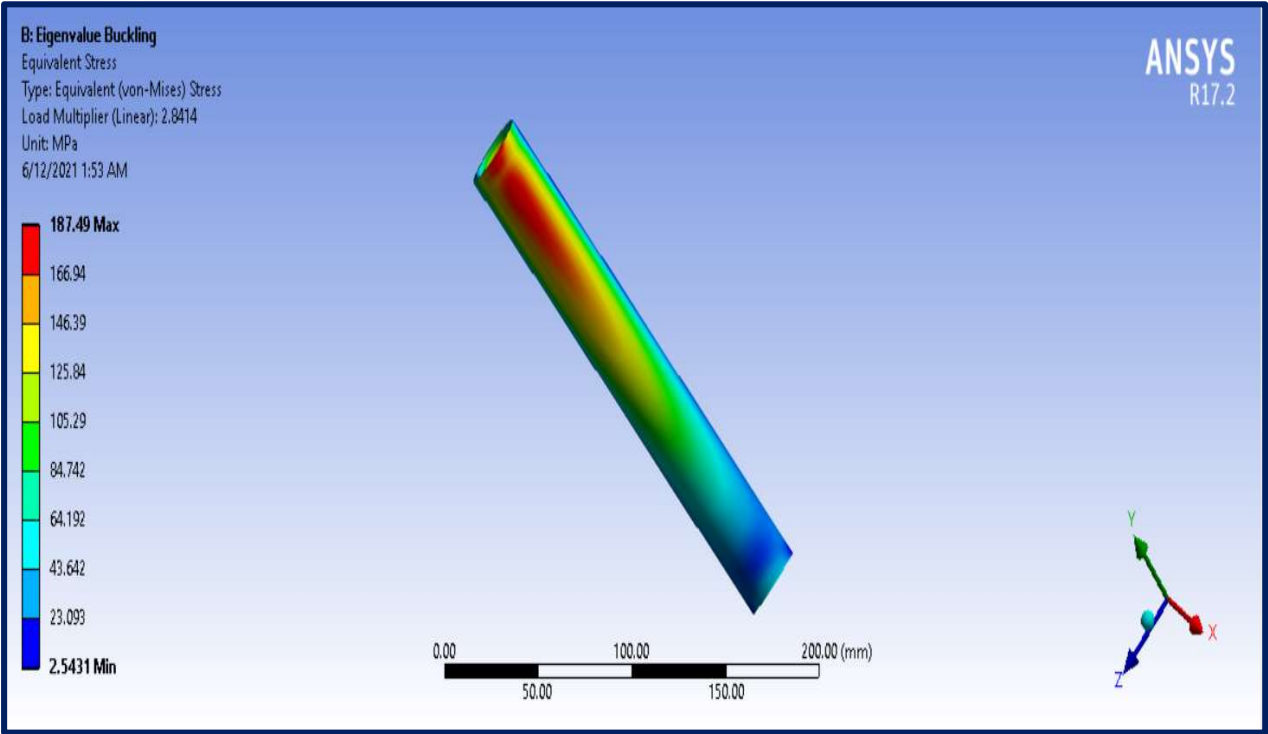


Figure (5.29) Max. Buckling stress for prosthetic pylon (I).



**Figure (5.30)** Max. Buckling stress for prosthetic pylon (II).

Figures (5.28 to 5.30) show the values of critical buckling stress are (211.65 MPa, 199.65 MPa, and 187.49 MPa) for the standard pylon, pylon(I), and pylon (II), respectively. It can be seen from these figures when the reinforcement fiber layers type (carbon or glass) changes will influence the value of critical buckling stress according to the properties of these fibers.

The best prosthetic pylon that resists compression load and has high properties was noticed by (ANSYS-17.2) was the pylon (I) that made of the sample (6), which contained three layers of carbon fibers with orientation (0°/90°), in orthocryl (617H19) lamination (80:20). This is because carbon fibers have better properties than glass fibers like modulus of elasticity, critical buckling load, etc. Figure (5.31) illustrates a comparison of critical buckling stress for pylons.

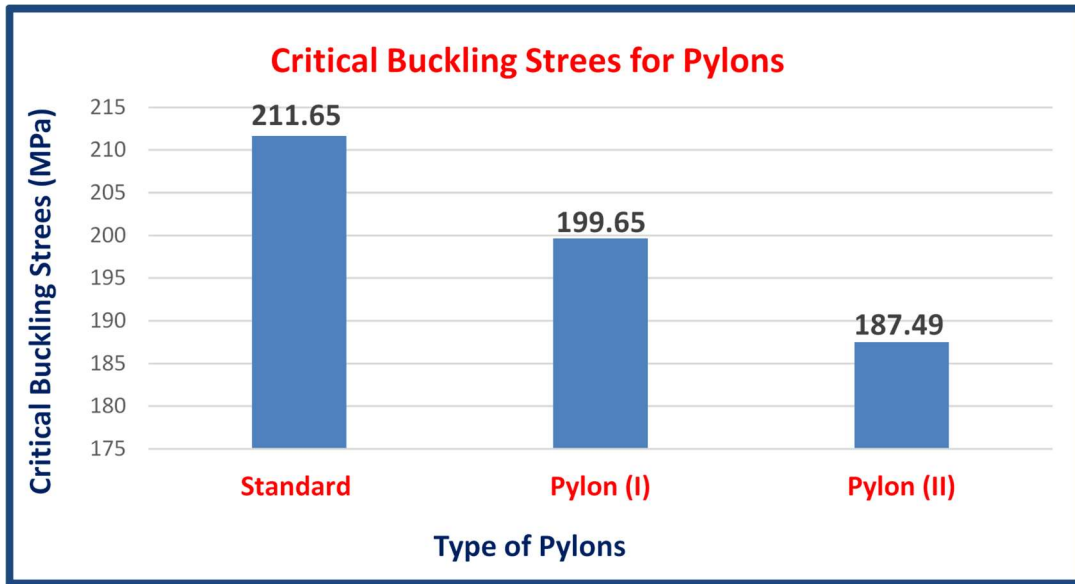


**Figure (5.31)** Comparison of the critical buckling stress(numerically) for pylons

Table (5.18) and figures (5.32) to (5.34) show the comparison between the experimental and numerical buckling stresses for all types of pylons. These results showed an excellent agreement between them as the discrepancy percentage did not exceed (3.01 %).

**Table (5.18)** Experimental and numerical buckling stresses for all types of pylons

Type of Pylon	Experimental Buckling Stress (MPa)	Numerical Buckling Stress (MPa)	Discrepancy = $\left  \frac{\text{Experimental} - \text{Numerical}}{\text{Experimental}} * 100\% \right $
<b>Metallic Pylon</b>	207	211.65	2.24
<b>Pylon(I)</b>	195	199.65	2.38
<b>Pylon (II)</b>	181	187.49	3.01



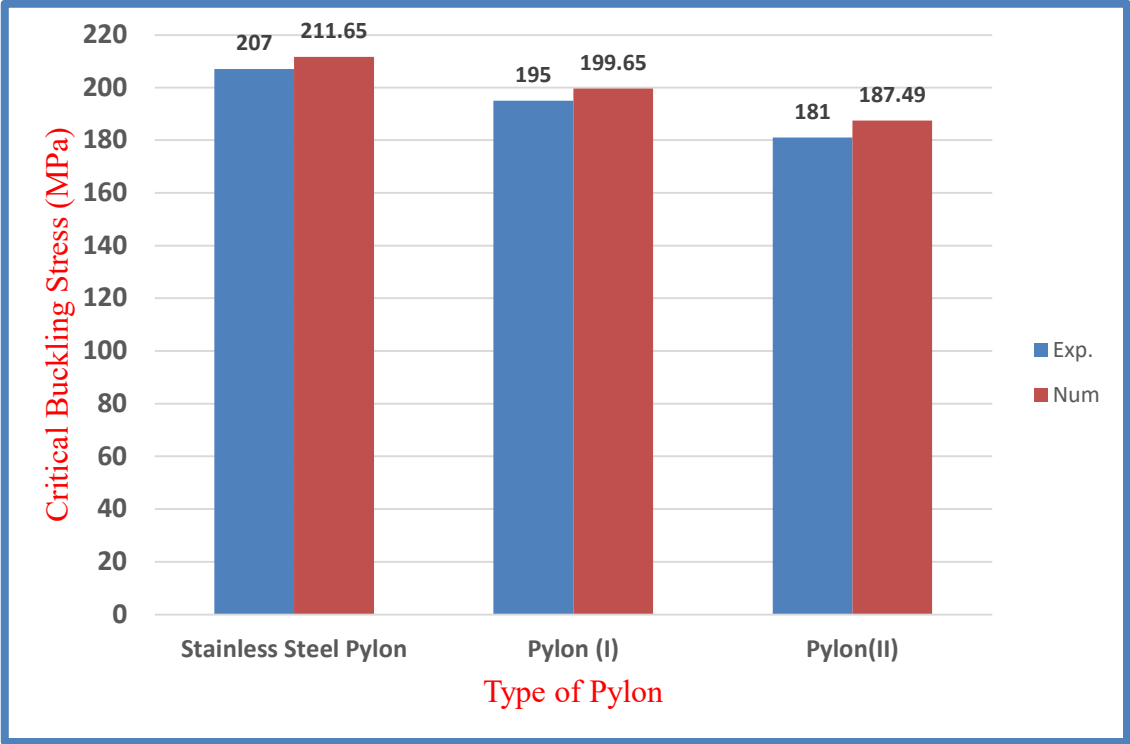


Figure (5.32) The experimental and numerical buckling stresses of all pylons.

---

# CHAPTER SIX

## CONCLUSION AND RECOMMENDATIONS

### FOR FUTURE WORK

The conclusions drawn from this research are presented in this chapter. It also makes recommendations that could be useful for future research.

#### 6.1 Conclusions

The most important conclusions that were obtained in this research, whether concerning the theoretical and experimental investigation for the suggested composite samples or concerning the experimental and numerical investigation for the manufactured pylons, are summarized as follows:

1. Mechanical properties:

- (a) Ultimate tensile stress, Young's modulus, ultimate flexural stress, flexural modulus of elasticity, and critical buckling load of the composite sample are the mechanical properties that increase with increasing fiber volume fraction for two types (glass and carbon) fiber. The higher values of these properties are found with samples with three carbon fiber layers at ( $V_f = 28.4\%$ ), equal to (175MPa, 4.63GPa, 230.769 MPa, 6.38 GPa, and 204.5N) respectively.
- (b) The critical buckling load reduces as the aspect ratio ( $L/T$ ) of the composite column increases.
- (c) The percentage of elongation is one of the mechanical properties which increases when the volume fraction decreases.

- 
2. The critical load theoretical and experimental results for the eight suggested samples give an excellent reasonable between them. The maximum difference between theoretical and experimental results was less than (6.4%).
  3. The results of the numerical part showed that the best suggested prosthetic pylon with the highest critical buckling stress to begin the failure was pylon(I), where the critical buckling stress was (204 MPa).
  4. A good agreement was obtained between the analytical and experimental results (buckling test) for both types of the new pylon. Critical buckling stress has been obtained with a maximum difference of less than (3.01%).
  5. The two types of the new pylons are cheaper and lighter compared with standard pylon, where the percentage reductions in cost and weight are up to (78%) and (82%), respectively, for the pylon (I). While it reached (86%) (79%) respectively in pylon (II). Besides the new two types of pylons, the more flexible this led to more impact-absorbing and more comfortable for the user than a standard metal pylon.
  6. Through the gait cycle test:
    - (a) It can be concluded that the percent of the difference in step length, step time, and other parameters were decreased with new pylons compared with the standard metallic pylon.
    - (b) The pylon (I) shows the best results; the COP approaches the foot's midst, like normal. The butterfly form appears. This is due to the high adjustment of a prosthetic pylon (I). The butterfly's symmetrical shape indicates that the difference in gait line length and single support line were (9mm) and (4mm), respectively. However, it was (14mm) and (8mm) respectively for the suggestion pylon (II), While for the standard pylon it was (21mm) and (15mm) respectively. That is, an improvement rate of (57%) and (33%) for pylon I and pylon II, respectively.

- 
- (c) Owing to the shift in ground reaction force with the gait cycle, the stress distribution for the new two forms of the pylon is maximum at heel strike, decreasing at midstance, and rising again at toe-off; this corresponds to the test results the amputee with the standard metallic pylon.
- (d) Relating to the foot rotation angle, the difference was decreased between the injured leg and the regular leg, where the improvement was by (95%) and (38%). At the same time, the step length has been enhanced by (75%) and (50%). In addition, the step time improved by (88%) and (66%) in pylon (I) and pylon (II), respectively.

## 6.2 Recommendations for Future Work

The following recommendations can be taken into consideration for the expansion of this study:

1. Developing new materials, determining mechanical properties, and determining the ability to absorb impact and fatigue.
2. Investigating the effects of different matrix materials such as acrylic or epoxy on the properties of a trans-tibial prosthetic pylon with natural fiber reinforcement.
3. Studying the effect of addition varying particle types like carbon nanotube (CNT) and titanium oxide (TiO<sub>2</sub>) on the trans-tibial prosthetic pylon.

## REFERENCES

- [1]- "Landmine – Statistics", One World International, London, 2002.
- [2]- Lenka, P. and R. Kumar "Gait Comparisons of Trans Tibial Amputees with Six Different Prosthetic Feet in Developing Countries." *Indian J Phys Med Rehabil* 21: 8-14, 2010.
- [3]- Challoor S. H., "Stress Relaxation Effect on The Prosthetic Below Knee Socket, " MSc Thesis, College of Engineering, Al-Mustansiriya University, 2014.
- [4]- Enderle, J. D., and Bronzino, J. D, "Introduction to Biomedical Engineering", Academic Press, 2012.
- [5]- Clynes, M., and Milsum, J. H., "Biomedical Engineering Systems 1970.
- [6]- Andrea Haberman "Mechanical Properties of Dynamic Energy Return Prosthetic Feet", M.Sc. Thesis Queen's University, Canada, 2008.
- [7]- Jason Wiersdorf, "Preliminary Design Approach for Prosthetic Ankle Joints Using Compliant Mechanisms", MSc. Thesis, Mechanical Engineering Department, Brigham Young University, December, 2005.
- [8]- Gerschutz M.J., Haynes M.L., Nixon DM, and Colvin J.M., "Tensile Strength and Impact Resistance Properties of Materials Used in Prosthetic Check Sockets, Copolymer Sockets, and Definitive Laminated Sockets". *J Rehabil Res. Dev.* ;48(8): 987–1004, 2011.
- [9]- Douglas G. Smith," The Transfemoral Amputation Level, Part 4 "Great Prosthetic Components are Good, but a Good Socket is Great" *Journal of in Motion*", Volume 14 · Issue 5 · September/October 2004.

- [10]- Dundass, C., Yao G.Z., Mechefske, C. K, "Initial Biomechanical Analysis and Modeling of Transfemoral Amputee Gait." JPO: Journal of Prosthetics and Orthotics 15(1): 20-26. 2003.
- [11]- Samira K. Radi, Haider F. Neama, "Analysis of Below Knee Prosthetic Socket", Journal of Engineering and Development, Vol.12, No. 2, pp.127-136, 2006.
- [12]- Michael Schuch C., CPO, FISPO, FAAOP, "Consumer Guide for Amputees: A Guide to Lower Limb Prosthetics: Part I - Prosthetic Design: Basic Concepts", Vol.8, No.2,1998.
- [13]- Muhsin J. Jweeg, Haider F. Neama, Samira K. Radhi, " An Experimental Comparative Study between Polypropylene and Laminated Lower Prosthetic Socket" Al-Khwarizmi Engineering Journal, 3(1), pp. 40-47, 2007.
- [14]- Allan G. A. Coombes, Christopher D. Greenwood, John J. Shorter, "Human Biomaterials Applications", Springer Science + Business Media New York, 1996.
- [15]- Cheung, H., Ho, M., Lau, K., Carona, F., and Hui, "Natural Fiber-Reinforced Composites", Journal of Science Direct, Vol.40, 2009.
- [16]- Cochran H., Orsi, and P., "Lower Limb Amputation, Part3: Prosthetics", Prosthetics & Orthotics International, 2001.
- [17]- Joaquin A. Blaya "Force - Controllable Ankle Foot Orthosis (AFO) to Assist Drop Foot Gait" M. Sc thesis, Mechanical Engineering Waterloo, Ontario, Canada, 2002.
- [18]- Benhamou, R. "The Artificial Limb in Preindustrial France" Technology and Culture, Vol.35, No. (4), 835-845,1994.
- [19]- Norton, K. "A Brief History of Prosthetics in Motion". Vol.17, No. 7, 1-3,2007.

- [20]- Karl F. Zabjek, "Biomechanical Analysis of Light Feet During Locomotion in Elderly People with Lower Limb Amputees" M. Sc. Thesis, University of Sherbrooke, Canada,1997.
- [21]- Vilagra, J., Sganzerla, C., and Walcker L. "Transtibial Prostheses: Items of Comfort and Safety". Rev. Thema Sci. 1(2), 107–112, 2011.
- [22]- Jacob Lenhart, Claire McGuire, and Mikaela Nocetti, "Prosthetics Limbs: History", El Camino Fundamental High School, 2015.
- [23]- Wevers H. W. and J. P. Durance, "Dynamic Testing of Below-Knee Prosthesis", Prosthetics and Orthotics International, Vol.11, pp.117-123, 1987.
- [24]- Thurston A. J., J. Rastorfer, Burian H., and Beasley A. W "The Flek- Shine: A Composite Material for Use in Flexible Shank Below-Knee Prosthesis", Prosthetics and Orthotics International, Vol. 13, pp.97-99, 1989.
- [25]- Bern N. Laws P. and Solomonidis S. "Mechanical characterization of vertical shock-absorbing pylons for lower limb", J. of engineering in Medicine, Vol.4, No.4, 1994.
- [26]- Coleman K. L., Boone D. A., Smith D. G., and Czerniecki J. M., "Effect of Trans-tibial Prosthesis Pylon Flexibility on Ground Reaction Forces During Gait", Prosthetics and Orthotics International, Vol.25, No.3, pp.195-201, 2001.
- [27]- Ian Brown and Ross Stewart, "Determining Inspection Intervals for Lower Limb Prosthetic Components", Rehab.Tech./Monash University/ Caulfield/VIC 3162, 2001.
- [28]- Winson C. C. Lee, Ming Zhang and David A. Boone Bill C., "Finite-Element Analysis to Determine Effect of Monolimb Flexibility on Structural Strength and Interaction Between Residual Limb and Prosthetic Socket", Journal of Rehabilitation Research &Development, Vol.41, No.6A, pp.775-786, 2004.

- [29]- Prasanna K. Lenka, Amit R. Chowdhury, and Ratnesh Kumar, “Design and Development of Lower Extremity Paediatric Prosthesis, A Requirement in Developing Countries”, IJPMR, Vol.19, No.1, pp.8-12, 2008.
- [30]- Shasmin H. N., Abu Osman N. A. and Abd Latif L., “Economical Tube Adapter Material in Below Knee Prosthesis”, Department of the Biomedical Engineering/ University of Malaysia, Vol. 21, pp.407-409, 2008.
- [31]- Shasmin H. N., N. A. Abu Osman and L. Abd Latif, “Comparison between Biomechanical Characteristics of Stainless Steel and Bamboo Pylons”, Department of Biomedical Engineering / University of Malaysia, Vol. 21, pp.851-853, 2008.
- [32]- Muhsin J. Jweeg, Kadhim K. Resan, and Muhand N. Mohammed, “Design and Manufacturing of a New Prosthetic Low-Cost Pylon for Amputee”, Journal of Engineering and Development, Vol.14, No.4, December (2010).
- [33]- Muslim M. Ali, Ali I., Jabbar H. Mohmmed, and Ali R. Yousif,” Study the Effect of Angle Dorsiflexion on Bending Stress of Prosthetic Pylon”, International Journal of Engineering Science and Technology (IJEST), Vol.4, No.12, pp.4818-4853, 2012.
- [34]- Albert E. Yousif, and Ahmed Ali Sadiq, “The Design, Development, and Construction of An Adjustable Lower Extremity”, Journal of Engineering (IOSRJEN), Vol.2, No.10, pp.30-42, 2012.
- [35]- Pitkin M., J. Pilling, and G. Raykhtsaum, “Mechanical Properties of Totally Permeable Titanium Composite Pylon for Direct Skeletal Attachment”, National Institute of Health, Vol. 100, No. 4, May 2012.
- [36]- Jawad K. Oleiwi, and Shaymaa Jumaah Ahmed. “Tensile and Buckling of Prosthetic Pylon Made from Hybrid Composite Materials” Eng. &Tech. Journal, Vol.34, Part (A), No.14, 2016.



- [37]- Richard H. Jones, M.D., and Chester C. Nelson, C.P. “(Pylon-Prosthetic) Devices for Lower Extremity Congenital Skeletal Limb Deficiencies”, From the Shriner's Hospital for Crippled Children, Minneapolis, Minnesota, 1965.
- [38]- Myer Kutz, Arif Iftekhar, “Biomedical Engineering and Design Handbook”, University of Minnesota, Minneapolis, 2<sup>nd</sup> edition, 2009.
- [39]- Lawrence E. Murr, “Handbook of Materials Structures, Properties, Processing, and Performance: Classification of Composite Materials and Structures”, Springer International Publishing Switzerland, 2014.
- [40]- Mallick P. K., “Fiber-Reinforced Composite: Materials, Manufacturing, and Design”, International Standard Book, 3<sup>rd</sup> edition, (2007).
- [41]- Mustafa Akay, “An Introduction to Polymer-Matrix Composites”, First edition, Bookboon, 2015.
- [42]- Ramakrishna, S., Mayer, J., Wintermantel, E., and Leong, K. W., “Biomedical Application of Polymer-Composite Materials”, National University of Singapore, Vol.61, No.9, 2001.
- [43]- Laszlo P. Kollar and George S. Springer, "Mechanics of Composite Structures. Mechanics of Composite Structures", Cambridge University Press, 2003.
- [44]- Jones, R. M, "Mechanics of Composite Materials", (Vol.193). Washington, DC: Scripta Book Company, 1975
- [45]- Department of Defense Handbook, "Composite Materials Handbook", Polymer Matrix Composites, Materials Usage Design and Analysis, MIL-HDBK-17-3F, Vol. 3, 2002.
- [46]- Mallick P. K., “Composites Engineering Handbook”, New York, Marcel Dekker, 1<sup>st</sup> edition, 1997.

- [47]- Robert M. Jones and Karen S. Devens, “Mechanics of Composite Materials”, New York, 1998.
- [48]- Andriacchi T.P Ogle and Galante Jo.,” Walking Speed as a Basis for Normal and Abnormal Gait Measurements”, Journal of Biomechanics, Vol.10, No.4, 1977.
- [49]- Lynn S. Lippert, MS, PT, "Clinical Kinesiology and Anatomy”, F. A. Davis Company, Fourth edition, 2006.
- [50]- Gerard Gorniak, "Upper and Lower Extremity Biomechanics", Bookboon, 2016.
- [51]- Mario C. Faustini, Richard R. Neptune and Richard H. Crawford " The Quasi-Static Response of Compliant Prosthetic Sockets for Transtibial Amputees Using Finite Element Methods " J. of Med. Eng. Phys., Vol.28, pp.113-121,2006.
- [52]- Jacquelin Perry and Judith M. Bumfield, “Gait Analysis: Normal and Pathological Function”, The Journal of the American Medical Association, Vol.304, No.8, 2010.
- [53]- Brian Durward, Gillian Baer, and Philips Rowe, “Functional Human Movement”, Butterworth- Heinemann, 1999.
- [54]- Arthur F.T. Mak, Ming Zhang, and David A. Boone, “State of the Art Research in Lower Limb Prosthetics Biomechanics-Socket Interface”, Journal of Rehabilitation Research and Development, Vol. 38, No. 2, 2001.
- [55]- Ross Stewert, “Stress Paths of AK Prosthetic Socket”, Monash Rehabilitation Technology Research Unit; Research, 1991
- [56]- “Standard Test Method for Tensile Properties of Plastics D638-03”, Annual Book of ASTM Standard, New York, 2004.

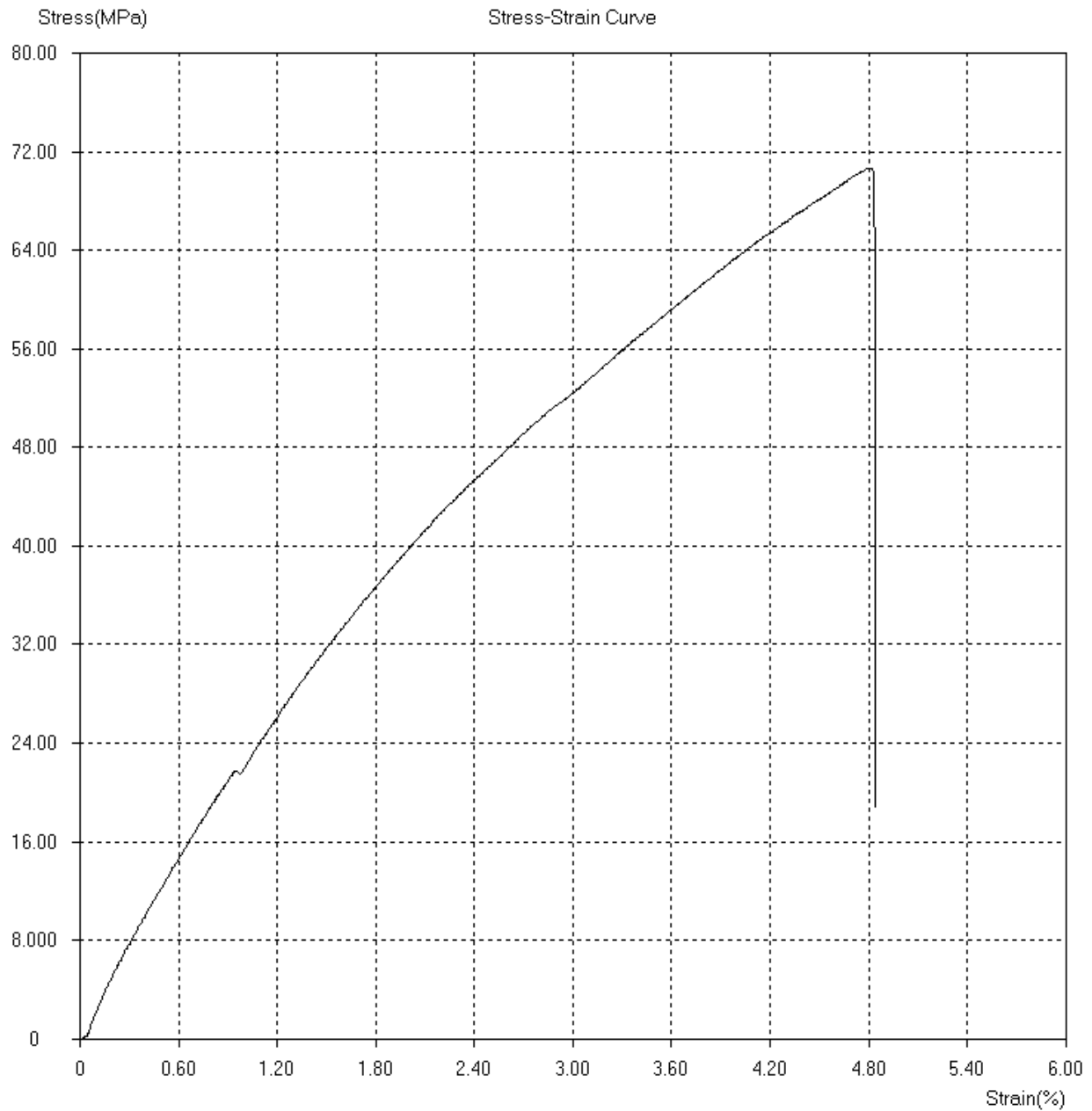
- [57]- Donald R. Askeland, Pradeep P. Fulay, and Wendelin J. Wright, “The Science and Engineering of Materials”, 6<sup>th</sup> edition, Cengage Learning Inc., 2011.
- [58]- “Standard Test Method for Flexural Properties of Unreinforced and Reinforced Plastics and Electrical Insulating Materials D790-02”, Annual Book of ASTM Standard, New York, 2002.
- [59]- Mott, R. L., "Applied Strength of Materials", 5<sup>th</sup> edition, John Wiley, U.K., 1993.
- [60]- E.J. Hearn, “Mechanics of Materials”, Vol. 2, Second Edition, Pergamon Press, 1985.
- [61]- Assakkaf, I.A., "Mechanics of Materials", Mc–Graw-Hill, 3rd edition 2003.
- [62]- Nautiyal, B.D., "Introduction to Structural Analysis", New Age International Ltd, Publisher.4835/24, Ansari Road Darya Ganj, New Delhi-110002, 2001.
- [63]- Dainal, L.S., "Structures", 5th edition, Prentice-Hall, 2004.
- [64]- F.A. Crane and J.A. Charles "Selection and Use of Engineering Materials "Butter Worth & Co. (Publishers) Ltd. 1987.
- [65]- Rao, S. S, "The Finite Element Method in Engineering", 5th, Boston: Elsevier, 2011.
- [66]- ANSYS theory reference. "ANSYS Composite Prep-Post User's Guide", ANSYS, Inc. South Point, Canonsburg, November 2013.
- [67]- Callister, W.D, "Materials Science and Engineering", an Introduction, 7<sup>th</sup> Edition, John Wiley & Sons, Inc. 2007.

- [68]- “Standard Test Method for Density and Specific Gravity (Relative Density) of Plastics by Displacement D792-08”, Annual Book of ASTM Standard, New York, 2008.
- [69]- Mohsin A. Al-Shammari and Ahmed K. Abdulameer," Fatigue Strength and Stiffness to Weight Ratio Determination of Syme's Amputation Prosthesis Socket “, M.Sc. thesis, College of Engineering, University of Baghdad, 2018.
- [70]- Shigley, J. E., "Shigley's Mechanical Engineering Design", Tata McGraw-Hill Education, 2011.
- [71]- Jameel.A.N., and Al-mawash.A. D, “Experimental and Theoretical Buckling Analysis of Cracked Laminated Composite Thin Plates”, M.Sc. thesis, college of engineering, Baghdad university; 2014.
- [72]- Whittle, M.W., "Gait analysis: An Introduction". Butterworth-Heinemann, 2014.
- [73]- Matthew J. Major, Rebecca L. Stine and Steven A. Gard “The effects of walking speed and prosthetic ankle adapters on upper extremity dynamics and stability-related parameters in bilateral transtibial amputee gait” NIH Public Access 38(4): 858–863. doi:10.1016/j. gait post. 2013.
- [74]- Mohsin A. Al-Shammari, Emad Q. Hussein, Ameer A. Oleiwi “Fatigue strength and stiffness/weight ratio determination of through knee prosthetic” M.Sc. thesis, College of Engineering, University of Kerbala, 2017.

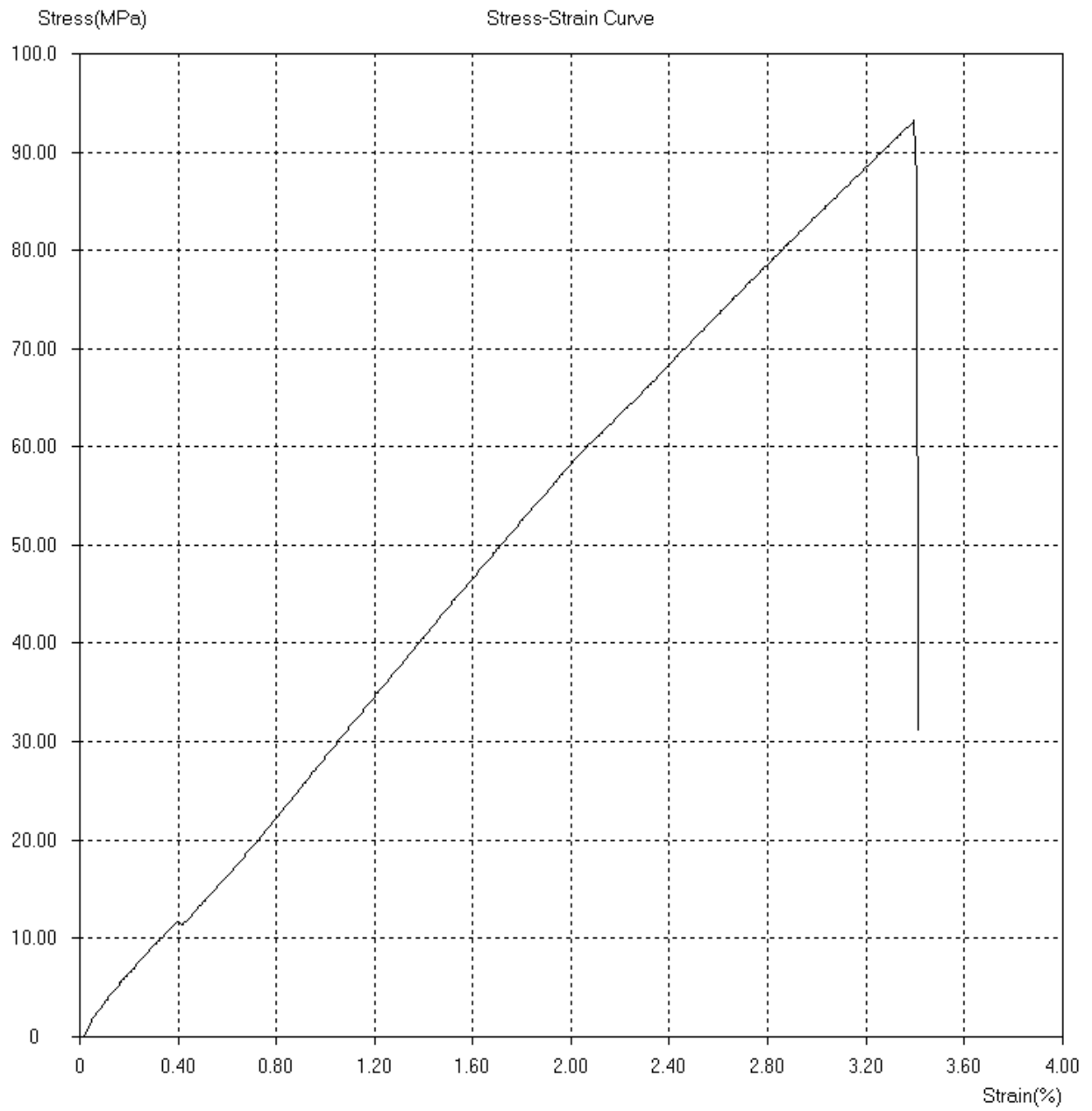
## Appendix A

The Ministry of Higher Education and Scientific Research- University of Technology- laboratories of Department of Materials Engineering about results of tensile test for the suggested samples.

### Sample 1



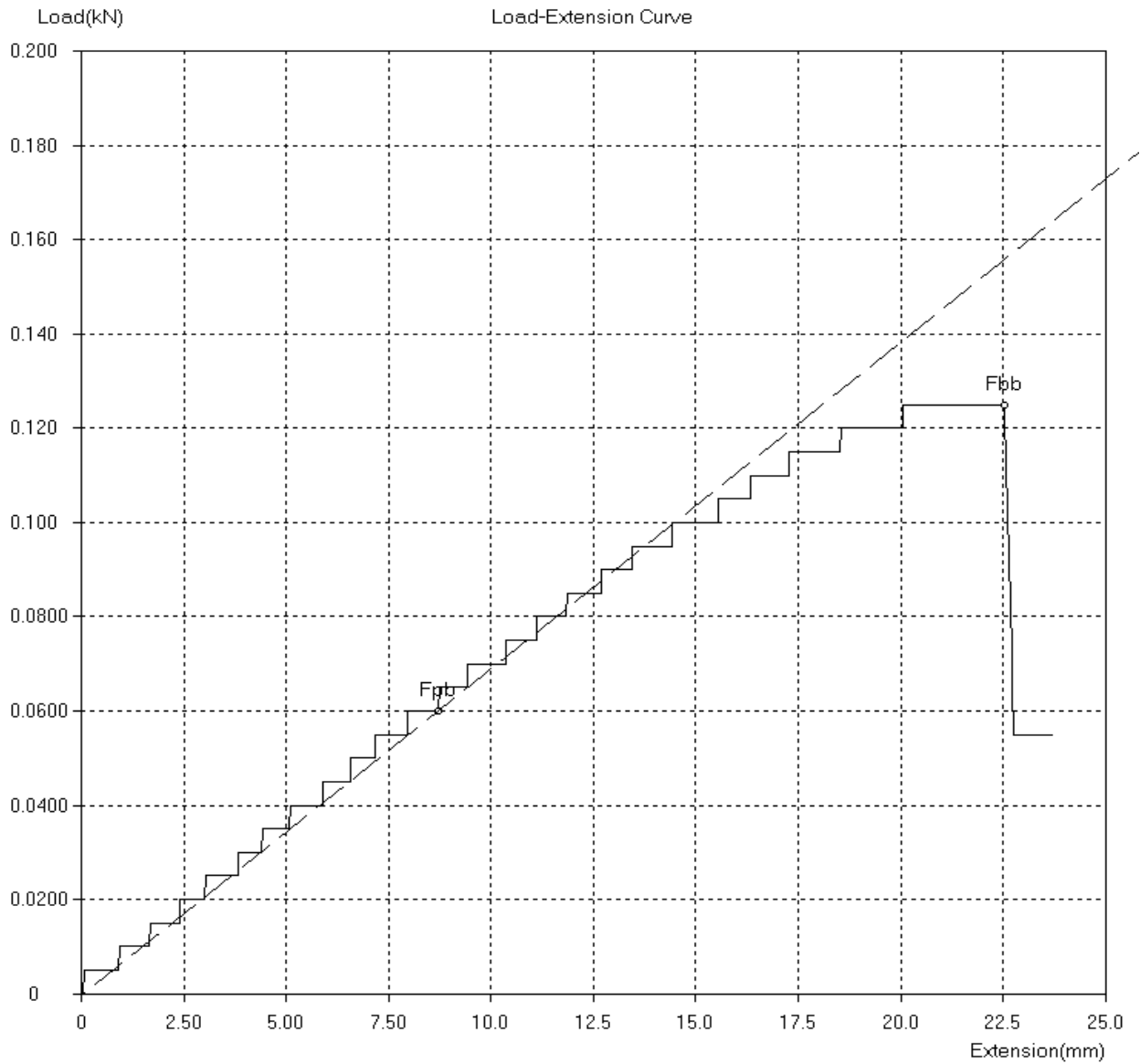
## Sample 2



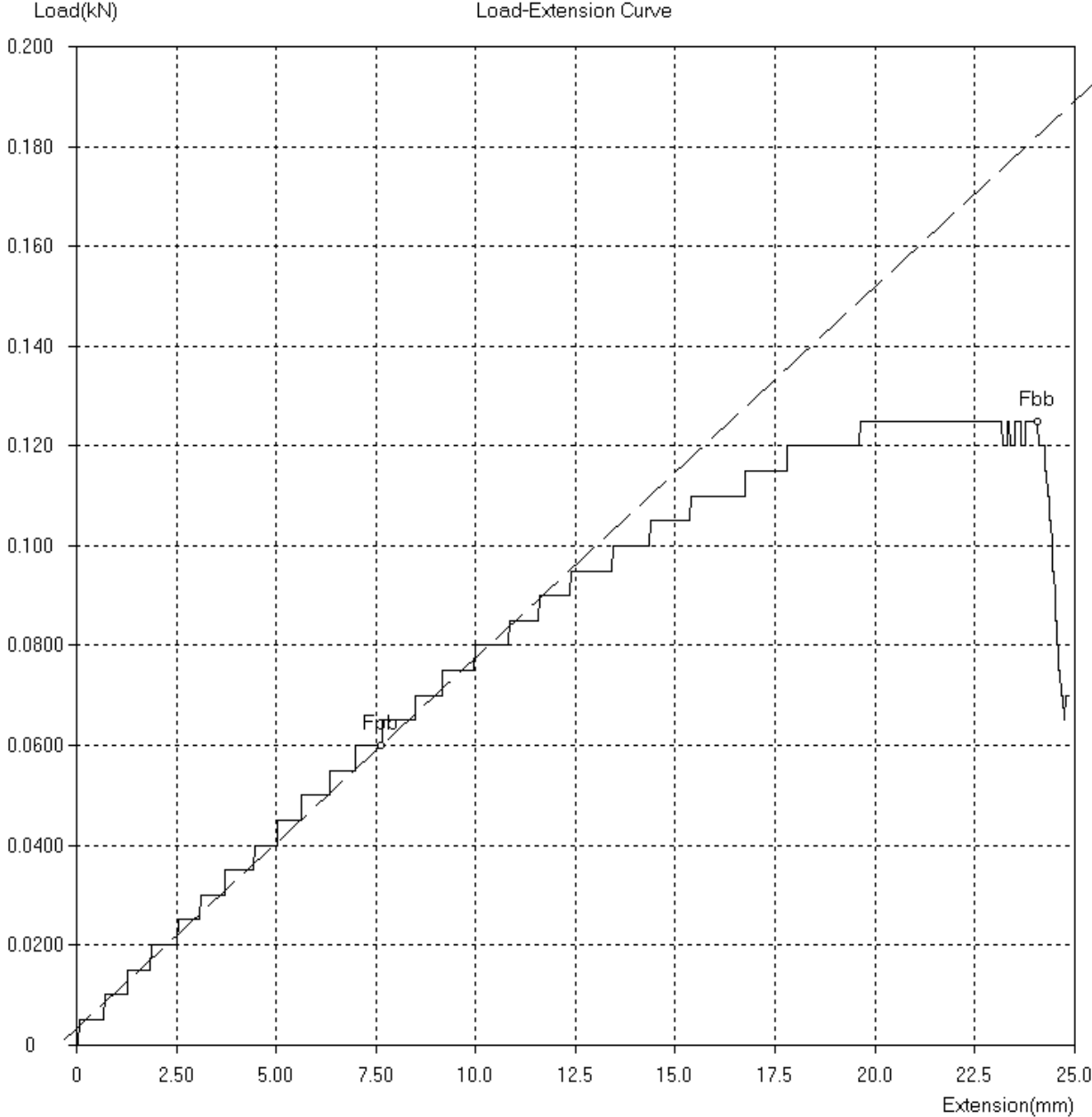
## Appendix B

The Ministry of Higher Education and Scientific Research- University of Technology- laboratories of Department of Materials Engineering about bending test results for the suggested samples.

### Sample 5



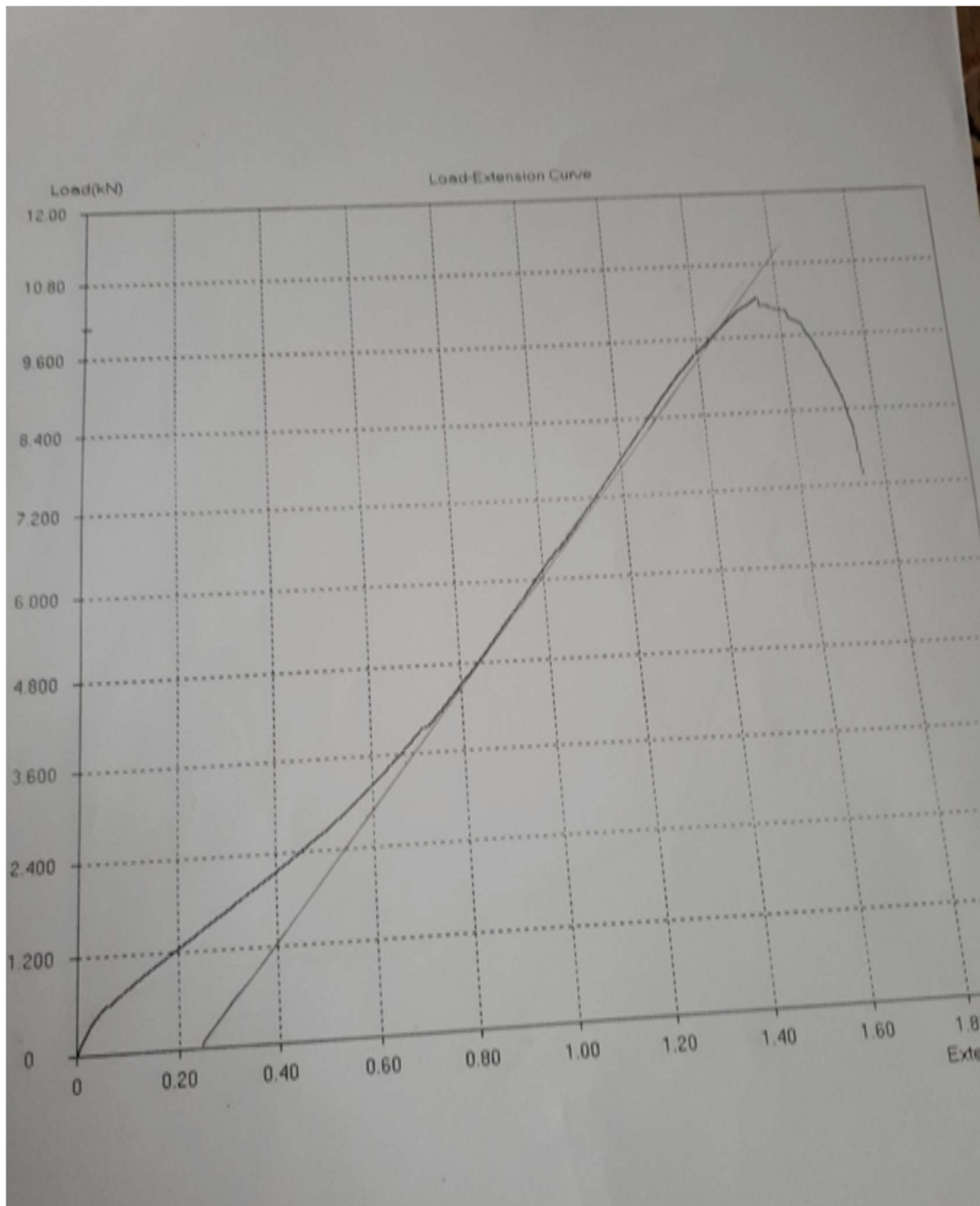
Sample 8

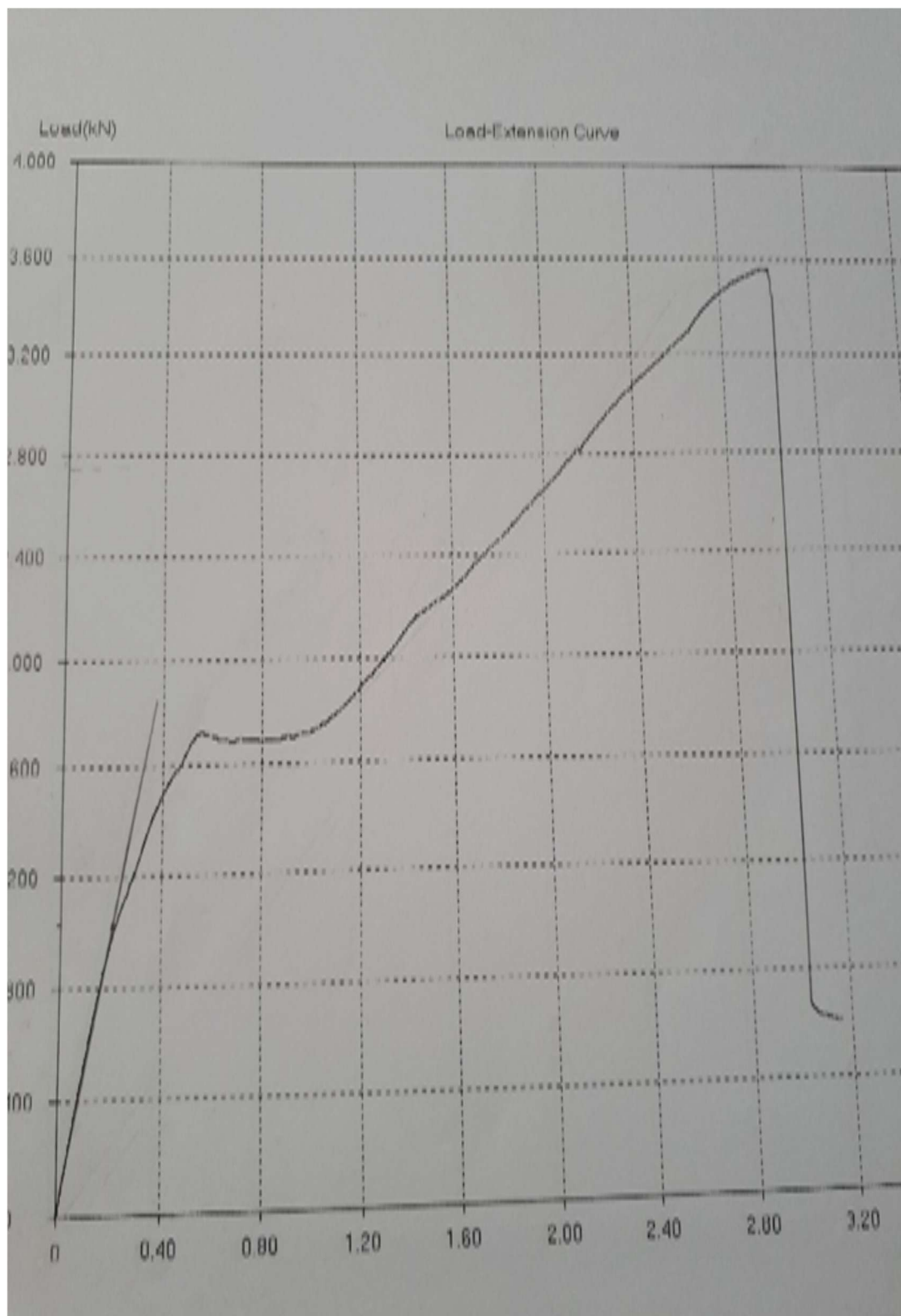




## Appendix C

The Ministry of Higher Education and Scientific Research- University of Technology- laboratories of Department of Materials Engineering about results of pylon buckling test.





## الخلاصة

يعد الساق الاصطناعي جزءًا مهمًا من الطرف الاصطناعي السفلي، وهو مجال مثير للاهتمام في الهندسة الطبية الحيوية هذا اليوم. يتم تصنيع الساق الاصطناعي بشكل عام من معدن خفيف الوزن مثل الألومنيوم والتيتانيوم والفولاذ المقاوم للصدأ أو سبيكة من هذه المعادن.

يهدف هذا البحث إلى تطوير الساق الاصطناعي من خلال تصنيعه من مواد مركبة جديدة تجعله أخف وزنا وأقل تكلفة وأكثر راحة للمستخدم من ذوي الاحتياجات الخاصة.

تتكون العينات المقترحة من عدد ثابت من طبقات البرلون وعدد مختلف (طبقة واحدة أو طبقتان أو ثلاث) من ألياف الكربون أو الألياف الزجاجية باتجاه (0/90) نسبة للحمل المسلط كمواد تقوية بالإضافة الى (أورثوكريل 80:20 (617H19)) كمادة أساس وقد اعتمدت تقنية التعبئة الفراغية (الحقيبة المفرغة من الهواء) في تصنيعها.

تم إجراء اختبارات الخصائص الميكانيكية مثل الشد والانتشاء والانبعاج وبعض اختبارات الخصائص الفيزيائية كاختبار الكثافة.

نظريًا، تم حساب هذه الخصائص باستخدام المعادلات المناسبة، وقد كان هناك توافقًا جيدًا بين النتائج التجريبية والنظرية حيث بلغت نسبة التفاوت (6.4%) فقط.

بناءً على هذه النتائج تم تصنيع نوعين من السيقان، الأول من العينة السادسة والتي تتكون من الطبقات (2) برلون، 3 ألياف كربونية، 2 برلون)، والآخر من العينة الثالثة والتي تتكون من الطبقات (2) برلون، 3 ألياف زجاجية، 2 برلون). وقد اجري اختبار الانبعاج للساقين المصنوعين من المواد مركبة بالإضافة إلى الساق المعدني المستخدم حاليًا والمصنوع من الفولاذ المقاوم للصدأ للتحقق من حمل الانبعاج الحرج وأقصى انحراف لكل عمود.

باستخدام طريقة العناصر المحدودة (ANSYS WORKBENCH 17.2) تم تحليل (التشوه الكلي، الانفعال المرن، اجهاد الانبعاج، وشكل الانبعاج) لكل من الساقين المركبين والساق المعدنية.

تمت مقارنة النتائج التجريبية مع النتائج العددية وظهر توافقًا ممتازًا بينهما حيث لم تتجاوز نسبة التفاوت (3.01%).

للتحقق من متانة السيقان الاصطناعية المقترحة في الدراسة الحالية ومقارنتها بالسيقان المعدنية المستخدمة من حيث القوة والوزن والمرونة وراحة المستخدم، تمت دراسة حالة أحد ذوي الاحتياجات الخاصة في مركز بابل للأطراف الاصطناعية، كان رجلا وزنه (80 كغم) وارتفاعه (1.7) م وعمره (55) سنة. بترت ساقه اليسرى تحت الركبة. وقد أجري له اختبار قوة رد فعل الأرض بالسيقان المقترحة وتمت مقارنة النتائج مع الساق القياسي، وقد كانت نتائج دورة المشي للشخص المبتور مع الساق الجديدة مع نظائرها من الساق الاصطناعية فيما يتعلق بزواوية دوران القدم، تم تقليل الفرق بين الساق المصاب والساق الطبيعية حيث كان التحسن بنسبة (95%) و (38%) أما بالنسبة لطول الخطوة فقد تم تحسينها بنسبة (75%) و (50%) كما تحسن زمن الخطوة بمقدار (88%)، و (66%) في الساق المقترحة (I) والساق (II) على التوالي.



جمهورية العراق  
وزارة التعليم العالي والبحث العلمي  
كلية الهندسة - جامعة كربلاء  
قسم الهندسة الميكانيكية

## " تشخيص الانبعاج لساق طرف صناعي متراكب "

رسالة مقدمة الى قسم الهندسة الميكانيكية - كلية الهندسة - جامعة كربلاء كجزء من متطلبات نيل درجة الماجستير في علوم  
الهندسة الميكانيكية

(ميكانيك تطبيقي)

من قبل

**حيدر زاهر كاظم عبد الأخوة الخفاجي**

بكالوريوس في علوم الهندسة الميكانيكية لسنة 2007

بإشراف

الأستاذ الدكتور عماد قاسم حسين

الأستاذ الدكتور محسن عبدالله الشمري

تمت

الحمد لله كما هو أهله

اللهم صل على محمد وآل محمد وعجل فرجهم